Thesis

Duality for Precise Locations of Critical Points in Random Spin Systems

Masayuki Ohzeki
Department of Physics, Tokyo Institute of Technology

August, 2008

Abstract

We derive the precise locations of the critical points in several random spin systems, the $\pm J$ Ising model, the Gaussian model, and the Potts spin glass on the square lattice, and the $\pm J$ Ising model on the triangular lattice. A relationship between different partition functions established by consideration with a symmetry, the duality, plays an important role in proving these results. This technique has been originally applied to non-random spin systems and given the exact solutions. Recently a variant technique has been proposed and predicted the locations of the critical points in classical spin systems with random couplings. However some results by this technique do not show good consistencies with existing results in several cases.

As an improved way, we use a systematic summation of a part of spins in the partition functions, the renormalization group analysis, to increase the precision of the predictions beyond a conventional technique. This technique shows greatly successful improvement especially for the random spin systems on special lattices with a convenient structure for such summation, the hierarchical lattices. The obtained results are in good agreement with the existing results by other approaches. We also attempt to predict precise locations of the critical points in several random spin systems defined on regular lattices such as the square, triangular, and hexagonal lattices. The technique established in this thesis is, possibly, a unique tool to analytically derive the location of the critical points in the finite-dimensional random spin systems.

Acknowledgement

First of all, it is a great pleasure to express my gratitude to my supervisor Professor Hidetoshi Nishimori for his encouragement, guidance, and spiritual support.

I also acknowledge greatly the guidance, fruitful discussions, and kindness of Professor A. Nihat Berker of Koç University and Feza Gürsey Institute in Turkey, when I visited his group in Turkey. It is a pleasure to thank Dr. Michael Hinczewski of Feza Gürsey Institute for useful comments while I was in Turkey and he visited our group. Members of Koç University and Feza Gürsey Institute in Turkey gave me the stimulating atmosphere and encouragement. I sincerely thank Professor Yutaka Okabe of Tokyo Metropolitan University for sending numerical data before publishing to examine the validity of my theory. I acknowledge also the warm atmosphere and encouragement by all members of the Nishimori group and the condensed matter theory group of Tokyo Institute of Technology.

This work was financially supported by CREST, JST, by the 21st Century COE Program at Tokyo Institute of Technology 'Nanometer-Scale Quantum Physics', and by the Grant-in-Aid for Scientific Research on the Priority Area "Deepening and Expansion of Statistical Mechanical Informatics" by the Ministry of Education, Culture, Sports, Science and Technology.

I thank my family for spiritual support, and I pray that my father's soul who has gone this March may rest in peace. Finally, I am sorry to hear about the death of Mr. Isamu Sakama who is a great teacher to lead me to the Physics. He has gone this August on which I have just finished written this thesis. I dedicate this thesis to him.

List of Papers

1. **"Multicritical Points for the Spin Glass Models on Hierarchical Lattices"**
   Masayuki Ohzeki, Hidetoshi Nishimori, and A. Nihat Berker
   Phys. Rev. E **77** 061116 (2008).

2. **"Multicritical Points of the Potts Spin Glasses on the Triangular Lattice"**
   Masayuki Ohzeki
   J. Phys. Soc. Jpn. **76** 114003 (2007).

3. **"Multicritical Points of the Potts Spin Glasses on the Triangular Lattice"**
   Masayuki Ohzeki
   Physica E **40** 394 (2007).

4. **"Internal Energy of the Potts Model on the Triangular Lattice with Two- and Three-body Interactions"**
   Masayuki Ohzeki and Hidetoshi Nishimori
   J. Phys. Soc. Jpn. **75** 114003 (2006).

5. **"Location of the Multicritical Point for the Ising Spin Glass on the Triangular and Hexagonal Lattices"**
   Hidetoshi Nishimori and Masayuki Ohzeki
   J. Phys. Soc. Jpn. **75** 034004 (2006).

Contents

Chapter 1

Introduction

We deal with the random spin systems in which the strength of interactions between the localized electron spins are not uniform in space. If the signs of interactions between two spins are not spatially definite, we find conflicts between two types of effects, which order spins in parallel and antiparallel directions, by ferromagnetic interactions and by antiferromagnetic interactions, respectively. Because of the competing interactions, we can see a peculiar phenomenon in a low-temperature region, the *spin glass*, which is quite a different phase from the ferromagnetic phase and the paramagnetic phase found in normal magnetic material. Therefore the phase diagram in random spin systems has a highly rich structure and has critical points related with the peculiar phase transitions and the critical phenomena. Random spin systems is one of the most attractive issues not only as an intrinsic problem to understand such different behaviors investigated in spin systems with randomness from those without any randomness, but also as applications to other fields beyond physics [1, 2, 3].

The aim of this thesis is to derive the precise locations of critical points on the phase diagrams in random spin systems. This study is of practical importance for numerical studies since precise values of the critical points give benchmarks for the numerical simulations and greatly facilitate to estimate the critical exponents characterizing the critical phenomena.

Before going into detailed theoretical discussions, we first review topics and history of spin glasses.

1.1 Spin Glass

A magnetic alloy like CuMn, which is one of the spin glass materials consisting of noble metals (Au, Ag, Cu, Pt) weakly diluted with transition metals (Fe, Mn), has curious interactions between localized spins with a potential which oscillates as a

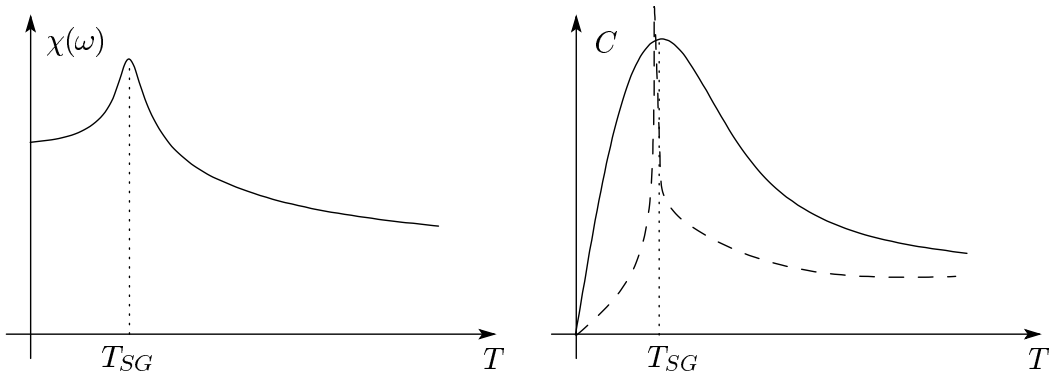

Figure 1.1: Sketch of the characteristic phenomena found in the spin glass. The left panel describes the cusp in the frequency-dependent susceptibility in a low field. The right panel expresses the behavior of a broad peak in specific heat. The dotted line is a sharp peak as found in ferromagnetic material for comparison. The spin glass transition temperature is written by T_{SG}.

function of the separation of the spins in the transition metal. This interaction is known as the RKKY (Ruderman-Kittel-Kasuya-Yosida) interaction [4, 5, 6] and is written as,

$$J_{ij} = \frac{\cos 2k_F r_{ij}}{r_{ij}^3}, \tag{1.1}$$

where J_{ij} is the strength of interaction between two spins, the subscript ij denotes the indices of spins in the transition metal, and r_{ij} is the distance between two spins. The quantity k_F is the Fermi wave number. This peculiar interaction generates a competition between parallel and antiparallel ordering effects for the direction of the localized spin, and causes a nontrivial behavior in the low-temperature region, the *spin glass*. Several characteristic phenomena observed in spin-glass materials are explained below. The cusp in the frequency-dependent susceptibility in low fields as shown in Fig. 1.1 was first observed as a peculiar behavior of the spin glass by Cannella and Mydosh [7]. This phenomenon of the cusp was also found in the insulator $Eu_xSr_{1-x}S$ [8] as well as in the dilute metallic alloys. Specific heat of the spin glasses at the critical point between the spin glass and paramagnetic phases has the behavior of a rather broad peak, which is different from one between the ferromagnetic and paramagnetic phases [9, 10].

To deal with random spin systems with spatially non-uniform interactions, we

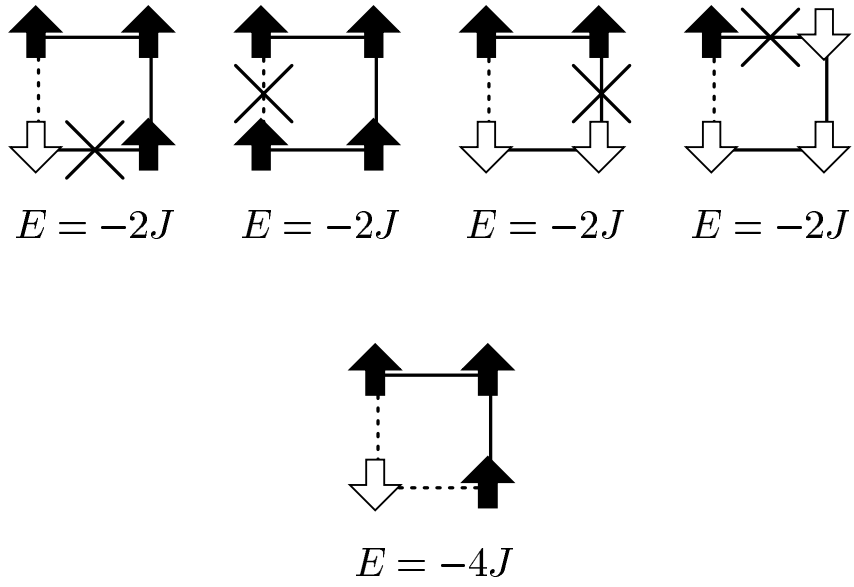

Figure 1.2: The upper figures are the possible configurations as the ground state for a four-bond system with a single antiferromagnetic interaction. The X symbols denote the unsatisfied bonds with a locally high energy $-J_{ij}S_iS_j = J$. The bottom figure denotes the one with two antiferromagnetic interactions.

have to construct a mathematical model, namely the *random-bond Ising model* defined through the Hamiltonian,

$$H = -\sum_{\langle ij \rangle} J_{ij} S_i S_j, \tag{1.2}$$

where S_i is the Ising spin taking the integer value ± 1, and J_{ij} expresses the strength of interactions between two spins.

In the high-temperature region, we can imagine the existence of a paramagnetic phase, similarly to pure ferromagnetic materials as the non-random Ising model. On the other hand, we find that the ground state obtained by minimizing the Hamiltonian shows quite a different behavior from the non-random Ising model. Simplifying the RKKY interaction, we consider the strength of interactions are uniform, expressed by J, but only the signs are non-uniform in space, because the crucial point of the spin glass is competing interactions between ferromagnetic and antiferromagnetic ones as explained below. This is called the $\pm J$ Ising model. As shown in Fig. 1.2, a single antiferromagnetic interaction yields several degeneracies in possible

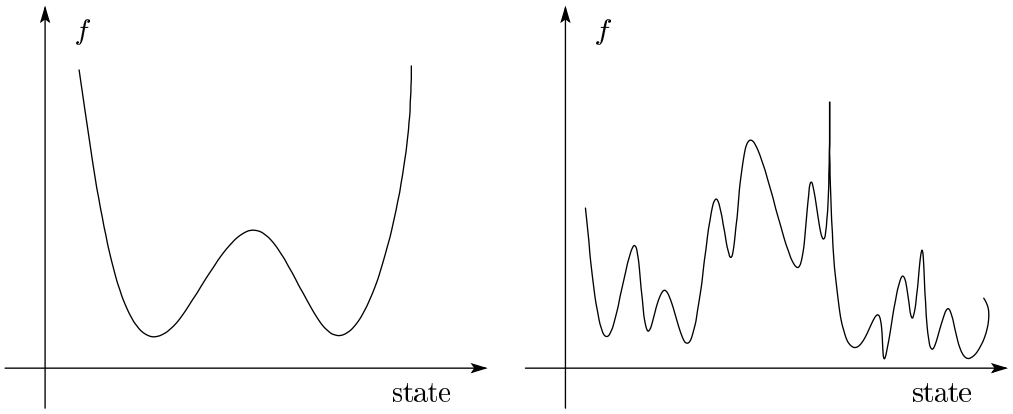

Figure 1.3: The structure of the free energy. The left panel expresses that with two valleys as for the ferromagnetic material. The right panel denotes maltivalley structure for the spin glass.

ground states. However two antiferromagnetic ones do not allow any configurations except for the global inversion degeneracy. It is known that odd numbers of antiferromagnetic interactions generates such degeneracies of the ground state and is explained by the concept of the *frustration* [11, 12]. This frustrations yield, in other words, many minima of the free energy and destroys the ferromagnetic order of spin directions in the low-temperature region. Therefore if the number of frustration increases, the free energy has complicated multivalley structure as in Fig. 1.3 [15, 16, 17, 18], and the ferromagnetic ordered state is violated.

However if we observe the behavior of change of spin orientations for a long time, they mostly do not change, but are frozen. This state, that is disorder in space but order in time, is called the spin glass phase. Usually the ordered phase is characterized by an order parameter. The spin glass order parameter is defined as,

$$q = \left[\langle S_i \rangle^2\right]_{\rm av} , \tag{1.3}$$

where two brackets $\langle \cdots \rangle$ and $[\cdots]$ are thermal and configurational averages for the random couplings J_{ij}, respectively. This order parameter describes, as explained below, the degree of freezing of the system inside a valley from a point of view of the multivalley structure of the free energy. In the spin glass phase, the spins should be randomly frozen. Thus the quantity $\langle S_i \rangle$ does not vanish at any site because the spin does not fluctuate significantly in time. On the other hand, its configurational averaged value $[\langle S_i \rangle]$ becomes zero, because the configurational average for J_{ij} reflects the average over various environments at a given spin and yields both of the

positive and negative values for $\langle S_i \rangle$. In the same situation, the spin glass parameter does not vanish because of the average of non-zero values $\langle S_i \rangle^2$. The spin glass phase is thus given by the condition that the spin-glass parameter has a non-zero value ($q \neq 0$), while the conventional magnetic order parameter is zero ($m = [\langle S_i \rangle] = 0$).

Let us further consider the spin glass state from a point of view of the multi-valley structure of the free energy. Imagine that we have performed a number of experiments. We let the system relax to the thermal equilibrium. Each experiment will be characterized by some equilibrium values of the local spin magnetizations m_i^a, where a expresses the index of the experiment. We then define the following quantity which describes how the states are close to each other obtained in different experiments,

$$q_{ab} = \frac{1}{N} \sum_i m_i^a m_i^b, \tag{1.4}$$

where the summation runs over all sites. This quantity has its maximum when the two states in the experiments a and b coincide. We introduce the distribution function $P(q)$ to consider the statistical properties of the overlaps q_{ab},

$$P(q) = \sum_{a,b} \delta(q_{ab} - q). \tag{1.5}$$

The paramagnetic phase is expressed by the unique global minimum of the free energy, in which the obtained magnetizations in all experiments become zero. If the free energy has a simple structure of two valleys with the magnetization $\pm m$ for the ferromagnetic phase as in Fig. 1.3, the distribution $P(q)$ is constituted only by two delta functions at $q = \pm m^2$ as in Fig. 1.4. On the other hand, for the case that q_{ab} has various values, $P(q)$ has a continuous part as in Fig. 1.4

Next some of analytic studies for the spin glass are introduced. The random-bond Ising model is also called the Edwards-Anderson model [13]. Edwards and Anderson demonstrated that the spin glass phase occurs within a novel form of the molecular-field theory (Curie-Weiss theory). Later Sherrington and Kirkpatrick proposed a variant of the Edwards-Anderson model, which can be exactly solved with the mean-field theory [14]. This pioneering work by the mean-field theory gave the phase diagram of the infinite-dimensional Edwards-Anderson model with the Gaussian distribution for J_{ij} as in Fig. 1.5. In the mean-field analysis, the spin glass order parameter emerges through the formulation by the *replica method* [19, 20, 21, 22]. The replica method enables us to evaluate the configurational averaged value for the various distributions of the random couplings J_{ij}. We then need to prepare copies of the random spin system with the replica spins $\{S_i^\alpha\}$. In

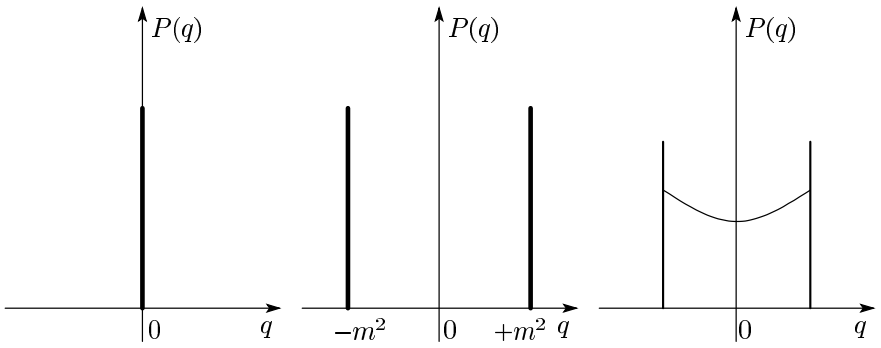

Figure 1.4: The distribution of the overlap q. The left panel shows the case for the paramagnetic phase, the middle one denotes that for the ferromagnetic phase, and the right one gives that for the spin glass phase.

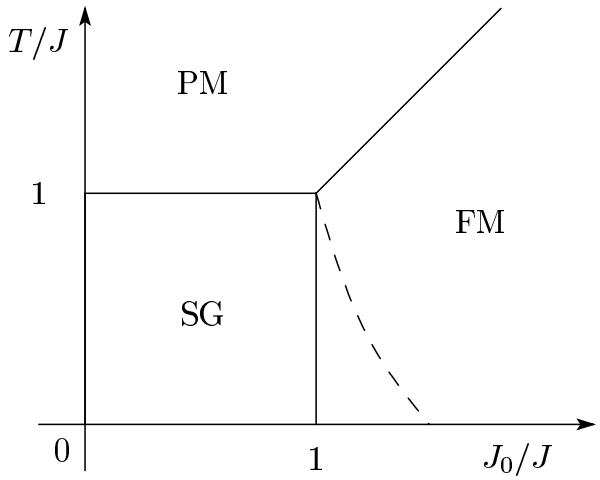

Figure 1.5: The phase diagram obtained by the mean-field theory. The paramagnetic phase is denoted as PM, the ferromagnetic phase is by FM, the spin glass phase is expressed by SG. The Sherrington and Kirkpatrick solution gives the phase boundary between the ferromagnetic and the spin-glass phases denoted by the dashed line. The Parisi solution developed by the concept of the replica symmetry breaking gives the correct answer as denoted a vertical line.

the analysis by the mean-field theory, two types of the order parameters are defined,

$$m_\alpha = [\langle S_i^\alpha \rangle]_{\rm av} \tag{1.6}$$

$$q_{\alpha\beta} = \left[\langle S_i^\alpha S_i^\beta \rangle\right]_{\rm av}, \tag{1.7}$$

where the indices α and β denote different copies in the replica method. Under the replica-symmetry assumption $q_{\alpha\beta} = q$, Sherrington and Kirkpatrick solved the equations of the state and gave indeed a solution with the spin glass state $m = 0$ and $q > 0$. However this Sherrington-Kirkpatrick solution has a problem with negative entropy. Parisi used the concept of the replica symmetry breaking [23, 24, 25], which states that a solution of the equations of the state is given by a matrix of $q_{\alpha\beta}$ with a special structure, solved this problem and he showed the correct phase diagram as in Fig. 1.5.

After then, mainly through analyses by the mean-field theory, many concepts related with the spin glass and other available techniques for analysis of behaviors in the spin glass were proposed and established. (the broken ergodicity [26], and the ultrametricity [27, 28], the TAP equation [29], and the renormalization group analysis [30, 31, 32, 33].)

1.2 Toward Finite Dimensional Spin Glass

The mean-field theory indeed showed the existence of the spin glass phase [14], as well as ferromagnetic and paramagnetic phases as in Fig. 1.5. A natural question is whether such a rich structure of the phase space appears or not in finite-dimensional systems, which expresses more realistic situations. It is in general very difficult to investigate two- and three- dimensional systems by analytical methods. Current studies are predominantly by the numerical methods. Various numerical approaches by the recent development of the computational power have been suggested and elucidated phenomenon in random spin systems. Owing to the effort by such numerical approaches, we have found that the spin glass phase is spread out for finite-temperature region in three-dimensional systems as in Fig. 1.6 [35, 36, 37, 38]. On the other hand, in two-dimensional systems, there is a general consensus that the spin glass phase exists only in the ground state [36, 39, 40, 41, 42].

Though we explained the studies on the spin glass above, in this thesis, our main interest does not lie directly in issues of the properties and the existence of the spin glass phase in finite dimensions. We instead will concentrate ourselves on the precise determination of the structure of phase diagram of finite-dimensional spin glasses. This study is of practical importance for numerical studies since, in numerical simulations or even experiments, the possibility of numerically approaching the critical point and extrapolating to the thermodynamic limit is in general restricted.

This restriction is remarkable for spin glasses, in which there are severe technical difficulties. For instance, there are long equilibration times and necessity of average over many realizations of the random systems to make error bars small enough. These problems make us to study with systems of relatively small size in numerical approaches. Therefore exact values of critical points greatly facilitate reliable estimates of critical exponents in finite-size scaling. In addition, it is not yet clear how reliable the numerical results are. For instance, the estimations of one of the critical exponents, ν, for the three-dimensional $\pm J$ Ising model have significantly changed during the years as summarized in Ref. [43]. Two examples of the recent estimations show deviations as $\nu = 2.72(8)$ [44] and $2.39(5)$ [43]. Such a problem on the reliability of the numerical estimations appears in one of the most challenging current studies on the spin glass. The nature of ordering in spin glass phase for three-dimensional system remains a controversial issue which the droplet theory [45, 46, 47], and the replica symmetry breaking theory [23, 24, 25] introduced above are valid for the description of the spin glass phase. An crucial difference between these theories concerns the estimations of low energy excitations for the large-scale system. To solve the most important issue on the spin glass in the future, the reliability of the numerical simulations is strictly appraised.

In the present contribution, we show a systematic analysis related with the phase diagram on the spin glass, which is also applicable broadly in random spin systems. Unfortunately we cannot give a direct solution on the issue mentioned above on the spin glass, but can contribute to the development of the numerical approaches in terms of setting the benchmarks for their reliability. Very little analytical systematic work exists in the random spin systems, especially for the spin glass. An exception is a symmetry argument using gauge invariance. We have some rigorous results in a limited subspace with the gauge symmetry on the phase diagram, the *Nishimori line*, for several types of the random spin systems [34]. These exact and rigorous results have succeeded in clarifying a part of problems related with the structure of the phase diagram for several random-bond Ising models. One of the possibilities for the establishment of the systematic theory is considered to elucidate the deep meaning of the role of the gauge invariance for the spin glass. In this thesis, several random-bond Ising models with the Nishimori line are analyzed by the further use of a symmetry, the *duality* as explained below and then we establish an analytical systematic approach for the phase transition in the spin glass by the development of the theory using the gauge invariance on the Nishimori line.

We first restrict ourselves to the $\pm J$ Ising model, which is our main platform to establish a new method. First we explain the published results related with the structure of the phase diagram especially in two-dimensional system in the next section.

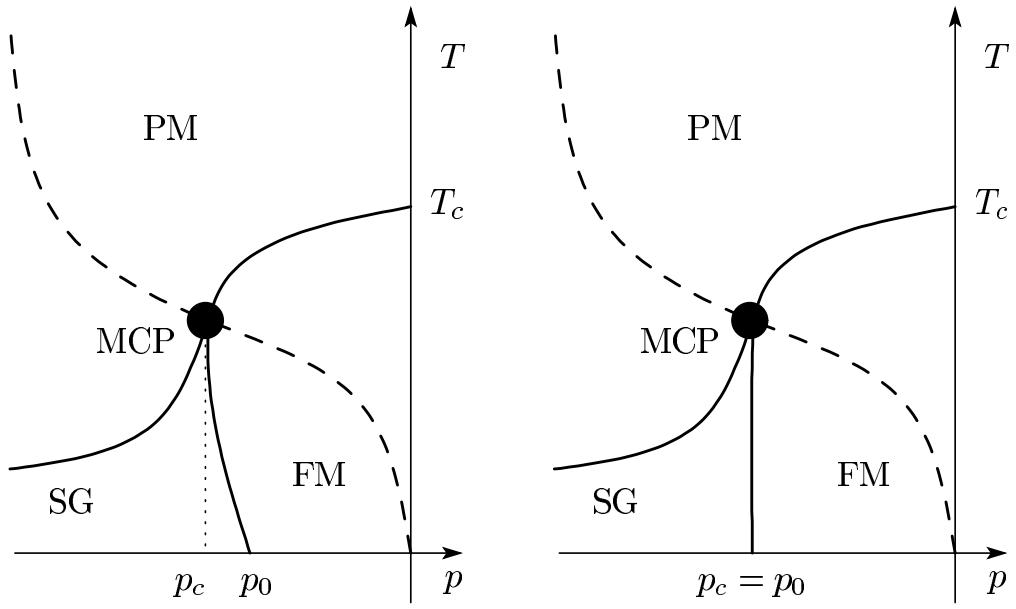

Figure 1.6: Two possible phase diagrams of the $\pm J$ Ising model. The left panel gives the case for $p_c \neq p_0$ (the reentrant scenario). The right one is for $p_c = p_0$ (the vertical scenario). The dashed line stands for the Nishimori line. The point denoted as MCP is the multicritical point.

1.3 Phase Diagram and Multicritical Point

A great number of investigations of the phase diagram of the random-bond Ising model in the two- and three-dimensional systems have been carried out mainly by numerical approaches such as series expansion, transfer matrix, and Monte-Carlo simulation for the finite-temperature region. In addition, some computing algorithms for an optimization problem are applied to the observation of the phase transition in the ground state.

The phase diagram of the $\pm J$ Ising model is restricted to two possible scenarios with the reentrant and vertical phase boundaries as in Fig. 1.6 from the prediction by a correlation inequality with the gauge invariance. The dashed line denotes the special line with the gauge symmetry, namely the Nishimori line [3, 34]. On the Nishimori line, we can obtain the exact internal energy, the upper bound for the specific heat, and several types of correlation inequalities. This is a piece of few exact results for finite-dimensional systems. In addition, the free energy of the $\pm J$ Ising model on the Nishimori line has a relationship with the distribution of frustration

p_c	Value	Method	Size	Year
SQ $\pm J$	0.89(1)	MCRG	64×64	Ozeki, *et. al.* (1987) [52]
SQ $\pm J$	0.889(2)	Transfer Matrix	14×10^5	Ozeki, *et. al.* (1987) [53]
SQ $\pm J$	0.886(3)	Series Expansion	19th order	Singh, *et. al.* (1996) [54]
SQ $\pm J$	0.8872(8)	Non-equilibrium	2501×2500,	Ozeki, *et. al.* (1998) [55]
SQ $\pm J$	0.8905(5)	Transfer Matrix	14×10^8	Aarao Reis, *et. al.* (1999) [56]
SQ $\pm J$	0.8906(2)	Transfer Matrix	12×10^6	Honecker, *et. al.* (2001) [57]
SQ $\pm J$	0.8907(2)	Fermionic TM	$32 \times 2 \times 10^8$	Merz, *et. al.* (2002) [58]
SQ $\pm J$	0.8900(5)	Transfer Matrix	12×10^6	de Queiroz (2003) [59]
SQ $\pm J$	0.8894(9)	Non-equilibrium	10001×10000,	Ito, *et. al.* (2003) [60]
SQ $\pm J$	0.8906(2)	Transfer Matrix	12×10^6	Picco, *et. al.* (2006) [61]
SQ $\pm J$	0.89081(7)	Monte-Carlo	64×64	Hasenbusch, *et. al.* (2008) [62]
Cubic $\pm J$	0.767(4)	MCRG	$32 \times 32 \times 32$	Ozeki, *et. al.* (1987) [52]
Cubic $\pm J$	0.7656(20)	Series Expansion	17th order	Singh (1991) [63]
Cubic $\pm J$	0.7673(3)	Non-equilibrium	$161 \times 161 \times 162$	Ozeki, *et. al.* (1998) [55]
Cubic $\pm J$	0.76820(4)	Monte-Carlo	$80 \times 80 \times 80$	Hasenbusch, *et. al.* (2007) [64]

Table 1.1: The location of the multicritical point p_c for the $\pm J$ Ising model estimated by various approaches. MCRG means the Monte-Carlo renormalization group and TM expresses the transfer matrix.

[48]. The interest of the Nishimori line goes further, since it has been shown that this line is invariant under renormalization [49, 50, 51]. If we see again the phase diagram of Fig. 1.6, we find that the intersection of phase boundaries between three phases is located on the Nishimori line. This is the *multicritical point*. The multicritical point is a nontrivial unstable fixed point from a point of view of the renormalization group [49, 50, 51]. Because of the simple form of the Hamiltonian and distributions of the random couplings J_{ij} of the $\pm J$ Ising model, a number of estimations exist and their results are listed in Table 1.1. It is thus now very adequate time that we construct a new analytic theory related with the phase transition in random spin systems, because we have many references as in Table 1.1, the locations of the multicritical point, for the validity of the theory which will be established in this thesis. In addition, the multicritical point is located on the Nishimori line, on which the gauge invariance and several exact and rigorous results are available. The results on the Nishimori line have played a role of the judgment of the reliability of the numerical methods. Recent development of the computational power and the guidance by the properties of the Nishimori line have given great progress of the numerical methods in the random spin systems. Conversely, in this thesis, we use many results for the location of the multicritical point by the numerical approaches as references of validity of our study. At this time, we have to be attentive to even a small difference between our predictions and numerical estimations.

Nevertheless, unfortunately, the numerical estimations include some conflicts that the multicritical point is expected to be located at about $p_c \approx 0.8900$ [59, 60] or $p_c \approx 0.8908$ [57, 58, 61, 62] on the two-dimensional square lattice. The conflict of $p_c \approx 0.8900$ versus $p_c \approx 0.8908$ without overlap of the error bars is very small but a serious problem on the reliability of each numerical calculation. It is thus worthwhile to establish a technique to derive the location of the multicritical point with the higher precision to the fourth digit than the current numerical estimations to solve this conflict and to provide a new standard reference for the numerical methods in the future.

We should remark that our study is initiated by not only such problems on the reliability of the numerical estimations but also an intrinsic interest in the multicritical point and the physics behind its property. Despite recent analytical approaches by supersymmetry [65], the exact characterization of the universality class of the multicritical point is also still unknown. For accurate analysis of the critical behaviors around the multicritical point and precise estimations of the critical exponents, determination of the location of the multicritical point is essential and important work also in this sense. Further interest in the location of the multicritical point stems from analogies with the quantum Hall transition [65, 66, 67, 68] and applications in coding theory for the classical [69, 70, 71, 72] and quantum [73, 74] information processing.

Let us take a look also at the ground state briefly. As seen in Fig. 1.2, frustration generates unsatisfied bond with the extra energy such as $-J_{ij}S_iS_j = J$. In addition, pair of the plaquettes under frustration arises adjacently to an antiferromagnetic bond. Therefore we have to find the set of minimal-length strings connecting frustrated plaquettes to minimize the whole energy of the $\pm J$ Ising model. Searching the ground state of the $\pm J$ Ising model is one of the classes of the optimization problems. An increase of concentration of the negative sign for J_{ij} of the $\pm J$ Ising model expressed by the value of $1 - p$ destroys ordered state. The location of the critical point in the ground state is expressed as p_0 as in Fig. 1.6. We list the previously published results on the location of p_0 in Table 1.2. The location of such a transition point p_0 is one of the targets of studies on the random-bond Ising model. This is why the ground state of the random-bond Ising model corresponds to one of the classes of optimization problems, which is the Chinese postman's problem and solved by an efficient algorithm [81, 82, 83]. A further interesting reason is to verify the verticality to the p-axis of the phase boundary in the region under the Nishimori line as in Fig. 1.6, which is predicted by an argument from a point of view of the entropy of the distribution of frustration [48], and expected by the result of analysis used by a modified mathematical model from the $\pm J$ Ising model [84]. Therefore we need results with high precision for the locations of the multicritical point p_c and the critical point p_0 in the ground state to judge two possible scenarios of the phase boundary under the Nishimori line.

p_0	Value	Method	Year
SQ $\pm J$	~ 0.901	Series Expansion	Grinstein *et. al.* (1979) [75]
SQ $\pm J$	0.895(1)	Matching Algorithm	Freund *et. al.* (1989) [76]
SQ $\pm J$	$0.892 < p_c < 0.905$	Matching Algorithm	Bendish *et. al.* (1994) [77]
SQ $\pm J$	0.896(1), 0.894(2)	Exact Ground State	Kawashima *et. al.* (1997) [78]
SQ $\pm J$	0.885	Ground State Emulation	Blackman *et. al.* (1998) [79]
SQ $\pm J$	0.8969(1)	Exact Ground State	Wang *et. al.* (2003) [74]
SQ $\pm J$	0.897(1)	Exact Ground State	Amoruso *et. al.* (2004) [80]

Table 1.2: The location of the critical point p_0 in the ground state.

Before closing this section, again we emphasize that the results shown above are by numerical simulations and estimations because, for finite-dimensional system, we have little analytic and systematic approaches. We show a new analytical systematic study, using the duality, to derive the exact, or highly precise, location of the critical points, especially the multicritical point lying on the Nishimori line, of the random-bond Ising model in the present contribution. The additional purpose of this study is to provide the standard reference for the reliability of various numerical approaches, as well as resolution toward the conflict between $p_c \approx 0.8900$ and $p_c \approx 0.8908$. The results obtained in this thesis show indeed the very close coincidence to a part of the current numerical estimations, which are considered to be correct answers, with very high precision.

1.4 Conjecture

In the previous section, we reviewed the published results on the location of the critical points of the $\pm J$ Ising model, especially the multicritical point on the square lattice. We mentioned that our purpose is to derive the location of such critical points in random spin systems.

We deal with the multicritical point mainly by a technique of a symmetry, namely the duality, which has been one of the analytical tools to obtain the exact location of the critical points in non-random spin systems [85, 86]. For the last decade, the conjecture on the location of the multicritical point has been proposed [87, 88]. The conjecture is established by the duality with the replica method and the gauge symmetry on the Nishimori line. The conjecture predicts the location of the multicritical point for the $\pm J$ Ising model on the square lattice as $p_c = 0.889972$ [87, 88]. This prediction is in good agreement with a part of the published results within their error bars as seen in Table 1.1. It was first believed that the conjecture $p_c = 0.889972$ is the exact solution. However, some cases show that the conjecture is outside the accuracy range of numerical results. In addition, there is a more

serious problem on the validity of the conjecture. The conjecture was applied to the multicritical points on hierarchical lattices with nesting units of bonds, on which the renormalization group analysis should be exact [89, 90, 91]. The conjecture derived different answers from the exact results obtained by the renormalization group analysis [92].

It is thus important work to elucidate the reasons why such deviations exist between the conjecture and the exact results on the hierarchical lattices. We should reconsider the validity of the conjecture especially on the hierarchical lattices. This investigation improves the conventional conjecture on the hierarchical lattice and, moreover, gives a possible way to analytically derive the precise locations of the multicritical point for the $\pm J$ Ising model also on the regular lattices such as the square, triangular, hexagonal lattices. Along this line, we propose an analytical technique to derive the location of the multicritical point with precision to the fourth digit and open up a way to obtain an exact solution or a very close estimation to the answer in finite-dimensional random spin systems in this thesis.

1.5 Overview of Thesis

We describe the organization of this thesis below.

In the next chapter, the duality and its applications are detailed. The way how to derive the critical point in non-random spin systems is given as well as the application of the duality; the calculation of the exact value of the internal energy. In this chapter, we also show applications of the duality to other lattices than the square lattice.

In Chapter 3, there are introductive sections for the random-bond Ising model and the replica method. We explain the gauge transformation and review the results obtained on the Nishimori line. The duality for the random-bond Ising model is considered here and several problems are also pointed out.

Chapter 4 is written about the conjecture on the location of the multicritical point. We focus on the duality on the Nishimori line. All of the results previously obtained by the conjecture are shown and compared with the existing results by other approaches. After that, we show the cases on the hierarchical lattices with deviations between the conjecture and the exact answers by the renormalization group analysis.

Chapter 5 is one of the most important parts of this thesis. The improved conjecture for the hierarchical lattices is considered in this chapter. The idea for improvement is inspired by the renormalization group analysis on the hierarchical lattices. We show that the obtained locations of the multicritical points by the improved version of the conjecture are in better agreement with the exact results by the renormalization group analysis than those by the conventional conjecture. The

improvement influences the duality in other regions as well as the Nishimori line. The slope of the critical point on the phase diagram is estimated and is closer to the exact solution than the conventional conjecture, which has failed to derive a precise slope.

In Chapter 6, we establish the improved conjecture as a reliable tool to derive the precise location of the multicritical points on the regular lattice. We can gradually increase the accuracy of the predictions by a systematic way. Therefore, if we estimate the location of the multicritical point by the systematic way, the predicted locations of the multicritical points converge on some point, which is expected to be the exact solution. We show that this improvement is also successful in several regions as well as the Nishimori line, and other random spin systems than the spin-glass models.

In the last chapter, we summarize our results and the properties of the improved conjecture.

Chapter 2

Duality Transformation

Our goal in this thesis is to derive the critical points in random spin systems. One of the useful tools to obtain the exact location of the critical point is the duality. This technique has been applied to spin models without randomness. The duality for the random spin systems has been also considered. One of the applications of the duality for the random spin systems is the conjecture on the location of the multicritical point in the random spin systems as discussed in Chapter 4. Before going into the application to the random spin systems, we review detailed formulations and roles of the duality in this chapter.

2.1 Symmetry of Partition Functions

We first remark what we can derive from the duality before the detailed calculation. The duality is very useful especially in spin systems defined on two-dimensional lattice to analyze the location of the critical points. Additional applications are the derivation of the exact value of the internal energy and the restriction of the behavior of the specific heat by the duality.

Originally the duality was proposed by the symmetry found between the high-temperature and low-temperature expansion of the partition function of the non-random Ising model on the square lattice [85]. Let us first take a look at the explicit form of the high-temperature expansion of the Ising model. The Hamiltonian of the non-random Ising model is defined as,

$$H = -\sum_{\langle ij \rangle} J S_i S_j, \tag{2.1}$$

where S_i takes integers ± 1, and J denotes the uniform interaction between two spins. The summation is taken over the nearest neighboring pairs of spins. The

partition function is given as,

$$Z(K) = \sum_{\{S_i\}} \prod_{\langle ij \rangle} \mathrm{e}^{K S_i S_j}. \tag{2.2}$$

Here we use the coupling constant K defined by $K = \beta J$ for simplicity. We use an identity to consider the high-temperature expansion,

$$\mathrm{e}^{K S_i S_j} = \cosh K + S_i S_j \sinh K. \tag{2.3}$$

Using this identity, we step to establish the high-temperature expansion ($\tanh K \ll 1$) as follows,

$$Z(K) = (\cosh K)^{N_B} \sum_{S_i} \left(1 + \sum_{m=1}^{N_B} \tanh^m K \sum_{m \text{ bonds}} \prod_{m \text{ pair}} S_i S_j \right). \tag{2.4}$$

Here the summation with the subscript "m bonds" is over the any configurations with m bonds and the product is over m pairs of $S_i S_j$. The quantity N_B denotes the number of the bonds. However the terms without constructing closed path vanish after the summation over $\{S_i\}$, because of the property that $\sum_{S_i} S_i = 0$ as shown in Fig. 2.1. Therefore we obtain the following expression of the high-temperature expansion, as a result,

$$Z(K) = 2^{N_s} (\cosh K)^{N_B} \sum_{C} \tanh^m K, \tag{2.5}$$

where N_s is the number of the sites, C denotes the summation over the closed paths and m expresses the length of each closed path. The minimum length of the closed path is $m = 4$ and forms the elementary square. The number of such closed path is N_s.

On the other hand, the low temperature expansion ($\mathrm{e}^{-2K} \ll 1$) is given as, by consideration of contributions by flipped spins from the ground state as in Fig. 2.2,

$$Z(K) = 2\mathrm{e}^{N_B K} \left(1 + N_s \mathrm{e}^{-8K} + \cdots \right), \tag{2.6}$$

where $2\mathrm{e}^{N_B K}$ corresponds to the partition function for the ground state. The term e^{-8K} arises from the contribution of 4 bonds surrounding one flipped spin and we can find N_s terms. which are similar to the closed paths.

If we compare two symmetric expansions, we find the correspondence between closed paths around the plaquettes and bonds around flipped spins at sites. In addition, we prepare two partition functions $Z(K^*)$ and $Z(K)$ in low and high-temperature regions, respectively. The low-temperature expansion for $Z(K^*)$ and

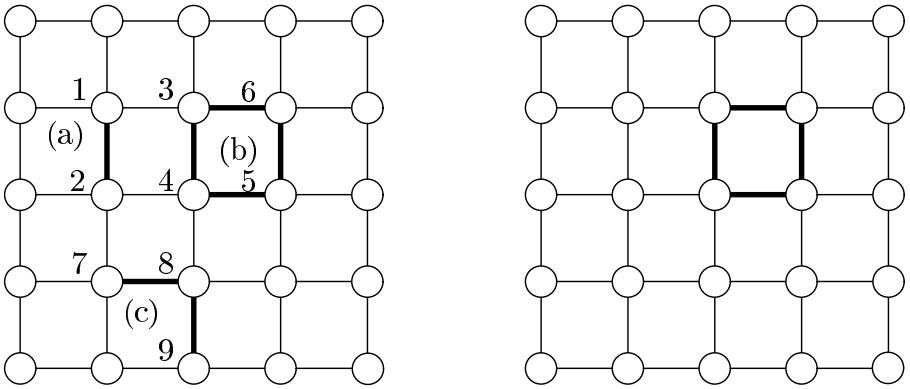

Figure 2.1: The high-temperature expansion. Each cluster of the bold bonds denotes the example of the configuration appearing in Eq. (2.4). After the summation over spin variables $\{S_i\}$, we obtain the following terms (a) $\sum_{\{S_i\}} S_1 S_2 = 0$, (b) $\sum_{\{S_i\}} (S_3 S_4)(S_4 S_5)(S_5 S_6)(S_6 S_3) = 2^{N_s}$, and (c) $\sum_{\{S_i\}} (S_7 S_8)(S_8 S_9) = 0$. Therefore the high-temperature expansion corresponds to the collection of the contributions of the possible closed paths on the square lattice as in the right panel.

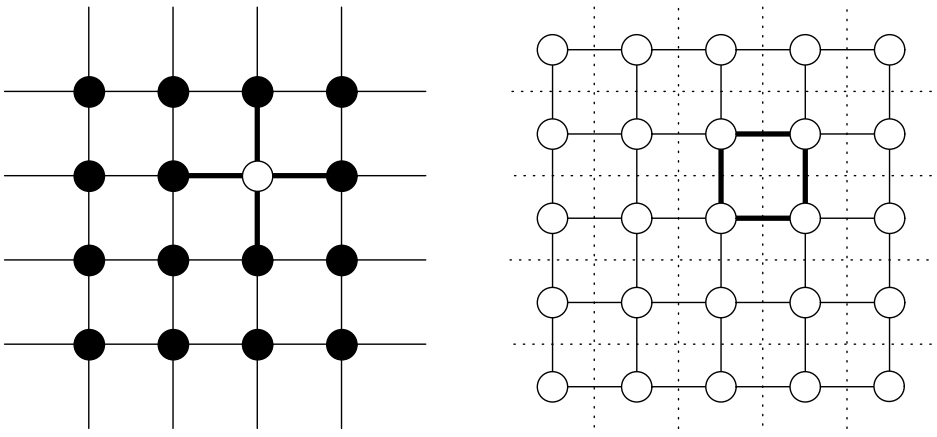

Figure 2.2: The low-temperature expansion. The filled circles are up-pointing spins, and the white site denotes flipped spin from the ground state. The bold bonds express the excited bonds with the contribution e^{-2K}. Such a contribution is described as a closed path on another lattice as in the right panel.

the high-temperature expansions for $Z(K)$ establish the relationship between two different couplings,

$$\mathrm{e}^{-2K^*} = \tanh K. \tag{2.7}$$

Using this relation, we can construct an equation,

$$Z(K) = \frac{2^{N_s}(\cosh K)^{N_B}}{2\mathrm{e}^{N_B K^*}} Z(K^*). \tag{2.8}$$

Therefore we can find a relationship between the low-temperature partition function defined on the original square lattice and the high-temperature partition function defined on another square lattice. We can identify two square lattices especially in the thermodynamic limit ($N_s \to \infty$), though they are different from a strict observation. We use this symmetric property, the *duality*, of the spin systems in the following discussions.

However it is slightly inconvenient to apply the duality, the relationship between the low and high-temperature expansions, to other types of spin models and different forms of the lattices. In the next section, we introduce a general formulation of the duality for such applications by use of the Fourier transformation [86].

2.2 General Formulation of Duality

We restrict ourselves to the application of the duality for two-dimensional spin systems. The duality gives a relationship between two different non-random spin systems, in terms of partition functions and structure of lattices. We express the transformation of the lattice in Fig. 2.3. The general manner of change of the lattice is interchange between sites of the original lattice (black colored sites) and plaquettes of another lattice and conversely, as seen in the previous section. The black colored sites are the ones on the original lattice, which correspond to the plaquettes on another lattice, and the white-colored sites are the ones on another lattice, which are originally located at the plaquettes of the original lattice. We sometimes obtain the same form of a lattice as the one before the application of the duality. Such a lattice is called the *self-dual* lattice. For example, the square lattice is one of the self-dual lattices as in Fig. 2.3. The triangular lattice is not self-dual and related with the hexagonal lattice as in Fig. 2.3. Such pair of the lattices is called the *mutually dual pair*.

Another transformation by the duality is for partition functions as,

$$Z(K) = \Lambda Z^*_{\mathrm{D}}(K), \tag{2.9}$$

where $Z(K)$ is the partition function with a coupling constant K for the original spin system defined on the original lattice as the top figures in Fig. 2.3, and Z^*_{D} is

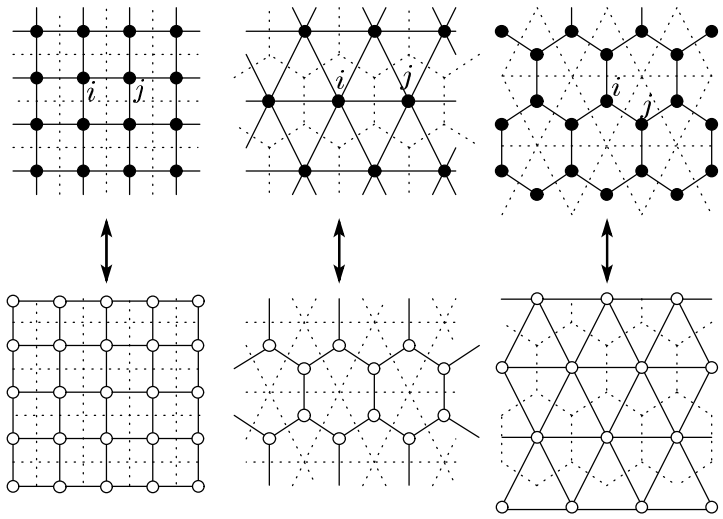

Figure 2.3: The top figures are the original lattices. The left figure is the square lattice, the middle one is the triangular lattice, and the right one is the hexagonal lattice. The bottom figures are the dual lattices.

that for another spin system defined on another lattice as the bottom figures in Fig. 2.3. The subscript "D" on the right-hand side expresses that the form of the lattice is different from the original system, and the asterisk means that the functional form of the partition function on the right-hand side is different from the original one. As seen in the previous section, the low-temperature partition function of the Ising model on the square lattice corresponds to the high-temperature one. However we cannot always find such a simple correspondence between two partition functions before and after the duality. The coefficient Λ is an important factor to derive the critical point as detailed in the following section.

In the case for the self-dual lattices as the square lattice, the relation is reduced to $Z^*_{\rm D}(K) = Z^*(K)$. We can derive the exact location of the critical point for systems by the duality, when the partition function is written by a single-variable function. In other words, the resulting partition function after the duality has the same dependence on the coupling constant, or equivalently the temperature, as the original partition function. Then we can establish the following relation,

$$Z^*(K) = Z(K^*), \tag{2.10}$$

where K^* stands for another coupling constant. Consequently, the relationship in

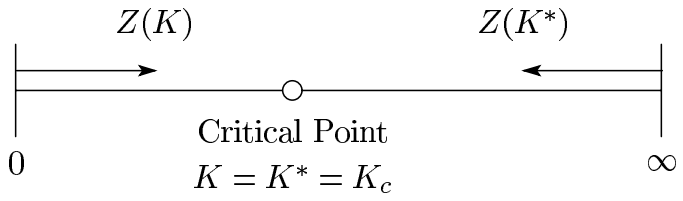

Figure 2.4: The schematic relationship between K and K^*.

Eq. (2.9) can be written as,

$$Z(K) = \Lambda Z(K^*). \tag{2.11}$$

This is called the *duality relation*. Detailed calculations for several examples are given in following sections. Now we show the useful properties for analysis of spin systems obtained from the duality relation (2.11).

2.2.1 Critical Point

If the system under consideration has a unique critical point, the duality relation (2.11) can give the exact location of the critical point. The duality relation (2.11) establishes the relationship between the two values of the coupling constants as $K^*(K)$. When monotone decrease of K^* for the increase of K is satisfied, (e.g. $K^* \to 0$ for $K \to \infty$) the duality relation gives a connection between the partition functions in high and low-temperature regions for the spin model under consideration as in Fig. 2.4. We can then find the fixed point as the boundary between the low and high-temperature region, which gives the location of the critical point as,

$$K = K^* \equiv K_c. \tag{2.12}$$

Then the coefficient Λ of the duality relation for the partition functions as in Eq. (2.11), becomes unity. This is a special feature of the duality relation for the partition functions (2.11) only at the fixed point of the duality, which is used throughout this thesis.

2.2.2 Exact Value of Internal Energy

The internal energy is given by the derivative of the free energy. If we find the duality relation in terms of the partition function as in Eq. (2.11), we obtain the

following equation by taking a logarithmic derivative of the duality relation as,

$$\frac{d}{dK}\log Z(K)\bigg|_{K} = \frac{1}{\Lambda}\frac{d\Lambda}{dK} + \frac{d}{dK}\log Z(K)\bigg|_{K^*}\frac{dK^*}{dK}. \tag{2.13}$$

This equation gives a relation between the internal energies at different temperatures corresponding to K and K^*. Setting $K = K^* = K_c$, we predict the exact value of the internal energy at the critical point by Eq. (2.13) as follows, if the internal energy is continuous,

$$E(K_c) = -\frac{d}{dK}\log Z(K)\bigg|_{K_c} = -\left(1 - \frac{dK^*}{dK}\bigg|_{K_c}\right)^{-1}\frac{d\Lambda}{dK}\bigg|_{K_c}, \tag{2.14}$$

where we used the identity $\Lambda = 1$ at the critical point.

2.2.3 Specific Heat

We can infer the behavior of the specific heat at the critical point by the duality relation (2.11), that is whether it is continuous or not. We obtain the relation of two specific heats by the derivative of the free energy, similarly to the internal energy. The derivative by K of Eq. (2.13) gives

$$-T^2C(K) = \frac{1}{\Lambda^2}\left(\frac{d\Lambda}{dK}\right)^2 - \frac{1}{\Lambda}\frac{d^2\Lambda}{dK^2} - T^{*2}C(K^*) + E(K^*)\frac{d^2K^*}{dK^2}, \tag{2.15}$$

Therefore, near the critical point expressed by $K = K_c + \delta$ and $K^* = K_c - \delta$, the difference between the specific heat in low and high-temperature regions is given by

$$\begin{aligned} &-T^2\left\{C(K_c+\delta) - C(K_c-\delta)\right\} \\ &\quad= \left(\frac{d\Lambda}{dK}\bigg|_{K_c}\right)^2 - \frac{d^2\Lambda}{dK^2}\bigg|_{K_c} - \left(1 - \frac{dK^*}{dK}\bigg|_{K_c}\right)^{-1}\frac{d\Lambda}{dK}\bigg|_{K_c}\frac{d^2K^*}{dK^2}\bigg|_{K_c}. \end{aligned} \tag{2.16}$$

The specific heat will be divergent near the critical point or will be continuous through the critical point when all the terms on the right-hand side vanish. On the other hand, the specific heat will be discontinuous if the right-hand side gives non-zero value.

We show several detailed calculations to obtain the duality relation and demonstrate the above introduced applications in the following sections.

2.3 Duality on the Square Lattice

We give several examples of calculations of the duality on the square lattice here. The Ising model and the Potts model on the square lattice are considered.

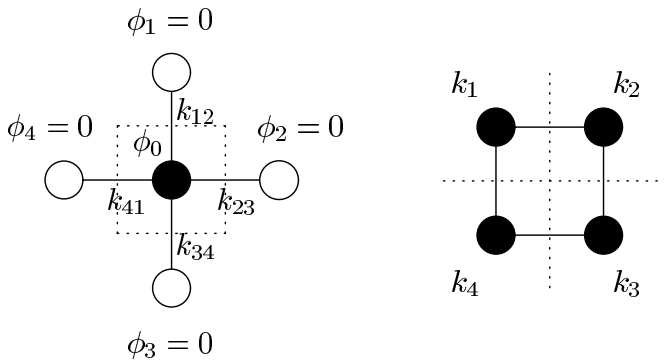

Figure 2.5: The duality for the simple four bonds. The filled circles express the summed spins in the evaluation of the partition function.

2.3.1 Simple Lattice

Let us consider the duality to a simple lattice as in Fig. 2.5, before going into the case of the square lattice. We can find a significant feature of the duality through this simple lesson. We consider a q-component spin system as well as the Ising model ($q = 2$) for general applications of the duality to other spin systems. The partition function for spin systems only with nearest neighboring interactions is given as,

$$Z = \sum_{\{\phi_i\}} \prod_{\langle ij \rangle} x(\phi_i - \phi_j), \tag{2.17}$$

where $\{\phi_i\}$ denotes the summation over all the spin variables between 0 and $q-1$, and the product runs over all the bonds on the lattice. The quantity x is called the edge Boltzmann factor. This edge Boltzmann factor has q elements denoted as $x(0), x(1), \cdots, x(q-1)$, and depends on the difference between neighboring spins. In addition, we assume that this q-component spin system has the edge Boltzmann factor with a period q, that is the so-called Z_q model. For example, the non-random Ising model, the Hamiltonian is usually written as in Eq. (2.1). We here use another expression for convenience as follows,

$$H = -J \sum_{\langle ij \rangle} \cos \pi \phi_{ij}, \tag{2.18}$$

where $\phi_{ij} \equiv \phi_i - \phi_j$, the spin variable ϕ_i takes the integer of 0 and 1. Therefore $\pi\phi_{ij}$ denotes the difference of the angle between the neighboring spins. We take the difference of spins ϕ_{ij} from top to bottom $\phi_{10} = \phi_1 - \phi_0$ and $\phi_{03} = \phi_0 - \phi_3$, and

from left to right $\phi_{40} = \phi_4 - \phi_0$ and $\phi_{02} = \phi_0 - \phi_2$ in Fig. 2.5. Then the partition function is written as,

$$Z = \sum_{\{\phi_i\}} \prod_{\langle ij \rangle} \mathrm{e}^{K \cos \pi \phi_{ij}}, \tag{2.19}$$

where we use again here the coupling constant K which is the product βJ. The edge Boltzmann factor for the Ising model is,

$$x_K(\phi_{ij}) = \exp\left\{K \cos\left(\pi \phi_{ij}\right)\right\}. \tag{2.20}$$

We regard the partition function as a multi-variable function of the set of the values of the edge Boltzmann factor. We express this fact by the angular brackets as $Z[\cdot]$ in this thesis for simplicity. In addition, for the Potts model, the Hamiltonian is defined as

$$H = -J \sum_{\langle ij \rangle} \delta(\phi_{ij}), \tag{2.21}$$

where ϕ_{ij} also expresses the difference of orientation between the neighboring spins, which takes the integer from 0 to $q-1$. we can obtain the edge Boltzmann factor, from e^K for parallel state and 1 for the others,

$$x_K(\phi_{ij}) = \exp\left\{K \delta\left(\phi_{ij}\right)\right\}, \tag{2.22}$$

We define the dual Boltzmann factor as, by the Fourier transformation,

$$x^*(k_{ij}) = \frac{1}{\sqrt{q}} \sum_{\phi_{ij}=0}^{q-1} x(\phi_{ij}) \exp\left(\mathrm{i} \frac{2\pi}{q} k_{ij} \phi_{ij}\right), \tag{2.23}$$

and, as the inverse transformation,

$$x(\phi_{ij}) = \frac{1}{\sqrt{q}} \sum_{k_{ij}=0}^{q-1} x^*(k_{ij}) \exp\left(\mathrm{i} \frac{2\pi}{q} k_{ij} \phi_{ij}\right), \tag{2.24}$$

where we omit the subscript K because of the absence of confusion.

We write the partition function for a system with four bonds and spins on four sites up $\{\phi_i = 0\}$ as in Fig. 2.5,

$$Z[x] = \sum_{\phi_0=0}^{q-1} x^4(\phi_0), \tag{2.25}$$

where x is the edge Boltzmann factor for a single bond. We here use the form of the Fourier transformation of the edge Boltzmann factor (2.24) and substitute it into the above relation,

$$Z[x] = \left(\frac{1}{\sqrt{q}}\right)^4 \sum_{\{k_{ij}\}} x^*(k_{12})x^*(k_{23})x^*(k_{34})x^*(k_{41}) \sum_{\phi_0=0}^{q-1} \exp\left\{ \mathrm{i}\frac{2\pi}{q}(k_{12}+k_{23}+k_{31}+k_{41})\phi_0 \right\}. \tag{2.26}$$

The summation over the site variables ϕ_0 gives the Kronecker's delta,

$$Z[x] = q\left(\frac{1}{\sqrt{q}}\right)^4 \sum_{\{k_{ij}\}} x^*(k_{12})x^*(k_{23})x^*(k_{34})x^*(k_{41})\delta\left(k_{12}+k_{23}+k_{31}+k_{41}\right). \tag{2.27}$$

Therefore the partition function is transformed into the summation over bond variables k_{ij} with restrictions by the Kronecker's delta with modulus q. We introduce new variables $\{k_i\}$, which satisfy the constraint by the Kronecker's delta,

$$k_{12} = k_1 - k_2, \quad k_{23} = k_2 - k_3, \quad k_{31} = k_3 - k_1, \quad k_{41} = k_4 - k_1. \tag{2.28}$$

One notices that the contribution to the partition function is invariant if we shift these variables $\{k_i\}$ to $\{k_i + u\}$ by an integer u from 0 to $q-1$. We should remove this arbitrariness by dividing the partition function by q. We then find that the partition function is transformed into the one with the dual edge Boltzmann factor x^* and dual site variables $\{k_i\}$,

$$Z[x] \;=\; \frac{1}{q}\, q\left(\frac{1}{\sqrt{q}}\right)^4 \sum_{\{k_i\}} x^*(k_1-k_2)x^*(k_2-k_3)x^*(k_3-k_4)x^*(k_4-k_1).$$

We emphasize the following features found in this relation, The factor $1/q$ on the right-hand side is by arbitrariness of the dual site variables $\{k_i\}$. The next factor q is obtained by the summation over the spin variable ϕ_0 on the original site, whose exponent is given by the site number $N_s = 1$. In addition, $\left(1/\sqrt{q}\right)^4$ is given as the factors by the Fourier transformation for the edge Boltzmann factors. The number 4 stems from the number of the bonds $N_B = 4$ on the original lattice as in Fig. 2.5. As the most important fact, we look at the product over four dual edge Boltzmann factors around the original site. Their arguments express that the dual system consists of four bonds and four sites connected with each other as in Fig. 2.5. We thus find that the form of the lattice is changed from the left-hand side figure to the right-hand side one in Fig. 2.5, and the duality transforms the original edge Boltzmann factor x into the dual one x^*. The changes of the lattice are regarded as the interchanges between the original sites and the dual plaquettes and between

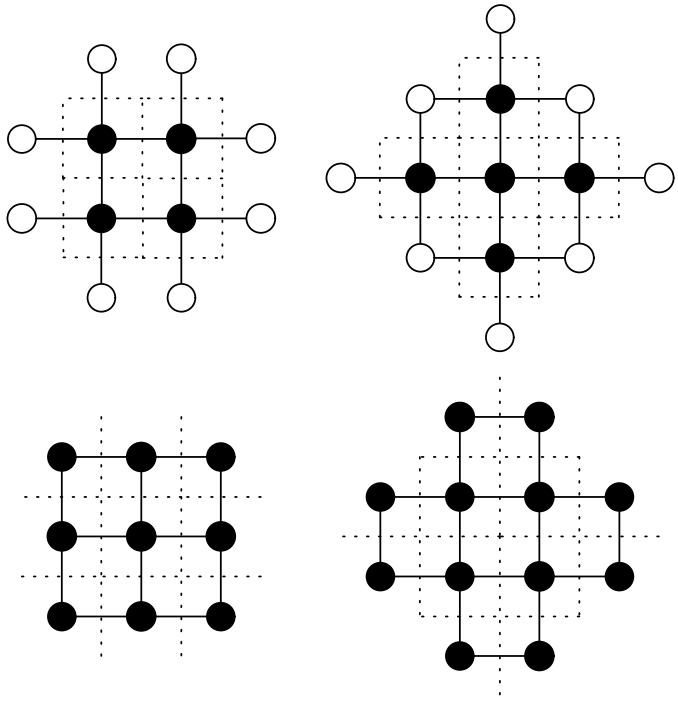

Figure 2.6: Two examples of the duality. The top figures express the original lattices and the bottom figures are their dual systems. The filled sites are the target of the summation, while white ones are fixed in up directions.

the original plaquettes and the dual sites. In addition, the orientations of the bonds rotate 90 degrees. These properties of the duality found in all the lattices [86]. We show two further examples describing the change of the lattice in Fig. 2.6.

We expect that the duality for a general lattice gives a relation as, by the features explained above,

$$Z[x] = q^{N_s - \frac{N_B}{2} - 1} Z_{\mathrm{D}}[x^*], \tag{2.29}$$

where D expresses the lattice in a different form from the original lattice.

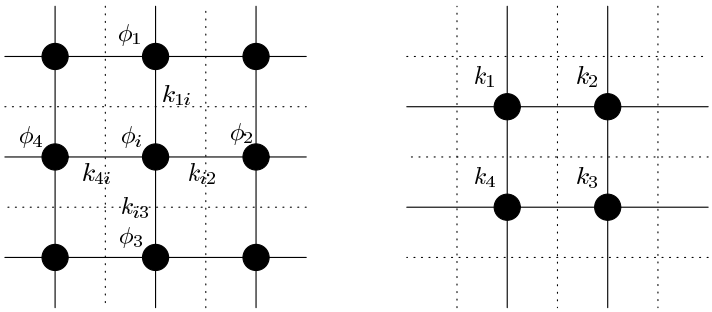

Figure 2.7: The sites and plaquettes on the square lattice.

2.3.2 Square Lattice

We write the partition function for a system defined on the square lattice as,

$$Z[x] = \sum_{\{\phi_i\}} \prod_{\langle ij \rangle}^{\text{square}} x(\phi_i - \phi_j). \tag{2.30}$$

Substituting the form of the Fourier transformation of the edge Boltzmann factor (2.24) into the partition function, we can rewrite Eq. (2.30) as,

$$Z[x] = \left(\frac{1}{\sqrt{q}}\right)^{N_B} \sum_{\{k_{ij}\}} \prod_{\langle ij \rangle}^{\text{square}} x^*(k_{ij}) \sum_{\{\phi_i\}} \prod_{\langle ij \rangle}^{\text{square}} \exp\left\{ \mathrm{i}\frac{2\pi}{q} k_{ij}(\phi_i - \phi_j) \right\}. \tag{2.31}$$

Here we consider the product of the exponential terms over all the bonds on the right-hand side, similarly to the case of the simple lattice. As in Fig. 2.7, we consider the adjacent four bonds to the site ϕ_i, and take the summation over this site variable as follows,

$$\begin{aligned} &\sum_{\{\phi_i\}} \prod_{\langle ij \rangle}^{\text{square}} \exp\left\{ \mathrm{i}\frac{2\pi}{q} k_{ij}(\phi_i - \phi_j) \right\} \\ &= \sum_{\phi_i} \prod_i \exp\left\{ \mathrm{i}\frac{2\pi}{q}(-k_{1i} + k_{i2} + k_{i3} - k_{4i})\phi_i \right\} = q^{N_s} \prod_i \delta\left(-k_{1i} + k_{i2} + k_{i3} - k_{4i}\right), \end{aligned} \tag{2.32}$$

The partition function can be regarded as the summation over bond variables k_{ij} with restrictions by the Kronecker's delta with modulus q as in Eq. (2.27). We introduce again new variables $\{k_i\}$, similarly to the simple case,

$$k_{1i} = k_1 - k_2, \quad k_{i2} = -(k_2 - k_3), \quad k_{i3} = -(k_3 - k_4), \quad k_{4i} = k_4 - k_1, \tag{2.33}$$

These variables satisfy the constraints expressed by the Kronecker's delta in Eq. (2.32). As a result, we obtain a relation with another partition function with the dual edge Boltzmann factor x^*,

$$\begin{aligned} Z[x] &= q^{N_s-\frac{N_B}{2}-1}\sum_{\{k_i\}}\prod_{\langle ij\rangle}^{\text{square(D)}} x^*(k_i-k_j) \\ &= q^{N_s-\frac{N_B}{2}-1}Z_{\rm D}[x^*], \end{aligned} \tag{2.34}$$

where "square(D)" denotes that the product of the dual edge Boltzmann factors is over the bonds on the square lattice only with the different boundary condition as considered above as in Figs. 2.5 and 2.6. The subscript D of the partition function also expresses such a difference of the lattice. Here N_s and N_B in the exponent of the power expresses the number of the sites and bonds, respectively, and -1 stem from the removal of the arbitrariness of $\{k_i\}$, similarly to the simple lattice. If we consider the thermodynamic limit of $N_s \to \infty$, the exponent of -1 is negligible. In addition, the difference of the boundary conditions of two square lattices can also be ignored. We can identify Z with $Z_{\rm D}$.

The duality relation (2.34) for the square lattice is thus reduced to, because $N_B = 2N_s$,

$$Z[x] = Z[x^*]. \tag{2.35}$$

2.3.3 Ising Model

We consider the Ising model as an explicit example of the duality. The edge Boltzmann factor is given by Eq. (2.20). The dual Boltzmann factor is, as calculated by Eq. (2.23),

$$x_K^*(k_{ij}) = \frac{1}{\sqrt{2}}\left(\mathrm{e}^K + \mathrm{e}^{-K}\cos\pi k_{ij}\right). \tag{2.36}$$

We introduce the principal Boltzmann factor written as $x_0(K)$, which is defined as the edge Boltzmann factor of the state with edge spins parallel $\phi_{ij} = 0$. In the case of the Ising model, $x_0(K) = \mathrm{e}^K$ from Eq. (2.20) and $x_0^*(K) = (\mathrm{e}^K + \mathrm{e}^{-K})/\sqrt{2}$ from Eq. (2.36). We extract these principal Boltzmann factors from the partition fuction to measure the energy from the state with $\phi_{ij} = 0$ by dividing each edge Boltzmann factor x_K by $x_0(K)$, as follows,

$$x_0(K)^{N_B} z\left[\frac{x_K}{x_0(K)}\right] = x_0^*(K)^{N_B} z\left[\frac{x_K^*}{x_0^*(K)}\right], \tag{2.37}$$

where z is the normalized partition function. Considering arguments of two normalized partition functions, we find an important relationship for deriving the location of the critical point.

$$z\left[\frac{x_K}{x_0(K)}\right] = z\left(1, \mathrm{e}^{-2K}\right) \tag{2.38}$$

$$z\left[\frac{x^*_K}{x^*_0(K)}\right] = z\left(1, \tanh K\right). \tag{2.39}$$

Only the arguments $x_K(1)/x_0(K) = \mathrm{e}^{-2K}$ and $x^*_K(1)/x^*_0(K) = \tanh K$ are different between both normalized partition functions. If we use another coupling K^* satisfying $\mathrm{e}^{-2K^*} = \tanh K$, the duality relation (2.37) yields the relationship between the two Ising models with different couplings as

$$\begin{aligned} x_0(K)^{N_B} z(1, \mathrm{e}^{-2K}) &= x^*_0(K)^{N_B} z(1, \mathrm{e}^{-2K^*}) \\ \Longleftrightarrow\ Z[x_K] &= \left\{\frac{x^*_0(K)}{x_0(K^*)}\right\}^{N_B} x_0(K^*)^{N_B} z(1, \mathrm{e}^{-2K^*}) \\ \Longleftrightarrow\ Z[x_K] &= \left\{\frac{x^*_0(K)}{x_0(K^*)}\right\}^{N_B} Z[x_{K^*}], \end{aligned} \tag{2.40}$$

where we multiply the normalized partition function by the principal Boltzmann factor $x_0(K)$ on the left-hand side in the second line and put the principal term $x_0(K^*)$ with another coupling K^* back the partition function on the right-hand side in the last line. The extra coefficient Λ in this relation is explicitly rewritten as,

$$\Lambda = \left\{\frac{x^*_0(K)}{x_0(K^*)}\right\}^{N_B} = (\sinh 2K)^{\frac{N_B}{2}}. \tag{2.41}$$

In addition, the relation $\mathrm{e}^{-2K^*} = \tanh K$ shows a monotone decrease of K^* for increase of K. We also find that $K \to 0$ for $K^* \to \infty$, and inversely $K \to \infty$ for $K^* \to 0$ are satisfied. Therefore we can interpret that the relation $\mathrm{e}^{-2K^*} = \tanh K$ gives a connection between the two partition functions in high and low-temperatures as shown in Eq. (2.8). As a result, we can predict the critical point as $\mathrm{e}^{-2K_c} = \sqrt{2} - 1 = 0.414214$, or equivalently $T_c = 2.26919$ from the fixed point of the duality $\mathrm{e}^{-2K_c} = \tanh K_c$. We can also confirm the fact that Λ becomes unity by substituting K_c into Eq. (2.41).

The exact value of the internal energy at the critical point is also obtained as $-\sqrt{2}N_s$ from Eq. (2.14). Moreover the specific heat is considered to be continuous or divergent at the critical point by the vanishment of the right-hand side of Eq. (2.16) at $K = K_c$. These predictions by the duality are consistent with the exact solutions [93, 94].

2.3.4 Potts Model

For the Potts model, the edge Boltzmann factor is defined as in Eq. (2.22), and the dual Boltzmann factor is given as,

$$x_K^*(k_{ij}) = \frac{1}{\sqrt{q}} \left\{ \mathrm{e}^K - 1 + q\delta\left(k_{ij}\right) \right\}. \tag{2.42}$$

Similarly to the case of the Ising model, we consider the relation (2.37) of two normalized partition functions by the principal Boltzmann factors. Only the arguments $x_K(1)/x_0(K) = x_K(2)/x_0(K) = \cdots = x_K(q-1)/x_0(K) = \mathrm{e}^{-K}$ and $x_K^*(1)/x_0^*(K) = x_K^*(2)/x_0^*(K) = \cdots = x_K^*(q-1)/x_0^*(K) = (\mathrm{e}^K - 1)/(\mathrm{e}^K + q - 1)$ are different between the two normalized partition functions in the duality relation for the Potts model as,

$$z\left[\frac{x_K}{x_0(K)}\right] = z\left(1, \mathrm{e}^{-K}, \cdots, \mathrm{e}^{-K}\right) \tag{2.43}$$

$$z\left[\frac{x_K^*}{x_0^*(K)}\right] = z\left(1, \frac{\mathrm{e}^K - 1}{\mathrm{e}^K + q - 1}, \cdots, \frac{\mathrm{e}^K - 1}{\mathrm{e}^K + q - 1}\right). \tag{2.44}$$

If we introduce the dual coupling satisfying the relation given by

$$\mathrm{e}^{-K^*} = \frac{\mathrm{e}^K - 1}{\mathrm{e}^K + q - 1}. \tag{2.45}$$

we can obtain a similar relationship between two Potts models with different couplings K and K^* to the one as in Eq. (2.40). The extra coefficient Λ differs from the case of the Ising model and is calculated as, from $x_0(K^*) = \mathrm{e}^{K^*}$ and $x_0^*(K) = (\mathrm{e}^K + q - 1)/\sqrt{q}$,

$$\Lambda = \left\{ \frac{x_0^*(K)}{x_0(K^*)} \right\}^{N_B} = \left(\frac{\mathrm{e}^K - 1}{\sqrt{q}} \right)^{N_B}. \tag{2.46}$$

This extra coefficient becomes unity at the critical point given as, by setting $K = K^* = K_c$

$$\mathrm{e}^{K_c} = \sqrt{q} + 1. \tag{2.47}$$

The internal energy is computed as $E(K_c) = -N_s(1 + 1/\sqrt{q})$. For the Potts model with the state number $q \leq 4$, this value indeed gives the exact value of the internal energy [95]. On the other hand, the Potts model with $q > 4$ undergoes a different phase transition, the first-order transition, with discontinuity of the internal energy,

that is $E(K_c - \delta) \neq E(K_c + \delta)$ for infinitesimal δ [95]. We use a modified relation of Eq. (2.14) given as, for such cases,

$$E(K_c + \delta) - \left.\frac{dK^*}{dK}\right|_{K_c} E(K_c - \delta) = - \left.\frac{d\Lambda}{dK}\right|_{K_c}. \tag{2.48}$$

Fortunately the value of $dK^*/dK|_{K=K_c}$ becomes -1 at the transition point. Therefore we can obtain the value of the average between two internal energies in the lower and higher-temperature regions of the transition point. The value of the average for the Potts model with $q > 4$ is,

$$E_{\mathbf{av}}(K_c) = N_s(1 + 1/\sqrt{q}). \tag{2.49}$$

This result coincides with the exact solution [95].

2.4 Duality on the Triangular Lattice

The duality is also applicable to the triangular lattice similarly to the case of the square lattice and the resulting duality relation of the partition functions is again given by Eq. (2.34). However the dual lattice is different from the original one. The dual lattice for the triangular lattice is the hexagonal lattice as in Fig. 2.3. Therefore we cannot establish a relationship between two partition functions on the same triangular lattice. We use another technique with the duality to give a direct transformation from the triangular lattice into another triangular lattice [95]. Let us describe this transformation below and its application.

2.4.1 Simple Triangle

First we explain another technique to relate two partition functions defined on the triangular lattice through the consideration on a single down-pointing triangle as in Fig. 2.8. We consider the partition function for this system with three bonds and three sites,

$$Z_{\rm TR}[x] = \sum_{\{\phi_i\}} x(\phi_1 - \phi_2)x(\phi_2 - \phi_3)x(\phi_3 - \phi_1). \tag{2.50}$$

We find that the sum of the arguments, $\phi_1 - \phi_2$, $\phi_2 - \phi_3$ and $\phi_3 - \phi_1$, in three edge Boltzmann factors equals to zero. We can hence rewrite this partition function as, using the new variables $\{\phi_{ij}\}$ taking values from 0 to $q - 1$ and Kronecker's delta,

$$Z_{\rm TR}[x] = q \sum_{\{\phi_{ij}\}} x(\phi_{12})x(\phi_{23})x(\phi_{31})\delta(\phi_{12} + \phi_{23} + \phi_{31}), \tag{2.51}$$

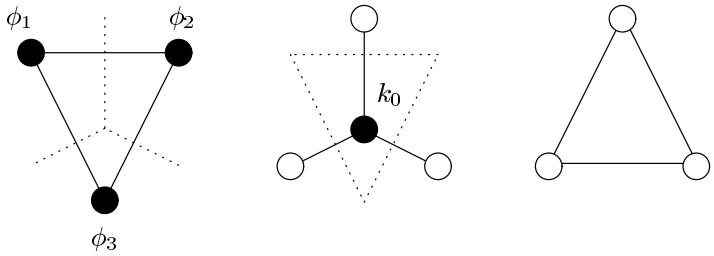

Figure 2.8: The duality for a single down-pointing triangle. The filled circles are the targets of the summation in the calculation of the partition function. The middle figure is the lattice after the duality, and the right figure expresses the lattice after the star-triangle transformation.

where the overall factor q on the right-hand side reflects the invariance of the system under the uniform change $\phi_i \to \phi_i + l$ (for $\forall i$ $0 \leq l \leq q-1$). We rewrite the Kronecker's delta as an exponential form,

$$Z_{\rm TR}[x] = q \, \frac{1}{q} \sum_{k_0=0}^{q-1} \sum_{\{\phi_{ij}\}} x(\phi_{12}) x(\phi_{23}) x(\phi_{31}) \mathrm{e}^{\mathrm{i}\frac{2\pi}{q}(\phi_{12}+\phi_{23}+\phi_{31})k_0}. \tag{2.52}$$

We can take the summations over $\{\phi_{ij}\}$. The Fourier transformation of the edge Boltzmann factor x in Eq. (2.24) enables us to rewrite this equation as,

$$Z_{\rm TR}[x] = q \, \frac{1}{q} \left(\sqrt{q}\right)^3 \sum_{k_0=0}^{q-1} \left\{x^*(k_0)\right\}^3 . \tag{2.53}$$

We then find that the partition function is transformed into the one with the dual edge Boltzmann factor x^* and dual site variables k_0. We can interpret that the partition function is transformed into the one of a system with three bonds and one site in a star shape as in Fig. 2.8 in a similar manner of change of the lattice to the case of the square lattice. If we calculate the summation over the single site variable k_0, we obtain another partition function with the dual edge Boltzmann factors on the up-pointing triangle as in Fig. 2.8. This summation is called the star-triangle transformation. We thus obtain the following relation for the two partition functions,

$$Z_{\rm TR}[x] \;\; = \;\; q \, \frac{1}{q} \left(\sqrt{q}\right)^3 Z_{\rm D,TR}[x^*]. \tag{2.54}$$

These partition functions are defined on the triangular lattices but their boundary conditions are different as denoted by D. One finds that the factor q on the right-hand side reflects a symmetry of the invariance of the uniform change of $\phi_i \to \phi_i + l$,

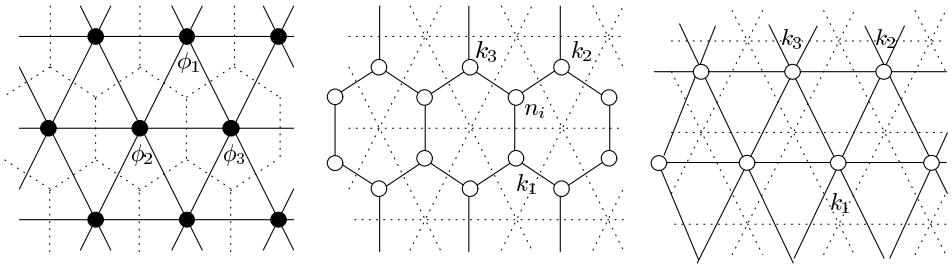

Figure 2.9: The duality for the triangular lattice. After the duality, the partition function on the triangular lattice is transformed into another partition function on the hexagonal lattice.

the exponent of $1/q$ expresses the number of the plaquette denoted by N_D and that of $\sqrt{q}$ means the number of the bonds. The simple lesson here gives and inference that the duality for the triangular lattice is given by a relation,

$$Z_{\rm TR}[x] \quad = \quad q^{1-N_D+\frac{N_B}{2}} Z_{\rm D,TR}[x^*]. \tag{2.55}$$

This is reduced to, by the Euler's relation $N_s + N_D = N_B + 1$,

$$Z_{\rm TR}[x] \quad = \quad q^{N_s-\frac{N_B}{2}} Z_{\rm D,TR}[x^*]. \tag{2.56}$$

The duality relation is again obtained similarly to the case on the square lattice.

2.4.2 Triangular Lattice

As seen in the previous example, a set of three edge Boltzmann factors always appear in the calculation of the duality for the triangular lattice. It is thus better to introduce the face Boltzmann factor for three bonds on an elementary triangle written by $A_K(\phi_{12}, \phi_{23}, \phi_{31})$. For example, the face Boltzmann factor for the Ising model is

$$A_K(\phi_{12}, \phi_{23}, \phi_{31}) = \exp\left\{K\left(\cos\pi\phi_{12} + \cos\pi\phi_{23} + \cos\pi\phi_{31}\right)\right\}, \tag{2.57}$$

where $\phi_{ij} = \phi_i - \phi_j$ and the subscripts denote sites on each elementary triangle as in Fig. 2.9. The use of the face Boltzmann factor enables us to deal with models with three-body interactions on the elementary triangle as shown below.

We omit the subscript expressing the coupling constant K below because of the absence of confusion. Use of the face Boltzmann factor permits us to write the

partition function for the triangular lattice as,

$$Z_{\rm TR}[A] = \sum_{\{\phi_i\}} \prod_{\triangle} A(\phi_1 - \phi_2, \phi_2 - \phi_3, \phi_3 - \phi_1), \tag{2.58}$$

where the symbol $\triangle$ denotes that the product runs over the N_s up-pointing triangles as in Fig. 2.9. The number of sites N_s is equal to the up-pointing triangles as found in Fig. 2.9. We consider the duality to the face Boltzmann factor, by introducing new variables $\{\phi_{ij}\}$ and Kronecker's delta for each triangle,

$$Z_{\rm TR}[A] = q \sum_{\{\phi_{ij}\}} \prod_{\triangle} A(\phi_{12}, \phi_{23}, \phi_{31}) \delta(\phi_{12} + \phi_{23} + \phi_{31}) \prod_{\triangledown} \delta \left(\sum_{ij} \phi_{ij} \right), \tag{2.59}$$

where the symbol $\triangledown$ expresses that the product runs over the down-pointing triangles, and the ij under the summation means the summation over the bonds on each down-pointing triangle. Similarly to the simple case, we rewrite the Kronecker's delta into the exponential form as, using variables k_i for the up-pointing triangles and n_i for the down-pointing triangles,

$$Z_{\rm TR}[A] = q \left(\frac{1}{q} \right)^{N_D} \sum_{\{k_i\}} \sum_{\{n_i\}} \sum_{\{\phi_{ij}\}} \prod_{i} A(\phi_{12}, \phi_{23}, \phi_{31}) \mathrm{e}^{\mathrm{i}\frac{2\pi}{q}\{(k_1+n_i)\phi_{23} + (k_2+n_i)\phi_{31} + (k_3+n_i)\phi_{12}\}}, \tag{2.60}$$

where N_D is the number of the plaquettes, which equals to $2N_s$. The sets of the variables $\{k_i\}$ and $\{n_i\}$ represent the site variables on the dual hexagonal lattice as in Fig. 2.9. Hence we can regard this partition function as another partition function defined on the dual hexagonal lattice. The summation over n_i gives a direct relationship between the two partition functions defined on the triangular lattice,

$$Z_{\rm TR}[A] = q^{1+N_D/2} \left(\frac{1}{q} \right)^{N_D} \sum_{\{k_i\}} \sum_{\{\phi_{ij}\}} \prod_{i} A(\phi_{12}, \phi_{23}, \phi_{31}) \mathrm{e}^{\mathrm{i}\frac{2\pi}{q}(k_1\phi_{23} + k_2\phi_{31} + k_3\phi_{12})} \delta(\phi_{12} + \phi_{23} + \phi_{31}). \tag{2.61}$$

This summation is called the star-triangle transformation. Therefore we obtain another partition function on the N_s down-pointing triangles. We here define the dual face Boltzmann factor as, by including the factor q^{-1} which corresponds to, $q^{-N_D/2}$, a part of the overall factors,

$$A^*(k_{12}, k_{23}, k_{31}) = q^{-1} \sum_{\{\phi_{ij}\}} A(\phi_{12}, \phi_{23}, \phi_{31}) \mathrm{e}^{\mathrm{i}\frac{2\pi}{q}(k_1\phi_{23} + k_2\phi_{31} + k_3\phi_{12})} \delta(\phi_{12} + \phi_{23} + \phi_{31}), \tag{2.62}$$

or equivalently, using the exponential form of the Kronecker's delta,

$$A^*(k_{12},k_{23},k_{31}) = q^{-2}\sum_{\{\phi_i\}} A(\phi_{12},\phi_{23},\phi_{31})\mathrm{e}^{\mathrm{i}\frac{2\pi}{q}(k_{12}\phi_3+k_{23}\phi_1+k_{31}\phi_2)}, \tag{2.63}$$

where $k_{ij} \equiv k_i - k_j$. Then we can establish a direct relationship between the two models defined on the triangular lattice without recourse to the hexagonal lattice as,

$$Z_{\mathrm{TR}}[A] = qZ_{\mathrm{D,TR}}[A^*], \tag{2.64}$$

where $Z_{\mathrm{D,TR}}$ is the partition function with the dual face Boltzmann factor defined on the down-pointing triangle as in Fig. 2.9. Similarly to the case of the square lattice, the extra coefficient q and the difference of the boundary conditions are negligible, if we consider the thermodynamic limit. We thus use the following relation in applications of the duality below,

$$Z_{\mathrm{TR}}[A] = Z_{\mathrm{TR}}[A^*]. \tag{2.65}$$

If we use again the representation of the edge Boltzmann factors x and x^*, from Eq. (2.62) and the exponential form of the Kronecker's delta,

$$\begin{aligned} A^*(k_{12},k_{23},k_{31}) &= q^{-2}\sum_{\{\phi_i\}}\sum_{n_i=0}^{q-1} x(\phi_{12})x(\phi_{23})x(\phi_{31})\mathrm{e}^{\mathrm{i}\frac{2\pi}{q}\{(k_1-n_i)\phi_{23}+(k_2-n_i)\phi_{31}+(k_3-n_i)\phi_{12}\}} \\ &= q^{-\frac{1}{2}}\sum_{n_i=0}^{q-1} x^*(k_1-n_i)x^*(k_2-n_i)x^*(k_3-n_i), \end{aligned} \tag{2.66}$$

where the summation over n_i means the star-triangle transformation. We obtain the same duality relation as Eq. (2.56) by inserting this expression into the duality relation (2.64).

2.4.3 Ising Model

The face Boltzmann factor for the non-random Ising model is given by Eq. (2.57). On the other hand, the dual face Boltzmann factor is computed by Eq. (2.63) as,

$$A_K^*(k_{12},k_{23},k_{31}) = \frac{1}{2}\left(\mathrm{e}^{3K} + \mathrm{e}^{K}\sum_{\triangle}\cos\pi k_{ij}\right), \tag{2.67}$$

where the up-pointing triangle means the summation over bonds 12, 23, and 31 surrounding each up-pointing triangle as in Fig. 2.9. We can rewrite the duality

relation (2.65) by extracting the principal Boltzmann factors A_0 and A_0^* for up-pointing triangles, in which spins are all up, as

$$A_0(K)^{N_s} z_{\rm TR}\left[\frac{A_K}{A_0(K)}\right] = A_0^*(K)^{N_s} z_{\rm TR}\left[\frac{A_K^*}{A_0^*(K)}\right], \tag{2.68}$$

where $z_{\rm TR}$ is the normalized partition function by the principal Boltzmann factor. These normalized partition functions have only the following difference in their arguments,

$$\mathrm{e}^{-4K} = \frac{A_K(0,1,1)}{A_0(K)} = \frac{A_K(1,0,1)}{A_0(K)} = \frac{A_K(1,1,0)}{A_0(K)} \tag{2.69}$$

$$\frac{1-\mathrm{e}^{-4K}}{1+3\ \mathrm{e}^{-4K}} = \frac{A_K^*(0,1,1)}{A_0^*(K)} = \frac{A_K^*(1,0,1)}{A_0^*(K)} = \frac{A_K^*(1,1,0)}{A_0^*(K)}. \tag{2.70}$$

If we consider all configurations for three edges of the elementary triangle, there are only these face Boltzmann factors except for the principal Boltzmann factors. Therefore we find the duality relation of the coupling constants,

$$\mathrm{e}^{-4K^*} = \frac{1-\mathrm{e}^{-4K}}{1+3\ \mathrm{e}^{-4K}}. \tag{2.71}$$

Using this dual coupling, we construct the relation between two Ising models on the triangular lattice with different couplings as

$$Z_{\rm TR}[A_K] = \left\{\frac{A_0^*(K)}{A_0(K^*)}\right\}^{N_s} Z_{\rm TR}[A_{K^*}]. \tag{2.72}$$

The extra coefficient Λ is explicitly given as,

$$\Lambda = \left\{\frac{A_0^*(K)}{A_0(K^*)}\right\}^{N_s} = \left(\frac{1}{2}\right)^{N_s} \left(\mathrm{e}^{3K}+3\mathrm{e}^{-K}\right)^{\frac{N_s}{4}} \left(\mathrm{e}^{3K}-\mathrm{e}^{-K}\right)^{\frac{3N_s}{4}}. \tag{2.73}$$

Similarly to the case of the Ising model on the square lattice, we obtain the critical point $T_c = 3.64096$, from the fixed point $\mathrm{e}^{-4K_c} = 1/3$ of Eq. (2.71) by setting $K = K^* = K_c$. The extra coefficient Λ given in Eq. (2.73) also becomes unity at the critical point. We can predict that the internal energy of the Ising model on the triangular lattice is $E(K_c) = -4N_s$ given by Eq. (2.14) and the specific heat will be continuous or divergent through the critical point as evaluated by Eq. (2.16).

2.4.4 Potts Model with Two- and Three-Body Interactions

We apply the duality and the star-triangle transformation to the general case rather than the Potts model only with two-body interactions, namely the Potts model with

two- and three-body interactions [96]. We show the results for the exact value of the internal energy of this model below. The Potts model with two- and three-body interactions is defined by the following face Boltzmann factor,

$$A_{K_2,K_3}(\phi_{12},\phi_{23},\phi_{31}) = \exp\left\{K_2\sum_{\triangle}\delta(\phi_{ij}) + K_3\prod_{\triangle}\delta(\phi_{ij})\right\}, \tag{2.74}$$

where the up-pointing triangle expresses that the summation and product run over bonds 12, 23, and 31 surrounding each up-pointing triangle as in Fig. 2.9. It is convenient to rewrite this Boltzmann factor in the following traditional form by using an identity $\mathrm{e}^{K\delta(x)} = 1 + v\delta(x)$,

$$\begin{aligned} A_{K_2,K_3}(\phi_{12},\phi_{23},\phi_{31}) &= 1 + v_2\sum_{\triangle}\delta(\phi_{ij}) + \left\{3v_2^2 + v_2^3 + (1+v_2)^3 v_3\right\}\prod_{\triangle}\delta(\phi_{ij}) \\ &= 1 + v_2\sum_{\triangle}\delta(\phi_{ij}) + y\prod_{\triangle}\delta(\phi_{ij}), \end{aligned} \tag{2.75}$$

where $v_i \equiv \mathrm{e}^{K_i} - 1$ for $i = 2$ and 3 and $y \equiv \mathrm{e}^{K_3+3K_2} - 3\mathrm{e}^{K_2} + 2$. Then the dual face Boltzmann factor is obtained by computing Eq. (2.63) as follows,

$$\begin{aligned} A^*_{K_2,K_3}(k_{12},k_{23},k_{31}) &= \frac{y}{q}\left\{1 + v^*\sum_{\triangle}\delta(\phi_{ij}) + y^*\prod_{\triangle}\delta(\phi_{ij})\right\} \\ &= \frac{y}{q}\,A_{K_2^*,K_3^*}(k_{12},k_{23},k_{31}), \end{aligned} \tag{2.76}$$

where $v^* = qv/y$ and $y^* = q^2/y$. Therefore we can establish the relation between two Potts models with two- and three-body interactions with different couplings as,

$$Z_{\mathrm{TR}}[A_{K_2,K_3}] = \left(\frac{y}{q}\right)^{N_s} Z_{\mathrm{TR}}[A_{K_2^*,K_3^*}]. \tag{2.77}$$

The partition function of the unfamiliar model, the Potts model with two- and three-body interactions, has two arguments as the function of couplings. Setting $K_2 = K_2^*$ and $K_3 = K_3^*$, we obtain the line of the fixed points described by $y = q$. Indeed this line gives a part of the critical points as shown by Wu and Zia. They argued that the line $y = q$ represents the critical surface if $J_3 + 3J_2 > 0$ and $J_3 + 2J_2 > 0$ [97].

We can take the logarithmic derivative of the free energy by K_2 and K_3. These logarithmic derivatives yield two relations concerning the internal energy as follows,

$$\left(1 - \frac{\partial K_2^*}{\partial K_2}\right)\left\langle\sum_{\triangle}\delta(\phi_{ij})\right\rangle - \frac{\partial K_3^*}{\partial K_2}\left\langle\prod_{\triangle}\delta(\phi_{ij})\right\rangle = \frac{N_s}{y}\frac{\partial y}{\partial K_2} \tag{2.78}$$

$$-\frac{\partial K_2^*}{\partial K_3}\left\langle\sum_{\triangle}\delta(\phi_{ij})\right\rangle + \left(1 - \frac{\partial K_3^*}{\partial K_3}\right)\left\langle\prod_{\triangle}\delta(\phi_{ij})\right\rangle = \frac{N_s}{y}\frac{\partial y}{\partial K_3}, \tag{2.79}$$

q	K_2	K_3	τ	energy
2	0.375530	0.347552	0.925497	−3.19412
3	0.291622	0.737724	2.52973	−3.95336
4	−0.062177	1.75913	−28.2924	−15.5884
4	−1.09861	4.39445	−4	−0.5

Table 2.1: Solutions of eq. (2.82) and $y = q$. Here $\tau \equiv K_3/K_2$.

where $\left\langle \sum_{\triangle} \delta(\phi_{ij}) \right\rangle$ is the logarithmic derivative of the free energy by K_2 and $\left\langle \prod_{\triangle} \delta(\phi_{ij}) \right\rangle$ is by K_3. It turns out that these two equations are not independent of each other. However we can give the exact value of the internal energy in a restricted subspace of (K_2, K_3). We define the internal energy as, for the Potts model with two- and three-body interactions, regarding the inverse temperature as K_2,

$$E(K_2, K_3) = \left\langle \prod_{\triangle} \delta(\phi_{ij}) \right\rangle + \frac{K_3}{K_2} \left\langle \prod_{\triangle} \delta(\phi_{ij}) \right\rangle . \tag{2.80}$$

Therefore we can obtain the exact value of the internal energy by relating the ratio of two and three-body interactions with the ratios of the coefficients of $\left\langle \sum_{\triangle} \delta(\phi_{ij}) \right\rangle$ and $\left\langle \prod_{\triangle} \delta(\phi_{ij}) \right\rangle$ in Eqs. (2.78) and (2.78). The condition for calculating the exact value of the internal energy is

$$\frac{K_3}{K_2} = \frac{\dfrac{\partial K_3^*}{\partial K_2}}{1 - \dfrac{\partial K_2^*}{\partial K_2}}. \tag{2.81}$$

This condition is reduced to

$$(K_3 + 3K_2)(3\mathrm{e}^{K_2} + q - 2)(\mathrm{e}^{K_2} - 1) = K_2 \mathrm{e}^{K_2}(3\mathrm{e}^{K_2} + 2q - 3). \tag{2.82}$$

There are solutions of this equation for the case with the state number $q = 2$, 3, 4, and $q \geq 69$. However the Potts model has a possibility of a first-order transition for $q \geq 5$ [95]. We therefore list the solutions only for $q = 2$, 3, and 4 and values of the internal energy for their cases from Eqs. (2.78) and (2.79) in Table 2.1.

We performed Monte-Carlo simulations as confirmations with linear system size 100 and 10500 MCS per spin for most cases. The results show the validity of the duality for the partition function with two coupling constants as in the present

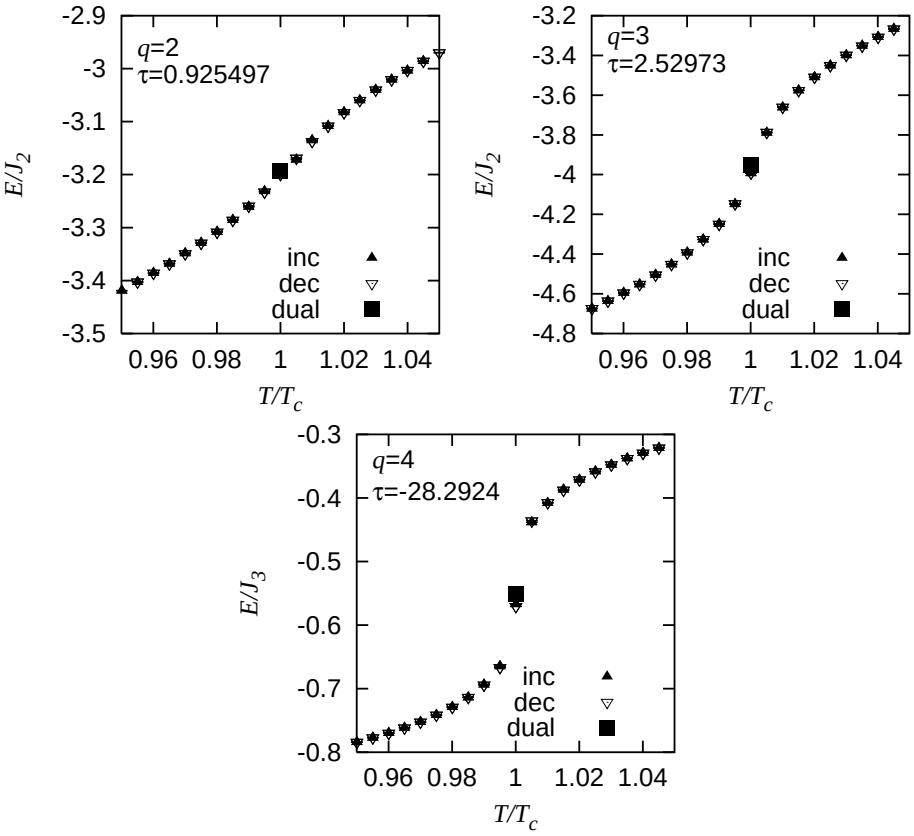

Figure 2.10: The internal energies at the fixed points of duality as in Table 2.1 except for $q = 4$, $\tau = -4$ and their numerical verifications by the Monte-Carlo simulation. The symbol 'inc' expresses the internal energy measured by increasing the temperature, 'dec' stands for the results by decreasing temperature, and 'dual' is for our results by the duality and the star-triangle transformation.

case as in Fig. 2.10. The data have been averaged over 100 independent runs. The case with $q = 4$ and $\tau = K_3/K_2 = -4$ is an exception, in which we took 250 independent runs of 4500 MCS. This case shows the hysteresis behavior of the first-order transition as in Fig. 2.11.

It is possible to understand the condition (2.81) for the internal energy to be calculable from a little different point of view. We plot $\tau = K_3/K_2$ and the dual $\tau^* = K_3^*/K_2^*$ as functions of K_2 in Fig. 2.12. As seen there, the two lines have the same slope (i.e. both are flat) at the fixed point $y = q$. This feature $dK_3^*/dK_2^* = dK_3/dK_2$ can be shown by a direct manipulation of the condition for calculation of the internal energy (2.81).

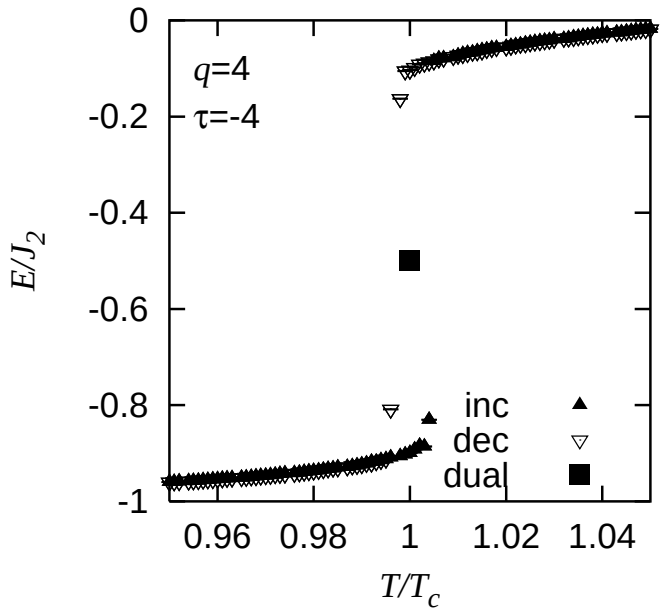

Figure 2.11: The internal energy at the fixed points of duality for $q = 4$, $\tau = -4$, which shows a characteristic hysteresis behavior, which is observed in the first-order transition. The symbols are similarly to ones used in Fig. 2.10.

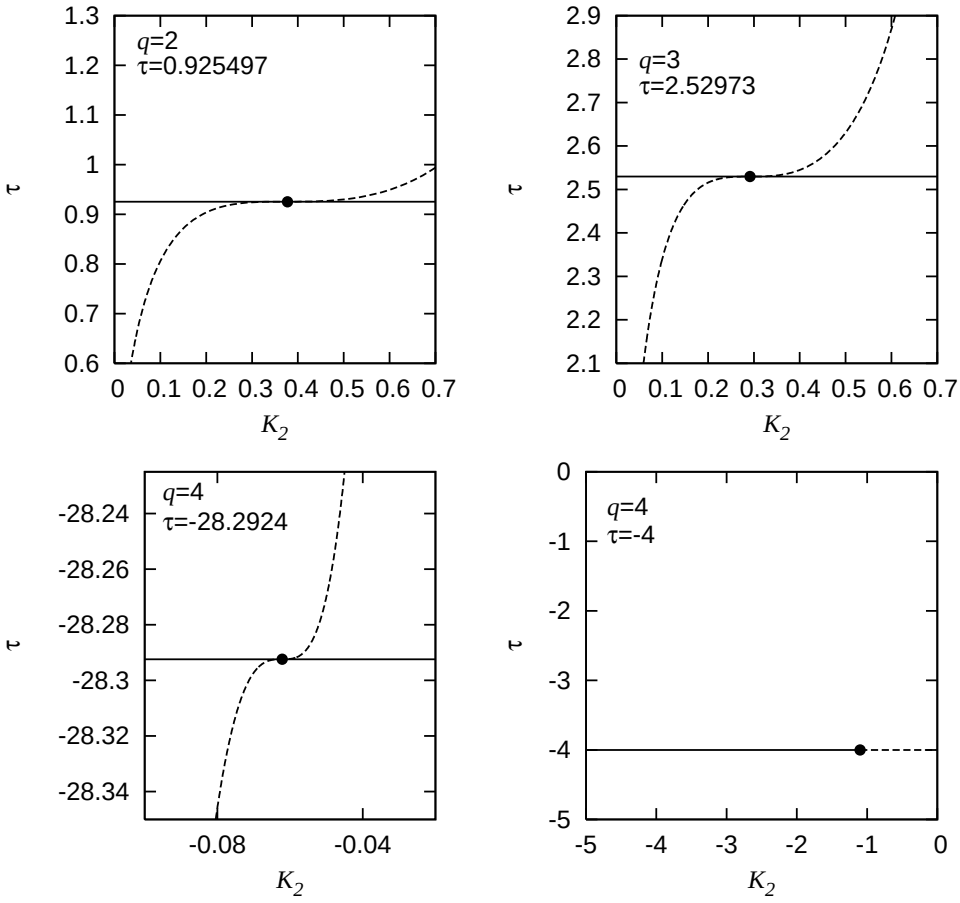

Figure 2.12: The behaviors around the solutions of Eq. (2.81). The horizontal solid line is the ratio K_3/K_2 for the original model and the dashed line is for the dual one K_3^*/K_2^*. These two lines intersect at the fixed point ($y = q$) shown in black dot.

Chapter 3

Analytic Properties of Random Spin Systems

In this chapter, we first review analytical properties of the random-bond Ising model in finite dimensional systems. The random-bond Ising model is a standard model to study the spin glass, and has quite a useful symmetry, the gauge symmetry, to facilitate to obtain analytical results such as the internal energy and the upper bound for the specific heat without any approximations. After then, we consider the duality for the random-bond Ising model. It is difficult to directly apply the duality transformation to the random-bond Ising model, because of the existence of antiferromagnetic interactions. Therefore we employ one of the useful techniques to analyze the random spin systems, the replica method, to map the random spin systems into effective non-random models but with multi-spin interactions. As a result, the replica method enables us to apply the duality to random-bond Ising model. However we then find some problems to derive the critical points by the ordinary procedure as introduced in the previous chapter.

3.1 Random Bond Ising Model

The random-bond Ising model is defined by randomizing the value of the coupling constant on each bond of the non-random Ising model as,

$$H = -\sum_{\langle ij \rangle} J_{ij} S_i S_j, \tag{3.1}$$

where S_i denotes Ising spin variable taking ± 1 on each site i, and J_{ij} expresses the random coupling constant. This random coupling constant J_{ij} changes slower than the motion of flipping of spins by thermal fluctuation. This type of randomness

is called "quenched" randomness. This model is one of the theoretical models for analysis of spin-glass behavior.

This spin-glass behavior is caused by the geometrical effect. Here we use the characteristic quantity defined as [11, 12],

$$f(C) = \prod_{(ij)\in C} \tau_{ij}, \tag{3.2}$$

where τ_{ij} expresses the sign of the random coupling and C denotes that the product is restricted over circumference of an elementary plaquette. When this quantity becomes negative, the spin configuration on the plaquette is under frustration, which affects remarkably the spin-glass behavior. If we consider a quenched random system with a number of the plaquettes, the degeneracy of the ground states increase enormously and spins do not always order in the same direction in space in the low-temperature region. This disorder effect is caused by the geometric property of quenched random couplings in space. On the other hand, investigating motion of spins for a long time, we find a particular behavior as frozen in time. This is the spin-glass behavior and such a phase is called the spin glass phase.

3.1.1 Configurational Average

In this thesis, we consider mainly two types of the distribution functions for the random coupling J_{ij} of the random-bond Ising model. One is the $\pm J$ Ising model with

$$P(J_{ij}) = p\delta(J_{ij} - J) + (1-p)\delta(J_{ij} + J), \tag{3.3}$$

where p denotes the probability of the ferromagnetic coupling J on each bond. This distribution function is rewritten as, for convenience,

$$P(J_{ij}) = \frac{\mathrm{e}^{\beta_p J_{ij}}}{2\cosh \beta_p J}, \tag{3.4}$$

where $\mathrm{e}^{-2\beta_p J} = (1-p)/p$. The other is the Gaussian Ising model with the distribution function

$$P(J_{ij}) = \frac{1}{\sqrt{2\pi J^2}} \exp\left\{ -\frac{1}{2J^2}(J_{ij} - J_0)^2 \right\}. \tag{3.5}$$

Here J_0 represents the average and J^2 is the variance of the Gaussian distribution. For convenience, we write this distribution function as follows, setting $J = 1$,

$$P(J_{ij}) = \frac{1}{\sqrt{2\pi}} \exp\left\{ -\frac{1}{2}(J_{ij}^2 + J_0^2) + J_0 J_{ij} \right\}. \tag{3.6}$$

The physical quantity in the equilibrium state is not only given by the thermal average as in the case of the non-random Ising model, owing to the existence of quenched random couplings following various distribution functions as introduced above. We need to evaluate the configurational average by J_{ij}. The double averages, thermal and configurational averages, make it difficult for us to directly analyze the random-bond Ising model. The thermal average is treated by the calculation of the free energy for each distribution of J_{ij}. After then, we have to evaluate the configurational average of the free energy by J_{ij} through the logarithmic dependence, recalling the free energy is given by the logarithm of the partition function. This calculation has not been exactly calculated as in the case of the non-random Ising model yet.

3.1.2 Replica Method

One of the useful techniques for the analysis of the random-bond Ising model with the configurational average is the replica method. Using the identity $\lim_{n\to 0}(x^n-1)/n = \log x$, we consider a relation

$$-\beta \left[F\right]_{\rm av} = \lim_{n\to 0} \frac{\left[Z^n\right]_{\rm av} - 1}{n}. \tag{3.7}$$

Instead of calculation of the logarithmic quantity for the evaluation of the free energy, we attempt to calculate the partition function to the power of n. If we assume that n is an integer, Z^n represents the partition function for a multiple spin system, which has different n-copied spins $\{S_i^\alpha\}$ $(\alpha = 1, 2, \cdots, n)$ and shares quenched random couplings $\{J_{ij}\}$ as,

$$Z^n = \sum_{\{S_i^\alpha\}} \prod_{\langle ij\rangle} \exp\left\{\beta J_{ij} \sum_{\alpha=1}^{n} S_i^\alpha S_j^\alpha\right\}. \tag{3.8}$$

The sketch of the replica method is given in Fig. 3.1. We find the n-replicated partition function of the random-bond Ising model after the configurational average generally expressed as

$$\left[Z^n\right]_{\rm av} = \sum_{\{S_i^\alpha\}} \prod_{\langle ij\rangle} \left[\int dJ_{ij} P(J_{ij}) \exp\left\{\beta J_{ij} \sum_{\alpha=1}^{n} S_i^\alpha S_j^\alpha\right\}\right]. \tag{3.9}$$

For example, we can write down explicitly the n-replicated partition function for the case of the $\pm J$ Ising model after the configurational average as,

$$\left[Z^n\right]_{\rm av} = \left(\frac{1}{\cosh \beta_p J}\right)^{N_B} \sum_{\{S_i^\alpha\}} \prod_{\langle ij\rangle} \cosh\left\{\beta_p J + \beta J \sum_{\alpha=1}^{n} S_i^\alpha S_j^\alpha\right\}. \tag{3.10}$$

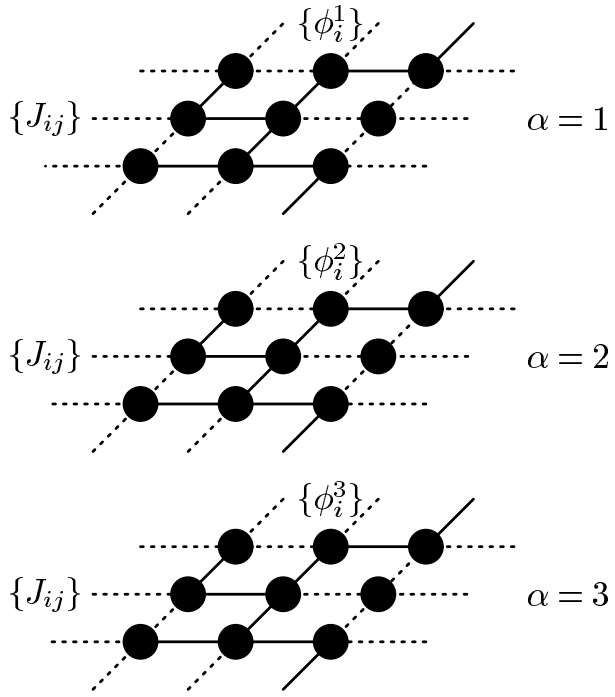

Figure 3.1: Sketch of the replicated system. The dashed lines are antiferromagnetic interactions and the solid lines are ferromagnetic ones for the $\pm J$ Ising model.

As seen in this equation, the replica method makes it possible to map a random spin system into an effective non-random system by evaluating the configurational average for the Boltzmann factor in advance. The effective edge Boltzmann factor is then given as,

$$x_n(\{S_i^\alpha\}) = \int dJ_{ij} P(J_{ij}) \exp\left\{\beta J_{ij} \sum_{\alpha=1}^{n} S_i^\alpha S_j^\alpha\right\}. \tag{3.11}$$

The replica method has been a greatly successful tool in the application of the mean-field theory to random spin systems, namely the Sherrington-Kirkpatrick model [14], though the n-replicated partition function of the finite dimensional random-bond Ising model has not been exactly evaluated yet. Analysis of the Sherrington-Kirkpatrick model by the replica method has shown the existence of the spin glass phase. We remark that whether the spin-glass phase exists even in a finite-dimensional system has not been shown rigorously.

3.1.3 Gauge Transformation

The Hamiltonian of the random-bond Ising model has a special symmetry known as the *gauge symmetry*. We define a local transformation as follows,

$$J_{ij} \rightarrow J_{ij}\sigma_i\sigma_j \tag{3.12}$$
$$S_i \rightarrow S_i\sigma_i, \tag{3.13}$$

where σ_i takes either -1 or $+1$. Therefore $\sigma_i^2 = 1$. We can easily find that the Hamiltonian is (3.1) invariant for this gauge transformation as follows,

$$H_G = -\sum_{\langle ij\rangle} J_{ij}\sigma_i\sigma_j S_i\sigma_i S_j\sigma_j = H, \tag{3.14}$$

where the subscript G denotes that the Hamiltonian is changed by the gauge transformation. On the other hand, the distribution function for J_{ij} is not generally conserved as shown below.

$\pm J$ Ising model

The distribution function of the $\pm J$ Ising model in Eq. (3.4) is changed into, after the gauge transformation,

$$P_G(J_{ij}) = \frac{\mathrm{e}^{\beta_p J_{ij}\sigma_i\sigma_j}}{2\cosh\beta_p J}. \tag{3.15}$$

Gaussian Ising model

We apply the gauge transformation to the distribution function and obtain

$$P_G(J_{ij}) = \frac{1}{\sqrt{2\pi}}\exp\left\{-\frac{1}{2}\left(J_{ij}^2 + J_0^2\right) + J_0 J_{ij}\sigma_i\sigma_j\right\}. \tag{3.16}$$

Both distribution functions have similar forms to the edge Boltzmann factor of the random-bond Ising model $\exp(\beta J_{ij}S_iS_j)$ with only difference of its argument as $\beta \rightarrow \beta_p$ for the $\pm J$ Ising model or $\beta \rightarrow J_0$ for the Gaussian Ising model. This feature is an advantage in the following analysis of the random-bond Ising model.

In addition, the gauge transformation leaves the distribution of frustration invariant. The quantity defined in Eq. (3.2) is transformed as

$$f_G(C) \rightarrow \prod_{(ij)\in C} \tau_{ij}\sigma_i\sigma_j = f(C). \tag{3.17}$$

Each gauge variable σ_i appears twice over bonds surrounding each plaquette. Therefore the distribution of frustration is not changed by the gauge transformation, because of $\sigma_i^2 = 1$.

We consider to evaluate the configurational average and thermal average of a gauge invariant quantity, written as Q, like the Hamiltonian (3.1) as,

$$[\langle Q\rangle]_{\rm av} = \int \prod_{\langle ij\rangle} P(Jij) dJ_{ij} \frac{1}{Z(\beta)} \sum_{\{S_i\}} Q \prod_{\langle ij\rangle} {\rm e}^{\beta J_{ij} S_i S_j}. \tag{3.18}$$

Here we consider the gauge transformation. The distribution function $P(J_{ij})$ changes as in Eqs. (3.15) and (3.16), while Q is invariant. The gauge transformation just changes the order of the sums over $\{J_{ij}\}$ for the $\pm J$ Ising model and the sums over only the signs of $\{J_{ij}\}$ in integration over $\{J_{ij}\}$ for the Gaussian Ising model. For example, the summation over $J_{ij} = \pm 1$ in the order 'first $+1$ and then -1' is changed into the order 'first -1 and then $+1$' by the gauge transformation $J_{ij} \to J_{ij}\sigma_i\sigma_j$ when $\sigma_i\sigma_j = -1$. Therefore the gauge transformations by any configurations $\{\sigma_i\}$ do not change the value of $[\langle Q\rangle]_{\rm av}$. We here consider the summation over all configurations of the gauge variables $\{\sigma_i\}$, which gives $2^{N_s}[\langle Q\rangle]_{\rm av}$ where N_s denotes the number of sites. We can thus evaluate $[\langle Q\rangle]_{\rm av}$ for the $\pm J$ Ising model as follows,

$$\begin{aligned}
[\langle Q\rangle]_{\rm av} &= \frac{1}{2^{N_s}(2\cosh\beta_p J)^{N_B}} \\
&\quad \times \sum_{\{J_{ij}\}} \sum_{\{\sigma_i\}} \prod_{\langle ij\rangle} {\rm e}^{\beta_p J_{ij}\sigma_i\sigma_j} \frac{1}{Z(\beta)} \sum_{\{S_i\}} Q \prod_{\langle ij\rangle} {\rm e}^{\beta J_{ij} S_i S_j} \\
&= \frac{1}{2^{N_s}(2\cosh\beta_p J)^{N_B}} \sum_{\{J_{ij}\}} \frac{Z(\beta_p)}{Z(\beta)} \sum_{\{S_i\}} Q \prod_{\langle ij\rangle} {\rm e}^{\beta J_{ij} S_i S_j},
\end{aligned} \tag{3.19}$$

where N_B stands for the number of bonds, and similarly for the Gaussian model,

$$[\langle Q\rangle]_{\rm av} = \frac{1}{2^{N_s}} \int \prod_{\langle ij\rangle} I(J_{ij}) dJ_{ij} \frac{Z(J_0)}{Z(\beta)} \sum_{\{S_i\}} Q \prod_{\langle ij\rangle} {\rm e}^{\beta J_{ij} S_i S_j}, \tag{3.20}$$

where we restrict J_{ij} to the positive range of the integration over J_{ij} and $I(J_{ij})$ is given by,

$$I(J_{ij}) = \frac{1}{\sqrt{2\pi}} \exp\left\{ -\frac{1}{2}\left(J_{ij}^2 + J_0^2\right)\right\}. \tag{3.21}$$

3.1.4 Exact Solution for the Internal Energy

Using the gauge transformation, we can rewrite the product of the distribution function over all bonds as the partition function of the random-bond Ising model

as in Eqs. (3.19) and (3.20). If we set $\beta = \beta_p$ in the $\pm J$ Ising model and $\beta = J_0$ in the Gaussian Ising model, both of the ratios $Z(\beta)/Z(\beta_p)$ and $Z(\beta)/Z(J_0)$ of two partition functions become unity in Eqs. (3.19) and (3.20). Therefore we can calculate the exact value of the internal energy under these conditions. For the case of the $\pm J$ Ising model, the internal energy is reduced to,

$$\begin{aligned}
[\langle H\rangle]_{\rm av} &= \frac{1}{2^{N_s}(2\cosh\beta_p J)^{N_B}}\sum_{\{J_{ij}\}}\sum_{\{S_i\}}\left(-\sum_{\langle ij\rangle}J_{ij}S_iS_j\right)\prod_{\langle ij\rangle}\mathrm{e}^{\beta_p J_{ij}S_iS_j} \\
&= -\frac{1}{2^{N_s}(2\cosh\beta_p J)^{N_B}}\frac{\mathrm{d}}{\mathrm{d}\beta_p}\sum_{\{S_i\}}\sum_{\{J_{ij}\}}\prod_{\langle ij\rangle}\mathrm{e}^{\beta_p J_{ij}S_iS_j} \\
&= -N_B J\tanh\beta_p J. \qquad (3.22)
\end{aligned}$$

The internal energy of the Gaussian Ising model is also rewritten as,

$$\begin{aligned}
[\langle H\rangle]_{\rm av} &= -\frac{1}{2^{N_s}}\int\prod_{\langle ij\rangle}I(J_{ij})dJ_{ij}\frac{\mathrm{d}}{\mathrm{d}J_0}\sum_{\{S_i\}}\mathrm{e}^{J_0 J_{ij}S_iS_j} \\
&= -N_B J_0. \qquad (3.23)
\end{aligned}$$

The above calculations hold for any lattices. The specialty of each lattice is reflected only in the number of bonds N_B.

The conditions, $\beta = \beta_p$ for the $\pm J$ Ising model and $\beta = J_0$ for the Gaussian Ising model, describe a particular line in the (p, T) plane for $\pm J$ Ising model and in the (J_0, T) plane for the Gaussian model. In other words, we find a special subspace on the phase diagram. The special line on the phase diagram is called the *Nishimori line*. Under the Nishimori-line condition, we find a way to rigorously evaluate several properties as well as the exact internal energy as shown below.

3.1.5 Upper Bound for the Specific Heat

Under the Nishimori-line condition, a cancellation of two factors expressed by the partition functions with different couplings occurs as in Eqs. (3.19) and (3.20). Therefore we can calculate the exact internal energy. In addition, we can evaluate the upper bound for the specific heat similarly to the case of the internal energy. The specific heat is given as,

$$\begin{aligned}
T^2C &= -\frac{\partial}{\partial\beta}[\langle H\rangle]_{\rm av} \\
&= \left[\langle H^2\rangle - \langle H\rangle^2\right]_{\rm av}. \qquad (3.24)
\end{aligned}$$

Here we set the Boltzmann constant $k_B = 1$. The first term of the last expression can be calculated as, similarly to the previous case with a cancellation of two partition

functions,

$$\begin{aligned}\left[\langle H^2\rangle\right]_{\rm av} &= \frac{1}{2^{N_s}(2\cosh\beta_p J)^{N_B}}\sum_{\{J_{ij}\}}\sum_{\{S_i\}}\left(-\sum_{\langle ij\rangle}J_{ij}S_iS_j\right)^2\prod_{\langle ij\rangle}\mathrm{e}^{\beta_p J_{ij}S_iS_j}\\ &= \frac{1}{2^{N_s}(2\cosh\beta_p J)^{N_B}}\frac{\mathrm{d}^2}{\mathrm{d}\beta_p^2}\sum_{\{S_i\}}\sum_{\{J_{ij}\}}\prod_{\langle ij\rangle}\mathrm{e}^{\beta_p J_{ij}S_iS_j}\\ &= J^2\left(N_B^2\tanh\beta_p J + N_B\frac{1}{\cosh^2\beta_p J}\right). \qquad (3.25)\end{aligned}$$

The second term in the second line of Eq. (3.24) has a denominator expressed by a remaining partition function even after use of the cancellation under the Nishimori-line condition. Therefore we cannot calculate this term exactly but can establish its lower bound by the Schwarz inequality as follows,

$$\left[\langle H\rangle^2\right]_{\rm av} \geq \left[\langle H\rangle\right]_{\rm av}^2 = N_B^2 J^2\tanh^2\beta_p J. \qquad (3.26)$$

By bringing Eqs. (3.25) and (3.26) together, we obtain the upper bound for the specific heat as,

$$T^2 C \leq N_B J^2\frac{1}{\cosh^2\beta_p J}. \qquad (3.27)$$

Similarly the upper bound on the specific heat for the Gaussian Ising model can be evaluated as,

$$T^2 C \leq N_B J^2. \qquad (3.28)$$

3.1.6 Frustration Entropy

Using the gauge transformation, we find another expression of the free energy. The free energy of the random-bond Ising model is written as follows,

$$-\beta\left[F\right]_{\rm av} = \int\prod_{\langle ij\rangle}P(J_{ij})dJ_{ij}\log Z(\beta,\{J_{ij}\}). \qquad (3.29)$$

Applying the gauge transformation, we take the summation over all configurations of the gauge variables $\{\sigma_i\}$ and obtain another expression, explicitly for the $\pm J$ Ising model,

$$-\beta\left[F\right]_{\rm av} = \frac{1}{2^{N_s}(2\cosh\beta_p J)^{N_B}}\sum_{\{J_{ij}\}}Z(\beta_p,\{J_{ij}\})\log Z(\beta,\{J_{ij}\}), \qquad (3.30)$$

and for the Gaussian Ising model,

$$-\beta \left[F\right]_{\rm av} = \frac{1}{2^{N_s}} \int_0^\infty \prod_{\langle ij \rangle} I(J_{ij}) dJ_{ij} Z(J_0, \{J_{ij}\}) \log Z(\beta, \{J_{ij}\}). \tag{3.31}$$

Each case shows that the free energy under the condition $\beta_p = \beta$ or $J_0 = \beta$ has reduced to the entropy $S(x) \equiv -\sum x \log x$. In addition the gauge transformation leaves the distribution of frustration invariant as in Eq. (3.17). Therefore we find that the free energy under the Nishimori-line condition gives the sum of the probabilities for various bond configurations with the same distribution of frustration. Seeing alternative expressions (3.30) and (3.31) of the free energy, we regard the free energy as the entropy of the distribution of frustration. The phase transition is caused by the singularity of the free energy. Therefore we can consider that the singularity of the distribution of frustration gives the location of the critical point on the Nishimori line. Frustration is a geometrical property of the random-bond Ising model. A phase transition in the ground state, where there are only geometrical effects without any thermal fluctuation, is expected to occur similarly by the geometrical singularity of frustration. We thus expect the existence of a phase boundary parallel to the T-axis on the phase diagram under the Nishimori line or equivalently a vertical phase boundary to p-axis for the $\pm J$ Ising model, and to J_0-axis for the Gaussian model. This is the vertical scenario as in Fig. 1.6. This expectation has not been rigorously proved yet but confirmed by the mean-field theory [14]. In addition, the method with the gauge transformation has succeeded in restricting two possibilities of the phase boundary under the Nishimori line for finite-dimensional systems by an inequality for the correlation functions,

$$|[\langle S_i S_j \rangle]| \leq \left| [\langle \sigma_i \sigma_j \rangle]_{\rm NL} \right| . \tag{3.32}$$

The phase boundary should be either vertical to p and J_0-axes or reentrant toward the ferromagnetic phase under the Nishimori line as in Fig. 1.6 [34].

3.2 Duality for Random Spin Systems

Let us consider the application of the duality to the partition function for the random-bond Ising model. The random-bond Ising model has quenched random couplings. In particular, the antiferromagnetic interaction such as $J_{ij} = -J$ prevents the duality from constructing a relationship between the original system and another system. If we consider the duality similarly to the non-random Ising model, the duality relation for the antiferromagnetic interaction produces an imaginary interaction. We explicitly write this situation as

$$\mathrm{e}^{-2K'} = -\tanh K, \tag{3.33}$$

where K' is the dual coupling for the antiferromagnetic interactions and has a complex value. Therefore we employ the replica method to map the random-bond Ising model into an effective non-random Ising model with multi-spin interactions. The configurational-averaged edge Boltzmann factor of the replicated random-bond Ising model in Eq. (3.11) is now rewritten as,

$$x_n(\{\phi_{ij}^\alpha\}) = \int dJ_{ij} P(J_{ij}) \exp\left\{\beta J_{ij} \sum_{\alpha=1}^{n} \cos\left(\pi\phi_{ij}^\alpha\right)\right\}, \tag{3.34}$$

where $\phi_{ij}^\alpha = \phi_i^\alpha - \phi_j^\alpha$ and $\pi\phi_i^\alpha$ expresses the angle of the spin on each site with the replica index α. The replica method gives a new point of view to consider random spin systems as another model with n-copied systems sharing common interactions as in Fig. 3.1. The present expression as in Eq. (3.34) permits us to regard the edge Boltzmann factor as a function of the differences ϕ_{ij}^α. Therefore the dual Boltzmann factor of the replicated random-bond Ising model is given by, similarly to the non-random case as in Eq. (2.23),

$$x_n^*(\{k_{ij}^\alpha\}) = \left(\frac{1}{\sqrt{2}}\right)^n \sum_{\{\phi_{ij}^\alpha\}} x_n(\{\phi_{ij}^\alpha\}) \exp\left(\mathrm{i}\pi \sum_{\alpha=1}^{n} k_{ij}^\alpha \phi_{ij}^\alpha\right). \tag{3.35}$$

It is straightforward to extend this relation for its application to q-component spin models with randomness like the Potts model,

$$x_n^*(\{k_{ij}^\alpha\}) = \left(\frac{1}{\sqrt{q}}\right)^n \sum_{\{\phi_{ij}^\alpha\}} x_n(\{\phi_{ij}^\alpha\}) \exp\left(\mathrm{i}\frac{2\pi}{q} \sum_{\alpha=1}^{n} k_{ij}^\alpha \phi_{ij}^\alpha\right). \tag{3.36}$$

The random-bond Ising model is the special case of $q = 2$. We can establish the duality relation for the partition function of the random spin system with q components, whose derivation is similar to the non-random case (2.34), as

$$Z_n[x_n] = q^{nN_s - \frac{nN_B}{2} - n} Z_n[x_n^*]. \tag{3.37}$$

For the square lattice, this duality relation is reduced to, by $N_B = 2N_s$ and the thermodynamic limit,

$$Z_n[x_n] = Z_n[x_n^*]. \tag{3.38}$$

We can construct the duality relation for the replicated spin systems defined on the triangular lattice. Then we use the face Boltzmann factor for convenience. For the case of the random-bond Ising model, the face Boltzmann factor is given by,

after the configurational average for the replicated edge Boltzmann factors as in Eq. (3.34),

$$A_n(\{\phi_{12}^\alpha,\phi_{23}^\alpha,\phi_{31}^\alpha\}) = x_n(\{\phi_{12}^\alpha\})x_n(\{\phi_{23}^\alpha\})x_n(\{\phi_{31}^\alpha\}). \tag{3.39}$$

Similarly to the case without randomness, we need the star-triangle transformation to establish a direct relationship between two models with randomness defined on the triangular lattice as well as the duality. We obtain a relationship between the replicated face Boltzmann factors as, similarly to Eq. (2.63),

$$A_n^*(\{k_{12}^\alpha,k_{23}^\alpha,k_{31}^\alpha\}) = \frac{1}{q^{2n}}\sum_{\{\phi_{ij}^\alpha\}} A_n(\{\phi_{12}^\alpha,\phi_{23}^\alpha,\phi_{31}^\alpha\})\mathrm{e}^{\mathrm{i}\frac{2\pi}{q}\sum_{\alpha=1}^n\left(k_{12}^\alpha\phi_3^\alpha+k_{23}^\alpha\phi_1^\alpha+k_{31}^\alpha\phi_2\right)}. \tag{3.40}$$

For the random-bond Ising model, this dual face Boltzmann factor is reduced to,

$$A_n^*(\{k_{12}^\alpha,k_{23}^\alpha,k_{31}^\alpha\}) = 2^{-\frac{1}{2}n}\sum_{\{n_i^\alpha\}} x_n^*(\{k_1^\alpha-n_i^\alpha\})x_n^*(\{k_2^\alpha-n_i^\alpha\})x_n^*(\{k_3^\alpha-n_i^\alpha\}). \tag{3.41}$$

Similarly to the square lattice, we can obtain the duality relation for the partition function as,

$$Z_{\mathrm{TR},n}[A_n] = Z_{\mathrm{TR},n}[A_n^*]. \tag{3.42}$$

3.2.1 Relationship between Replicated Models

We discuss the relationship between two partition functions related with the duality in random spin systems. We consider the case of the square lattice. The duality relation is given as in Eq. (3.38) As in the case of the non-random Ising model, we consider the normalization by the principal Boltzmann factors as,

$$x_0^{N_B} z_n\left[\frac{x_n}{x_0}\right] = x_0^{*N_B} z_n\left[\frac{x_n^*}{x_0^*}\right], \tag{3.43}$$

where x_0 and x_0^* are the principal Boltzmann factors of the original and the dual $\pm J$ Ising models, respectively. Here we use again the normalized partition function z_n. The principal Boltzmann factors are given by

$$x_0 = \left[\mathrm{e}^{n\beta J_{ij}}\right]_{\mathrm{av}} \tag{3.44}$$

$$x_0^* = \left[\left(\frac{\mathrm{e}^{\beta J_{ij}}+\mathrm{e}^{-\beta J_{ij}}}{\sqrt{2}}\right)^n\right]_{\mathrm{av}}. \tag{3.45}$$

We restrict ourselves to the case of the $\pm J$ Ising model on the square lattice here for simplicity. We give explicitly the edge Boltzmann factors for the $\pm J$ Ising model

from Eqs. (3.34) and (3.35) as,

$$x_n(\{\phi_{ij}^{\alpha}\}) = \frac{\cosh\left\{K_p + K\sum_{\alpha=1}^{n}\cos\pi\phi_{ij}^{\alpha}\right\}}{\cosh K_p} \tag{3.46}$$

$$x_n^*(\{k_{ij}^{\alpha}\}) = \sum_{\tau=\pm1}\frac{\mathrm{e}^{K_p\tau}}{2\cosh K_p}\prod_{\alpha=1}^{n}\left\{\mathrm{e}^{K\tau}+\mathrm{e}^{-K\tau}\cos\pi k_{ij}^{\alpha}\right\}. \tag{3.47}$$

Here we use expressions in terms of the coupling constants as $K_p = \beta_p J$, and $K = \beta J$, where $\mathrm{e}^{-2K_p} = (1-p)/p$. The quantity τ expresses the sign of the couplings for the $\pm J$ Ising model. We define the relative Boltzmann factor $u_{n,k} \equiv x_n(k)/x_0(K_p, K)$ for convenience for the following discussion, where $x_n(k)$ denotes the Boltzmann factor with k antiparallel pairs on the n-replica layer. Both of the original and the dual relative Boltzmann factors are explicitly written as

$$u_{n,k}(K_p, K) = \frac{\cosh\left\{K_p + (n-2k)K\right\}}{\cosh(K_p + nK)} \tag{3.48}$$

$$u_{n,k}^*(K_p, K) = \begin{cases}\tanh K_p \tanh^k K & k \in \text{odd} \\ \tanh^k K & k \in \text{even}\end{cases}, \tag{3.49}$$

We consider a relationship between two normalized partition functions, the original and dual ones, and their behavior on the n-dimensional hyper plain by consideration of change of their arguments $\{u_{n,k}\}$. Following the replica method, we have to consider the duality for the partition function of the n-replicated system with arbitrary number of n. After that, we consider an extrapolation to the quenched limit $n \to 0$. Let us consider several cases with various replica numbers below before taking the $n \to 0$ limit.

3.2.2 Special Cases

We consider that the replica number is less than three. For $n = 1$, the normalized partition function has a single argument similarly to the case of the non-random Ising model. The relative Boltzmann factors for the 1-replicated $\pm J$ Ising model is given as,

$$u_{1,1}(K_p, K) = \frac{\cosh(K_p - K)}{\cosh(K_p + K)} \tag{3.50}$$

$$u_{1,1}^*(K_p, K) = \tanh K_p \tanh K. \tag{3.51}$$

Therefore we can establish the duality relation for K_p and K as for the non-random Ising model.

$$\frac{\cosh\left(K_p^* - K^*\right)}{\cosh(K_p^* + K^*)} = \tanh K_p \tanh K. \tag{3.52}$$

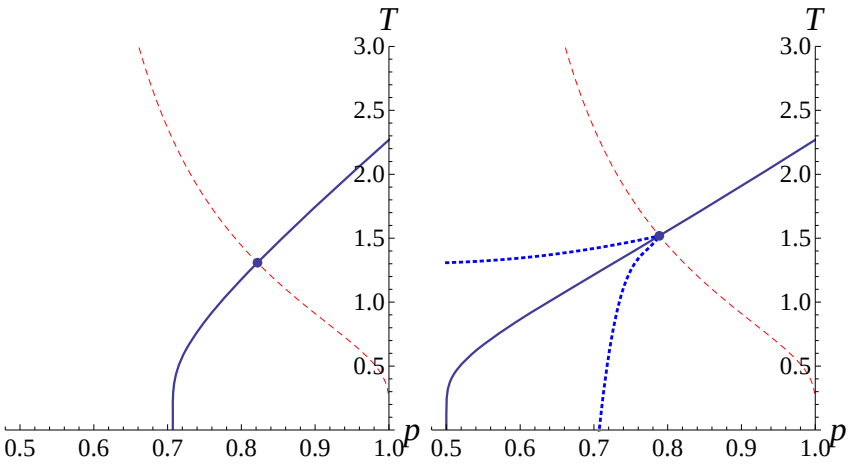

Figure 3.2: The phase diagram derived from the duality for the replica number 1 and 2. The dashed line is the Nishimori line. The points on the Nishimori line express the multicritical points for both of the cases. The bold line in the left panel expresses the phase boundary for the replicated $\pm J$ Ising model with $n = 1$. The bold line in the right panel expresses the phase boundary for the replicated $\pm J$ Ising model with $n = 2$ until the line meets the Nishimori line. The dotted lines in the right panel express exact phase boundaries in the region under the Nishimori line.

We derive a line from the fixed points given by setting $K = K^*$ and $K_p = K_p^*$. This line expresses the phase boundary for the 1-replicated $\pm J$ Ising model as in Fig. 3.2.

Let us next consider the case with $n = 2$. The relative Boltzmann factors of the 2-replicated $\pm J$ Ising model are

$$u_{2,1}(K_p, K) = \frac{\cosh K_p}{\cosh(K_p + 2K)} \tag{3.53}$$

$$u_{2,2}(K_p, K) = \frac{\cosh(K_p - 2K)}{\cosh(K_p + 2K)}. \tag{3.54}$$

We obtain also the dual ones,

$$u^*_{2,1}(K_p, K) = \tanh K_p \tanh K \tag{3.55}$$

$$u^*_{2,2}(K_p, K) = \tanh^2 K. \tag{3.56}$$

We here show the relationship between these relative Boltzmann factors described by two lines in the two-dimensional plane $(u_{2,1}, u_{2,2})$ in Fig. 3.3. As the temperature changes from 0 to ∞, the point representing $(u_{2,1}, u_{2,2})$ moves toward $(1, 1)$,

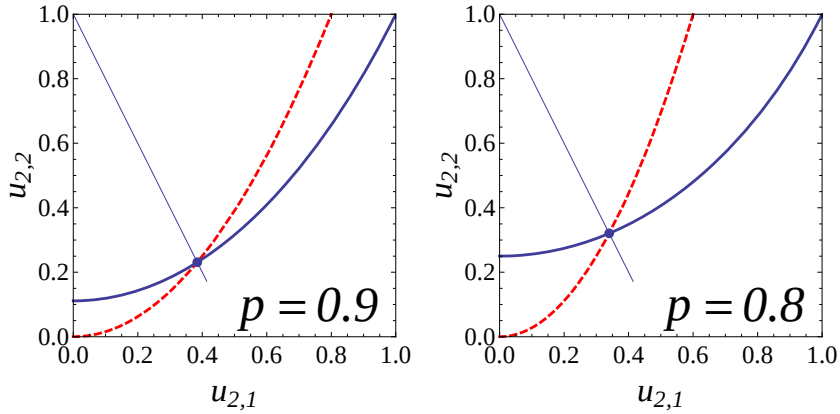

Figure 3.3: Behaviors of the relative Boltzmann factors for the 2-replicated $\pm J$ Ising model with concentration $p = 0.9$ and $p = 0.8$. The original ones are depicted by the solid lines and the dual ones are expressed by the dashed lines. The black points are the intersections which are the fixed points of the duality. The thin lines denote the fixed points of the duality for all p.

which corresponds the high-temperature limit, along the solid lines. Then the corresponding dual point $(u^*_{2,1}, u^*_{2,2})$ moves along the dashed lines in the opposite direction toward $(0, 0)$ as in Fig. 3.3. These behaviors are seen for any value of p. In the case of $p = 1$, that is the non-random Ising model, the solid line completely coincides with the dashed line as in Fig. 3.4. Therefore we can find a transformation $u^*_{2,k}(K) \to u_{2,k}(K^*)$. From this relationship, we obtain again the duality relation $\mathrm{e}^{-2K} = \tanh K$ for the non-random Ising model. On the other hand, there are the intersections of two lines as in Fig. 3.3, though we find that the solid line does not overlap the dashed line for $p < 1$. These correspond to the fixed points of the duality, which are given by $u_{2,k}(K_c) = u^*_{2,k}(K_c)$. We plot these fixed points for various values of p for the 2-replicated $\pm J$ Ising model as in Fig. 3.2. Indeed, the fixed points express the critical points above the Nishimori line. However, under the Nishimori line, the fixed points of the duality fail to give the critical points. Two phase boundaries under the Nishimori line exist, which is known by the previously published result [98]. Therefore the fixed points of the duality may not give the exact location of the critical points in the region under the Nishimori line.

Through two cases with the replica number 1 and 2, it seems that the duality can give the exact location of the critical points for the replicated $\pm J$ Ising model in the restricted region. In addition, we give a remark that we can derive these fixed points by a single equation $x_0(K_p, K) = x^*_0(K_p, K)$ similarly to the non-random spin models as seen previously.

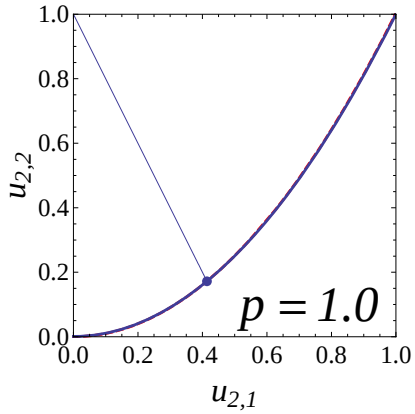

Figure 3.4: Behavior of the relative Boltzmann factors for the 2-replicated non-random Ising model. Two lines overlap as expressed by the solid line. The thin line denotes the fixed point of the duality.

3.2.3 General Cases

We consider the case of the 3-replicated $\pm J$ Ising model. We cannot find intersections, which are the fixed points of the duality, as found in the above cases except for $p = 1$, if the replica number becomes three and beyond. The relative Boltzmann factors are given by

$$u_{3,1}(K_p, K) = \frac{\cosh(K + K_p)}{\cosh(3K + K_p)} \tag{3.57}$$

$$u_{3,2}(K_p, K) = \frac{\cosh(-K + K_p)}{\cosh(3K + K_p)} \tag{3.58}$$

$$u_{3,3}(K_p, K) = \frac{\cosh(-3K + K_p)}{\cosh(3K + K_p)}. \tag{3.59}$$

We obtain also the dual ones,

$$u^*_{3,1}(K_p, K) = \tanh K_p \tanh K \tag{3.60}$$

$$u^*_{3,2}(K_p, K) = \tanh^2 K \tag{3.61}$$

$$u^*_{3,3}(K_p, K) = \tanh K_p \tanh^3 K. \tag{3.62}$$

We describe points corresponding to these relative Boltzmann factors on two-dimensional planes $(u_{3,1}, u_{3,2})$ and $(u_{3,1}, u_{3,3})$ as in Fig. 3.5. As seen in Fig. 3.5, we cannot obtain any fixed points of the duality for the 3-replicated $\pm J$ Ising model with $p \neq 1$. Therefore we find that the duality cannot predict the critical points as the fixed points. Only for the case of the non-random Ising model ($p = 1$) as in Fig. 3.6,

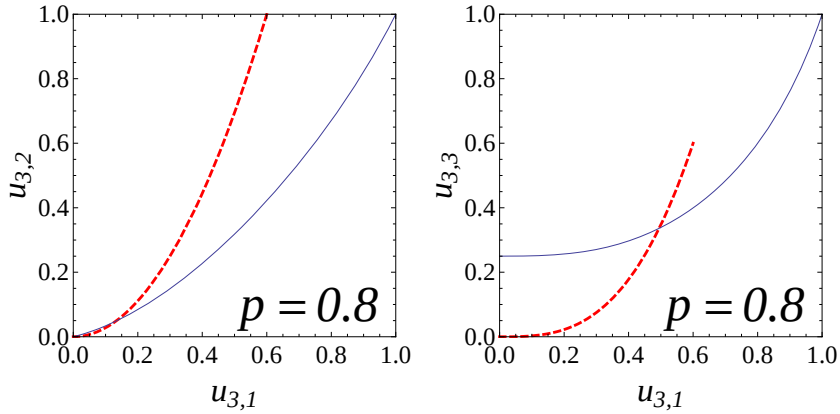

Figure 3.5: Behavior of the relative Boltzmann factors for the 3-replicated $\pm J$ Ising model. The original ones are depicted by the solid line and dual ones are expressed by the thick dashed line.

the solid line expressing $(u_{3,1}, u_{3,2}, u_{3,3})$ coincides with the dashed line representing $(u^*_{3,1}, u^*_{3,2}, u^*_{3,3})$ similarly to the previous cases. The problem of the absence of the fixed point remains for the n-replicated $\pm J$ Ising model with the replica number n beyond three and for the Gaussian Ising model.

The duality is a very useful tool to derive the exact locations of the critical points for non-random spin systems, but may not be applicable to random spin systems found in this section. In particular, before considering extrapolation to the limit $n \to 0$, we find that the duality with the replica method does not always give the fixed point.

In the next chapter, the conjecture on the location of the multicritical point is introduced. For a prediction of the precise location of the multicritical point, we consider the duality for the random-bond Ising model on the Nishimori line in the next chapter. On this line, some advantages for the application of the duality are found.

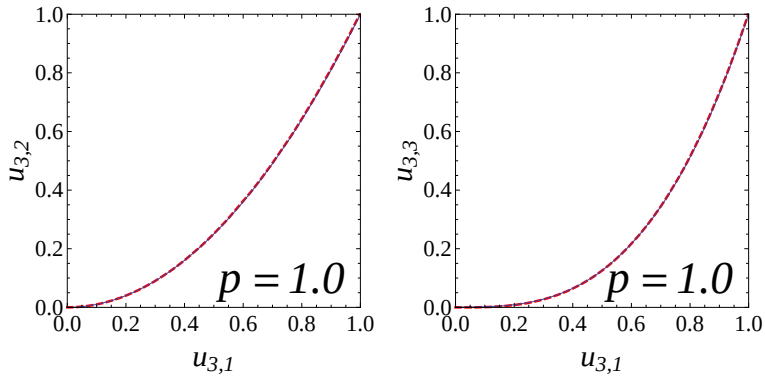

Figure 3.6: Behavior of the relative Boltzmann factors for the 3-replicated non-random Ising model. Two lines are overlap as expressed by the solid line.

Chapter 4

Conjecture on the Location of the Multicritical Point

In the previous chapter, we discussed the possibility to determine the location of the critical points for the $\pm J$ Ising model by the duality. Unfortunately it may be impossible to derive a phase boundary for the random-bond Ising model by the duality with the replica method. We again attempt to apply the duality to the random-bond Ising model by the aid of the gauge symmetry in this chapter. We consider the duality to derive the location of the critical point on the Nishimori line, the multicritical point, for the random-bond Ising model. To give a prediction, we assume some hypotheses. As seen below, it seems that the conjectures for the square and triangular lattices are in good agreement with the existing results with the precision to the third decimal point. Nevertheless the conjectures for the cases on the hierarchical lattices reveal evident inconsistencies with reliable estimations, which are by the exact renormalization group analysis on the hierarchical lattice. We discuss the reasons why such deviations between the conjectures and the exact results exist in this chapter.

4.1 Duality on the Nishimori Line

We start from the exact duality relation for the replicated partition functions of the random-bond Ising model in Eq. (3.43). As shown in the previous chapter, this relation is different from the duality relation for the non-random Ising model because the replicated partition function is a multi-variable function of many-component relative Boltzmann factors. Here we consider the duality relation for the replicated $\pm J$ Ising model on the Nishimori line by setting $K_p = K$.

We again use the relative Boltzmann factors to represent the relationship between two normalized partition functions. When $u_{n,1} = u_{n,2} = \cdots = u_{n,n} = 1$, which

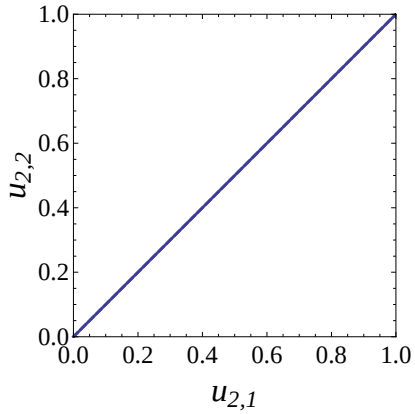

Figure 4.1: Behavior of the relative Boltzmann factors for the 2-replicated $\pm J$ Ising model on the Nishimori line. Two lines describing the original and dual relative Boltzmann factors completely coincide as expressed by the bold line.

corresponds to the high-temperature limit $T \to \infty$ ($K \to 0$), all spin configurations show up with equal probability. Therefore the normalized partition function just counts the number of all the possible spin configurations, 2^{nN_s}. On the other hand, in the low-temperature limit, which is expressed by $u_{n,1} = u_{n,2} = \cdots = u_{n,n} = 0$, the allowed spin configuration is the all-parallel state, for which we have set the energy 0, since the energy is measured from all spin-parallel state by dividing each edge Boltzmann factor by the principal Boltzmann factor x_0. Considering the global inversion degeneracy, we obtain that the partition function becomes 2. In addition, the normalized partition function is a monotonically decreasing function of T as shown in Ref. [99].

For the case with $n = 1$, we can find the duality relation for the coupling constant as in Eq. (3.52). On the other hand, we cannot obtain such a duality relation for $n = 2$ because two lines which describe changes of relative Boltzmann factors show different behaviors. However, on the Nishimori line, two lines coincide perfectly as in Fig. 4.1. Therefore we can establish the duality relation for the coupling K. Indeed it is given by, from correspondence between Eqs. (3.53) and (3.55) by setting $K = K_p$,

$$\frac{\cosh K^*}{\cosh 3K^*} = \tanh^2 K. \tag{4.1}$$

This equation is also obtained from Eqs. (3.54) and (3.56). We can thus obtain the multicritical point as the fixed point of the duality. The fixed point is also derived here from a single equation by the principal Boltzmann factors, similarly to the

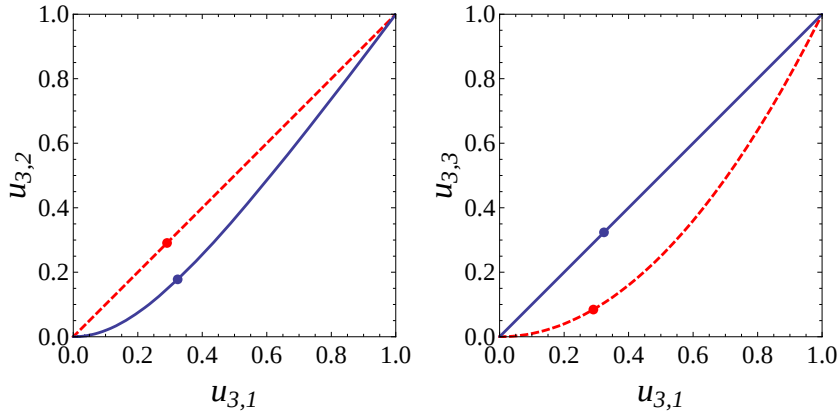

Figure 4.2: Behavior of the relative Boltzmann factors for the 3-replicated $\pm J$ Ising model on the Nishimori line. The solid line expresses the trajectory of the original relative Boltzmann factor and the dashed line denotes that of the dual one. Each dot expresses the solution of Eq. (4.2).

non-random spin systems,

$$x_0(K, K) = x_0^*(K, K), \tag{4.2}$$

where, from Eqs. (3.44) and (3.45)

$$x_0(K_p, K) = \frac{\cosh(K_p + 2K)}{\cosh K_p} \tag{4.3}$$

$$x_0^*(K_p, K) = 2\cosh^2 K. \tag{4.4}$$

These are explicit expressions for the $\pm J$ Ising model of Eqs. (3.44) and (3.45). We thus expect that the duality with the replica method is capable to derive only the exact location of the multicritical point for any number of n by the aid of the gauge symmetry as a special feature on the Nishimori line. Equation (4.2) then gives the location of the multicritical point.

Naturally one attempts to consider the case for the replicated $\pm J$ Ising model with $n = 3$. We show the behavior of the relative Boltzmann factors along the Nishimori line in Fig. 4.2. Unfortunately we find that two lines do not coincide in this case.

Whereas we cannot find the duality relation for the coupling even on the Nishimori line because of the absence of coincidence of two lines, the numerical estimation showed the multicritical point was at the given point by Eq. (4.2) within error bars [88]. Maillard, Nemoto, and Nishimori have then assumed that Eq. (4.2) gives the location of the multicritical point of the $\pm J$ Ising model. This is the conjecture to

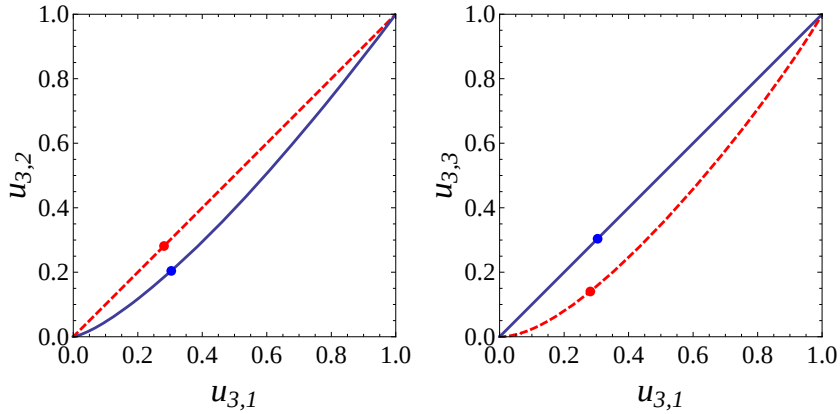

Figure 4.3: Behavior of the relative Boltzmann factors for the 3-replicated Gaussian Ising model on the Nishimori line. The solid line expresses change of the original relative Boltzmann factor and the dashed line denotes that of the dual one. Each dot expresses the solution of Eq. (4.2).

derive the location of the multicritical point of the $\pm J$ Ising model. As shown in Fig. 4.2, we remark that the solution of Eq. (4.2) is not give the fixed point of the duality. If we consider the principal Boltzmann factors similarly, we can construct the conjecture for other random-bond Ising models. One finds again that two lines of the original and dual relative Boltzmann factors do not overlap, if one considers the replicated system for the Gaussian Ising model with $n = 3$. Therefore the solution of Eq. (4.2) for the Gaussian Ising model is also not the fixed point of the duality. However we here have to point out a significant fact that the distance between the two points representing the solution of Eq. (4.2) is smaller than that for the $\pm J$ Ising model shown as in Fig. 4.3.

We here show the derivation of the conjecture of the quenched limit ($n \to 0$) for the case of the random bond Ising model with the general distribution function of J_{ij}. We assume that the conjecture holds valid in the quenched limit of $n \to 0$ of a single equation $x_0 = x_0^*$ similarly to Eq. (4.2), using definitions of the principal Boltzmann factors (3.44) and (3.45),

$$\left[\mathrm{e}^{n\beta J_{ij}}\right]_{\mathrm{av}} = \left[\left(\frac{\mathrm{e}^{\beta J_{ij}} + \mathrm{e}^{-\beta J_{ij}}}{\sqrt{2}}\right)^n\right]_{\mathrm{av}} . \tag{4.5}$$

We evaluate the leading term of the replica number n in this equation as,

$$1 + n\left[\beta J_{ij}\right]_{\mathrm{av}} = 1 - \frac{n}{2}\log 2 + n\left[\log\left(\mathrm{e}^{\beta J_{ij}} + \mathrm{e}^{-\beta J_{ij}}\right)\right]_{\mathrm{av}} . \tag{4.6}$$

From this equation, we obtain an equation for the multicritical point of the random-bond Ising model on self-dual lattices as,

$$\left[\log\left(1+\mathrm{e}^{-2\beta J_{ij}}\right)\right]_{\mathrm{av}} = \frac{1}{2}\log 2. \tag{4.7}$$

We will estimate the location of the multicritical point for several random-bond Ising models in the next section.

For the mutually dual-pair lattices as the triangular and the hexagonal lattices, we can establish the relation between locations of the multicritical points for the mutual pair. We consider the product of two partition functions with different couplings as $Z_n[x(\beta_1)]Z_{\mathrm{D},n}[x(\beta_2)]$. Here we use Z_n for the partition function defined on the original lattice and $Z_{\mathrm{D},n}$ is the one on the dual lattice. We apply the duality to this product of the partition functions and obtain the relation [100],

$$Z_n[x(\beta_1)]Z_{\mathrm{D},n}[x(\beta_2)] = Z_{\mathrm{D},n}[x^*(\beta_1)]Z_n[x^*(\beta_2)]. \tag{4.8}$$

We obtain a relation between the locations of the multicritical points on the mutually dual pair of lattices,

$$x_0(\beta_1)x_0(\beta_2) = x_0^*(\beta_1)x_0^*(\beta_2), \tag{4.9}$$

where β_i expresses the inverse temperature corresponding to the location of the multicritical point for each system. This relation yields, by taking the leading term of n, similarly to the case of the self-dual lattice,

$$\sum_{k=1}^{2}\left[\log\left(1+\mathrm{e}^{-2\beta_k J_{ij}}\right)\right]_{\mathrm{av}} = \log 2. \tag{4.10}$$

4.2 Multicritical Point

In this section, we show all the results obtained by the conjecture (4.7) and (4.10).

4.2.1 Random-Bond Ising Model on the Square Lattice

We can rewrite Eq. (4.7) for the $\pm J$ Ising model in terms of the probability p for $J_{ij} = J$ as,

$$-p\log_2 p - (1-p)\log_2(1-p) = \frac{1}{2}. \tag{4.11}$$

The left-hand side of this equation is the binary entropy defined as $H(p)$. Equation (4.11) gives $p_c = 0.889972$ as the prediction for the location of the multicritical point [87, 88].

Type	Conjecture	Numerical result
SQ $\pm J$	$p_c = 0.889972$ [87, 88]	0.8905(5) [56]
		0.8906(2) [57]
		0.8907(2) [58]
		0.8900(5) [59]
		0.8894(9) [60]
		0.8907(4) [61]
		0.89081(7) [62]
SQ Gaussian	$J_0 = 1.021770$ [87, 88]	1.02098(4) [61]
TR $\pm J$	$p_c = 0.835806$ [101]	0.8355(5) [59]
TR Gaussian	$J_0 = 0.798174$	—
HEX $\pm J$	$p_c = 0.932704$ [101]	0.9325(5) [59]
HEX Gaussian	$J_0 = 1.270615$	—
SQ Potts($q = 3$)	$p_c = 0.079731$ [87, 88]	0.079-0.080 [102]

Table 4.1: Comparisons between the conjecture and the existing numerical results. SQ denotes the square lattice. TR expresses the triangular lattice and HEX is the hexagonal lattice.

For the Gaussian Ising model, we cannot obtain an appealing expression as the case for the $\pm J$ Ising model. However we can estimate the location of the multicritical point by the numerical estimation of the following equation.

$$\int_{-\infty}^{\infty} P(J_{ij}) \log_2 \left(1 + \mathrm{e}^{-2J_0 J_{ij}}\right) = \frac{1}{2}, \tag{4.12}$$

where $P(J_{ij})$ is the distribution function of the Gaussian Ising model defined in Eq. (3.5). The left-hand side of this equation is expressed below as $G(J_0)$. The solution of $G(J_0) = 1/2$ gives $J_0 = 1.021770$ [87, 88]. The above conjectures for the $\pm J$ Ising model and the Gaussian model are compared with other results by various numerical approaches in Table 4.1. They are in good agreement to the third digit for the $\pm J$ Ising model and to the second digit for the Gaussian model with the existing results as in Table 4.1.

4.2.2 Potts Spin Glass on the Square Lattice

The conjecture is applicable to the Potts spin glass defined by the Hamiltonian,

$$H = -J \sum_{\langle ij \rangle} \delta \left(\phi_{ij} + l_{ij}\right), \tag{4.13}$$

where $\phi_{ij} \equiv \phi_i - \phi_j$ expresses the difference between adjacent Potts spins taking an integer value between 0 and $q-1$. The quantity l_{ij} is the random variable following the distribution function given as

$$P(l_{ij}) = \left\{ \begin{array}{ll} 1-(q-1)p & (l_{ij}=0) \\ p & (l_{ij} \neq 0) \end{array} \right\} = \frac{\mathrm{e}^{K_p \delta(l_{ij})}}{\mathrm{e}^{K_p}+q-1}, \tag{4.14}$$

where $\mathrm{e}^{K_p} \equiv \{1-(q-1)p\}/p$. The Potts spin glass has the gauge symmetry similarly to the random-bond Ising model. For the Potts spin variables and random variables, we define the gauge transformation as,

$$\phi_i \rightarrow \phi_i + s_i \tag{4.15}$$

$$l_{ij} \rightarrow l_{ij} - (s_i - s_j). \tag{4.16}$$

Here s_i is an integer between 0 and $q-1$. Therefore we can establish the Nishimori line by setting $\beta J = K_p$, where the internal energy can be calculated exactly and the specific heat can be bounded as in the case of the random-bond Ising model [103].

We give the conjecture for the location of the multicritical point from Eq. (4.2), similarly to the case (4.11) of the random-bond Ising model [87, 88].

$$-\{1-(q-1)p\}\log\{1-(q-1)p\} - (q-1)p\log p = \frac{1}{2}\log q. \tag{4.17}$$

The solutions are obtained as $p_c = 0.079731$ for $q=3$, $p_c = 0.063097$ for $q=4$, and $p_c = 0.052467$ for $q=5$. We list the conjecture for $q=3$ in comparison with the existing result for $q=3$ in Table 4.1. Though we show a comparison for one example in the Potts spin glass because of absence of other results, we find the conjecture works well to the third digit also for this model.

4.2.3 Random-Bond Ising Model on the Triangular Lattice

The triangular lattice is not a self-dual lattice. Therefore we need to use the star-triangular transformation to construct the direct relationship between the original triangular lattice and another triangular lattice. Then we assume that a single equation inspired by the non-random Ising model on the triangular lattice as in Eq. (2.73), similarly to the case for the random-bond Ising model on the square lattice as,

$$A_0 = A_0^*. \tag{4.18}$$

These principal Boltzmann factors are for the replicated random-bond Ising model on the triangular lattice. They are given by applications of the replica method and

configurational average to the definition of the face Boltzmann factor and the dual one as in Eqs. (3.39) and (3.41) with the random interactions as,

$$A_0 = \left[\mathrm{e}^{n\beta(J_{12}+J_{23}+J_{31})} \right]_{\mathrm{av}} \tag{4.19}$$

$$\begin{aligned} A_0^* &= \left[2^{-\frac{n}{2}} \sum_{S_0^\alpha} \prod_{i=1}^{3} \left(\frac{\mathrm{e}^{\beta J_{i0}} + \mathrm{e}^{-\beta J_{i0}} S_0}{\sqrt{2}} \right)^n \right]_{\mathrm{av}} \\ &= 2^n \left[\left(\prod_{i=1}^{3} \cosh \beta J_{i0} + \prod_{i=1}^{3} \sinh \beta J_{i0} \right)^n \right]_{\mathrm{av}} . \end{aligned} \tag{4.20}$$

The summation over S_0 corresponds to the star-triangle transformation. We attempt to apply the procedure of the conjecture to the face principal Boltzmann factors in Eqs. (4.19) and (4.20). Following the replica method, we take the leading terms of the replica number n and obtain the relation

$$\left[\log \left\{ \prod_{i=1}^{3} \cosh \beta J_{i0} + \prod_{i=1}^{3} \sinh \beta J_{i0} \right\} \right]_{\mathrm{av}} - \beta \left[(J_{12} + J_{23} + J_{31}) \right]_{\mathrm{av}} = -\log 2. \tag{4.21}$$

This equation gives an equation to predict the location of the multicritical point for the $\pm J$ Ising model on the triangular lattice as,

$$\begin{aligned} &2p^2(3-2p)\log p + 2(1-p)^2(1+2p)\log(1-p) + \log 2 \\ &\quad = p(4p-6p+3)\log(4p-6p+3) \\ &\qquad +(1-p)(4p^2-2p+1)\log(4p^2-2p+1). \end{aligned} \tag{4.22}$$

The location of the multicritical point is estimated as $p_c = 0.835806$ [101]. This can be related with the one on the hexagonal lattice by the relation (4.10), which is reduced to, for the case of the $\pm J$ Ising model,

$$H(p_{\mathrm{TR}}) + H(p_{\mathrm{HEX}}) = 1, \tag{4.23}$$

where p_{TR} and p_{HEX} denote the locations of the multicritical points on the triangular and hexagonal lattices, respectively. The location of the multicritical point for the $\pm J$ Ising model on the hexagonal lattice is predicted as $p_c = 0.932704$ [101]. Both of the results for the triangular and hexagonal lattices are compared with the results $p_{\mathrm{TR}} = 0.8355(5)$ and $p_{\mathrm{HEX}} = 0.9325(5)$ investigated with the help of finite-size scaling and conformal-invariance concepts [59]. In the case of the $\pm J$ Ising model on the triangular and hexagonal lattices, the conjecture is successful, with the precision to the third decimal point, in deriving the locations of the multicritical points as in Table 4.1.

We give also our predictions for the Gaussian Ising model on triangular lattice by numerical estimations of the relation (4.21), by the triple integration over $\{J_{ij}\}$, as

$$\int_{-\infty}^{\infty} \prod_{i=1}^{3} P(J_{0i}) dJ_{0i} \log \left\{ \prod_{i=1}^{3} \cosh \beta J_{i0} + \prod_{i=1}^{3} \sinh \beta J_{i0} \right\} - 3J_0^2 = -\log 2. \qquad (4.24)$$

where J_0 denotes the location of the multicritical point and $P(J_{ij})$ is the distribution function defined in Eq. (3.5). The result is $J_{0\mathrm{TR}} = 0.79817$ and this is related with $J_{0\mathrm{HEX}} = 1.27061$ the location of the Gaussian Ising model on the hexagonal lattice by the relation (4.9). We have not found published results by other approaches for the Gaussian Ising model on the triangular and hexagonal lattices. Therefore we cannot conclude whether the conjecture is valid or not.

Comparing the conjecture and other results as in Table 4.1, we accept that the conjecture can indeed derive the locations of the multicritical points with the precision to the third digit especially for the $\pm J$ Ising model, or at least second digit for the Gaussian Ising model, although two lines of the replicated spin systems for the original and dual random spin systems do not coincide. Unfortunately, there are also several cases that the conjecture does not always work well to the third digit, differently from the above cases. We show several inconsistent cases below, the conjecture for the hierarchical lattices.

4.2.4 Hierarchical Lattices

When we apply the renormalization group analysis to the regular lattice, we need some approximations to iterate the procedure of the renormalization in general. However the special structure of hierarchical lattices helps the renormalization group analysis to give the exact result. Construction of a hierarchical lattice starts from a single bond, and we iterate the process to substitute the single bond with a unit cell of more complex structure as in Fig. 4.4. Because a hierarchical lattice has such an iterative structure consisting of unit cells as shown in Figs. 4.4, we again obtain the same structure after we trace out the degrees of freedom, as denoted by white circles, on each unit cell in renormalization group calculations, which are the inverse processes of the construction. Therefore the renormalization by summation over white-colored sites in each unit cell gives another effective coupling constant by a relation,

$$A \mathrm{e}^{K^{(r)} S_i S_j} = \sum_{\{S_k\}} \mathrm{e}^{K^{(r-1)}(S_i S_1 + S_i S_2 + S_1 S_2 + S_1 S_j + S_2 S_j)}, \qquad (4.25)$$

where the superscript of the coupling constant denotes the step of renormalization and the indices of spins express sites as labeled in Fig. 4.4. This is reduced to the

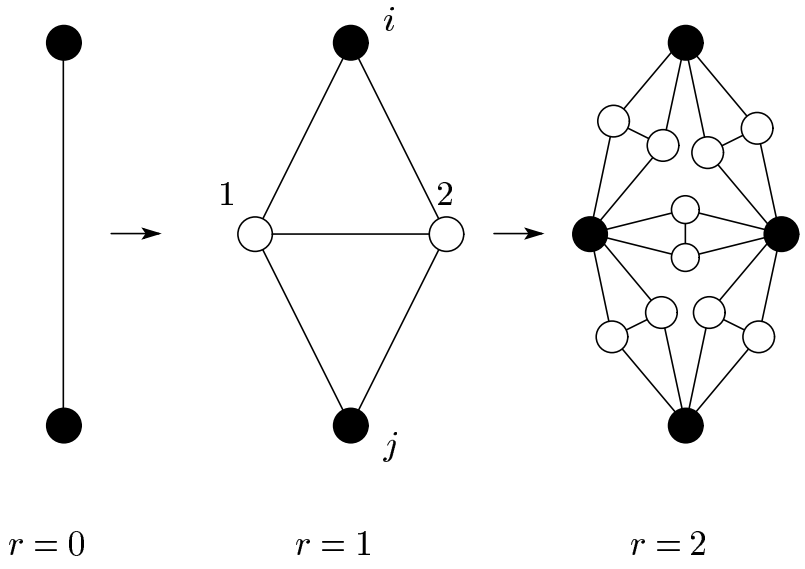

Figure 4.4: A self-dual hierarchical lattice.

following recursion relation for the coupling constant of the Ising model defined on the hierarchical lattice as in Fig. 4.4,

$$\mathrm{e}^{-2K^{(r)}} = \frac{4\cosh K^{(r-1)}}{\mathrm{e}^{5K^{(r-1)}} + 2\mathrm{e}^{-K^{(r-1)}} + \mathrm{e}^{-3K^{(r-1)}}}. \tag{4.26}$$

This recursion relation yields the flow of the renormalization as in Fig. 4.5. Depending on the initial temperature, the coupling constant changes into two different fixed points $K = 0$ and $K = \infty$ of the renormalization. These fixed points correspond to paramagnetic and ferromagnetic phases. The unstable fixed point is given as $K_c = 0.440687$, or equivalently $\mathrm{e}^{-2K_c} = \sqrt{2} - 1$. The critical point on the hierarchical lattice as in Fig. 4.4 is the same as the fixed point of the duality, because this hierarchical lattice is a self-dual lattice. As shown above, the structure of the hierarchical lattice enables us to obtain the exact location of the critical point from the evaluation of the simple recursion relation as in Eq. (4.26).

Even for the random spin systems, this advantage of the renormalization holds on hierarchical lattices. Our task is to evaluate recursion relations of coupling constants following the distribution function of bonds, which relates the sets of the coupling constants $\{K_{ij}^{(r)}\}$ after renormalization with $\{K_{ij}^{(r-1)}\}$ before renormalization. The examination of statistics of resulting coupling constants enables us to obtain another distribution depending on the initial temperature and randomness.

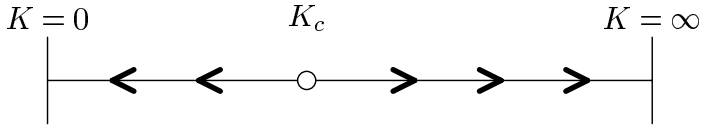

Figure 4.5: Flow of the renormalization for the non-random Ising model on the hierarchical lattice in Fig. 4.4.

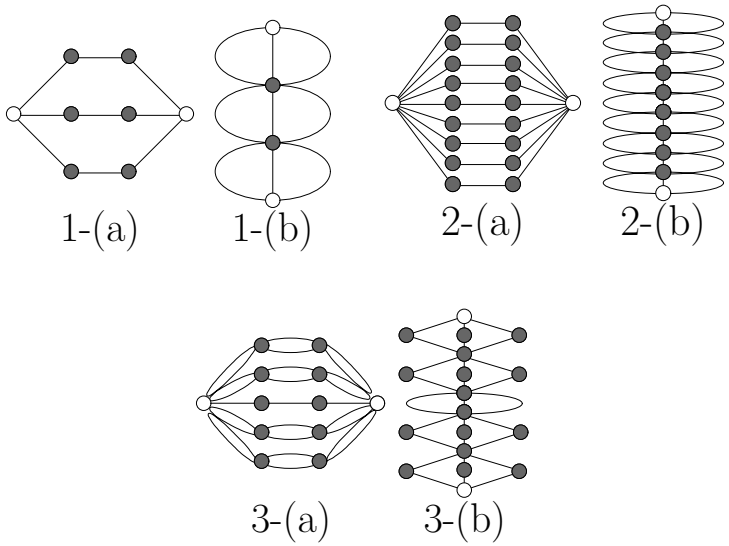

Figure 4.6: Three mutually dual pairs of hierarchical lattices.

The renormalized coupling constants reflect the phase of the random spin system under consideration.

Hinczewski and Berker investigated the locations of the multicritical points on three mutually dual pairs of hierarchical lattices as in Fig. 4.6 [92]. They examined the conjectured relation for the mutually dual pairs, which is expected to be satisfied similarly to the case of the pair of the triangular and hexagonal lattices,

$$H(p_a) + H(p_b) = 1, \tag{4.27}$$

where p_a and p_b denote the location of the multicritical point on the hierarchical lattices. The results were not perfectly consistent with the above relation as $H(p_a) + H(p_b) = 1.017, 0.983$ and 0.991. Similarly to these confirmations, here we show investigations of the validity of the relation (4.27) for the $\pm J$ Ising model and the

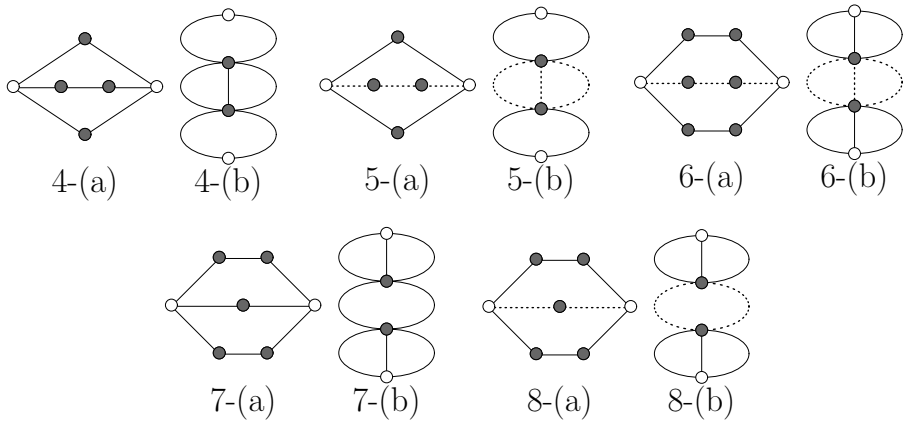

Figure 4.7: Additional five mutually dual pairs of hierarchical lattices. Bonds denoted by the dashed lines stay unrenormalized, whereas bonds expressed by the solid lines are replaced by the renormalized interactions at each renormalization.

Gaussian Ising model for other five mutually dual pairs as in Fig. 4.7 [104]. A stochastic calculation of the renormalization group analysis, proposed by Nobre [105] is carried out for the derivation of the location of the multicritical points for the mutually dual pairs. The Gaussian Ising model is expected to satisfy the similar relation to the case for the $\pm J$ Ising model

$$G(J_a) + G(J_b) = 1, \tag{4.28}$$

where J_a and J_b express the average of the Gaussian distribution corresponding to the locations of the multicritical points. The confirmations of the relation (4.27) for the $\pm J$ Ising model and of this relation for the Gaussian Ising model are shown in Table 4.2. We find small but non-negligible deviations in most cases. Remarkable results are found in the cases for the Gaussian Ising model. The discrepancies from the conjectured relation are much smaller than those for the $\pm J$ Ising model.

Verifications of the conjecture as shown above are carried out also for the self-dual hierarchical lattices with various types of the unit cell as in Fig. 4.8 [104]. The conjecture gives the same locations as that of the square lattice, because the conjecture does not depend on particular structure of the hierarchical lattices, but on the self duality. Nevertheless the locations of the multicritical point as shown in Table 4.3 are slightly different among each other, which reflect the individual structures of the unit cells of the hierarchical lattices. Therefore we have to reconsider the validity of the underlying hypothesis of the conjecture. This consideration will yield a way to improve the conjecture to derive more precise locations of the multicritical point as shown in the following chapters.

Lattice	p_a	p_b	$H(p_a)+H(p_b)$	J_a	J_b	$G(J_a)+G(J_b)$
1	0.9338(7)	0.8265(6)	1.017(4)	0.7605(5)	1.3174(9)	1.0005(8)
2	0.8149(6)	0.9487(7)	0.983(4)	0.7655(5)	1.3118(9)	1.0000(8)
3	0.7526(5)	0.9720(7)	0.991(5)	0.5569(4)	1.6151(11)	0.9999(7)
4	0.8712(6)	0.9079(6)	0.998(4)	0.9704(7)	1.0730(8)	1.0009(10)
5	0.8700(6)	0.9081(7)	1.000(4)	0.9701(7)	1.0733(8)	1.0009(10)
6	0.9337(7)	0.8266(6)	1.017(4)	1.3175(9)	0.7606(5)	1.0003(8)
7	0.9084(6)	0.8678(6)	1.005(4)	1.1450(8)	0.9040(6)	1.0001(9)
8	0.9065(6)	0.8686(6)	1.009(4)	1.1436(8)	0.9055(6)	1.0005(9)

Table 4.2: The locations of the multicritical points for the $\pm J$ and Gaussian Ising models on mutually dual pairs of hierarchical lattices. The results for lattices number 1 to 3 reproduce the results by Hinczewski and Berker.

Lattice	p_c	$2H(p_c)$
$b=2$ SD($\pm J$)	0.8915(6)	0.991(4)
$b=3$ SD($\pm J$)	0.8903(2)	0.998(1)
$b=4$ SD($\pm J$)	0.8892(6)	1.005(4)
$b=5$ SD($\pm J$)	0.8895(6)	1.003(4)
$b=6$ SD($\pm J$)	0.8890(6)	1.006(4)
$b=7$ SD($\pm J$)	0.8891(6)	1.005(4)
$b=8$ SD($\pm J$)	0.8889(6)	1.006(4)
Lattice	J_0	$2G(J_0)$
$b=3$ SD(Gaussian)	1.0209(3)	1.0011(4)

Table 4.3: The locations of the multicritical points for the $\pm J$ Ising and Gaussian models on the self-dual hierarchical lattices. Also shown are the values $2H(p_c)$ and $2G(J_0)$, which should be unity according to the conjecture.

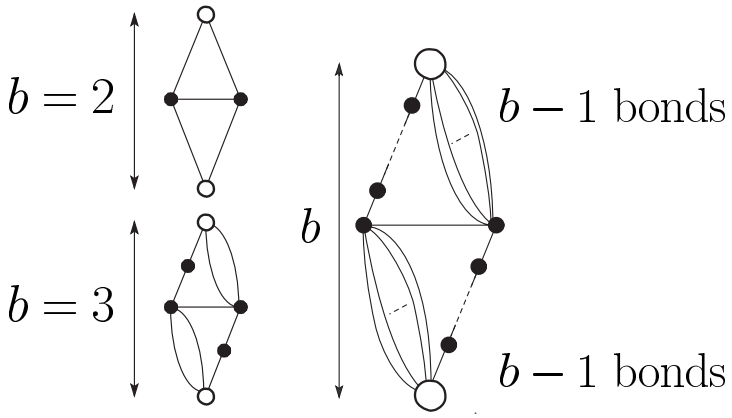

Figure 4.8: Several self-dual hierarchical lattices. The number of bonds is expressed by the scale factor b.

4.3 Phase Boundary and Historical Remarks

Before closing the present chapter, we explain some historical remarks and refer to the possibility of derivation of the critical points, except for the multicritical point, in random spin systems by the duality in conjunction with the replica method. The conjecture without restriction of the Nishimori-line condition gives predictions for the critical points. More explicitly, the following relation is the conjecture on the phase boundary for the $\pm J$ Ising model,

$$x_0(K_p, K) = x_0^*(K_p, K). \tag{4.29}$$

Considering the extrapolation of the $n \to 0$ limit, we obtain an equation from the leading term of the replica number n,

$$p \log\left(1 + \mathrm{e}^{-2\beta J}\right) + (1-p) \log\left(1 + \mathrm{e}^{2\beta J}\right) = \frac{1}{2} \log 2. \tag{4.30}$$

However this equation gives quite a different phase boundary from the expected one for the $\pm J$ Ising model as in Fig. 4.9, whereas the conjectured multicritical point is located at the lowest value of the concentration p shown rigorously by the gauge symmetry [34]. In the limit without any randomness, the duality can give the exact critical point that is the transition point of the non-random Ising model. Therefore we naturally expect that the duality can also derive the phase boundary near the critical point T_c of the non-random Ising model, because the effect by randomness is weak near T_c. The slope of T_c for the $\pm J$ Ising model is estimated by the conjectured

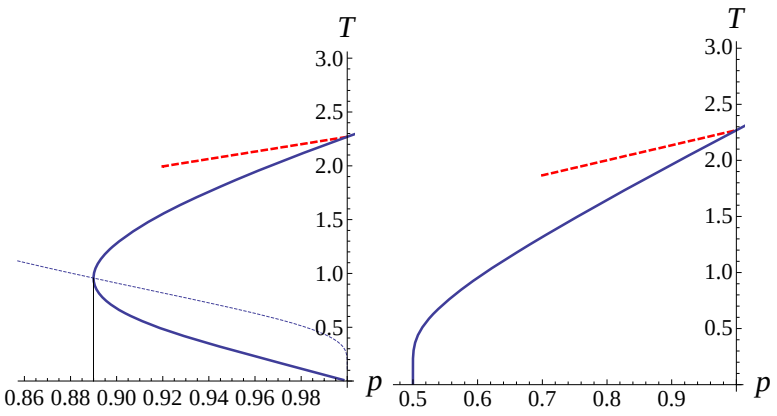

Figure 4.9: Conjectured phase diagram for the $\pm J$ Ising model and the dilute Ising model. The solid lines describe the conjectured phase boundaries and the dashed lines express the slope from the critical point of the non-random Ising model derived by the perturbation theory. For the $\pm J$ Ising model, the dotted line expresses the Nishimori line, and the vertical thin line is expected phase boundary in the low-temperature region.

relation (4.29) without restriction $K = K_p$ as,

$$\frac{1}{T_c}\left.\frac{dT}{dp}\right|_{T=T_c} = 3.41421. \tag{4.31}$$

However the perturbation theory shows that this result is inaccurate [106], because the slope should become

$$\frac{1}{T_c}\left.\frac{dT}{dp}\right|_{T=T_c} = 3.20911. \tag{4.32}$$

We find that the conjecture fails to derive the precise phase boundary even near T_c. The conjecture was proposed before the discovery of the Nishimori line [107, 108]. When the conjecture appeared, the conjecture was considered to be capable to describe the phase boundary for the random-bond Ising model, including the diluted Ising model defined by the distribution function,

$$P(J_{ij}) = p\delta(J_{ij} - J) + (1-p)\delta(J_{ij}). \tag{4.33}$$

Therefore the conjecture (4.7) yields the prediction for the phase boundary as

$$p \log\left(1 + \mathrm{e}^{-2\beta J}\right) + (1-p)\log 2 = \frac{1}{2}\log 2. \tag{4.34}$$

This equation describes the phase boundary as in Fig. 4.9. However this prediction is also an inaccurate solution near T_c, whereas the conjecture succeeded in deriving the exact solution for the critical point $p_c = 0.5$ in the ground state, and the slope around p_c [107, 109, 110] as in Fig. 4.9. The slope of T_c for the diluted Ising model by the conjecture is estimated as,

$$\frac{1}{T_c}\frac{dT}{dp}\bigg|_{T=T_c} = 1.34254. \tag{4.35}$$

On the other hand, the perturbation theory again gives the inconsistent result with this value [110],

$$\frac{1}{T_c}\frac{dT}{dp}\bigg|_{T=T_c} = 1.32926. \tag{4.36}$$

In the case for the Potts diluted model, it was also reported that the deviations for the slope from the non-random spin system between the result by the conjecture and the one by the perturbation theory as shown above [111, 112]. Therefore the conjecture, an application of the duality with the replica method, was considered not to be a reliable approach to precisely analyze the phase transitions in random spin systems. The duality with the replica method was argued by Aharony and Stephen [113]. They concluded that the duality in conjunction with the replica method for the random spin systems might not be applicable to the random spin systems, because the behaviors of the edge Boltzmann factors for the original and dual replicated random spin systems did not coincide in general as our discussion in the previous chapter.

However, for the last decade, we have found the possibility that the gauge symmetry on the Nishimori line enables us to predict the location of the multicritical point in good agreement with many numerical verifications [87, 88, 99, 100, 101]. The conjecture is again studied as a theory to derive the critical points in random spin systems. On the other hand the discrepancies have also been found in the cases on the hierarchical lattices as seen in the previous section. These are non-negligible problems on the conjecture. It is then necessary to reconsider the validity of the conjecture and to investigate reasons generating the deviations between the conjecture and exact solutions on the hierarchical lattices. The investigation for the phase transitions in random spin systems on hierarchical lattices has given the way to improve the conjecture to derive more precise locations of the critical points even for the slope of T_c as well as the location of the multicritical point as shown in next chapter.

Chapter 5

Improved Conjecture for Hierarchical Lattices

We found the deviations between the results by the conjecture and the renormalization-group analysis with the maximum discrepancy of 2% for the cases of the $\pm J$ Ising model on the mutually dual pairs of the hierarchical lattices labeled by 1 and 6 in Figs. 4.6 and 4.7 as in Table 4.2. It is considered that these crucial differences are caused by the fact that two lines of the relative Boltzmann factors do not overlap found in Chapter 3. We reconsider the duality with the replica method for the random-bond Ising model discussed in Chapter 3 from a point of view of the renormalization group. On the hierarchical lattices, we can deal with the renormalization group analysis by the evaluation of recursion relations as in Eq. (4.25). As will be seen later, two lines expressing changes of the relative Boltzmann factors show tendency to approach a common renormalized system after a sufficient number of renormalization steps. This fact enables us to identify the multicritical point as the fixed point of the duality.

5.1 Duality and Renormalization

We restrict ourselves to the n-replicated $\pm J$ Ising model defined on hierarchical lattices. After the configurational average, the replicated random spin systems become effective non-random spin systems without any randomness. For example, we consider the 3-replicated $\pm J$ Ising model under the Nishimori-line condition $K_p = K$ with the following relative Boltzmann factors, from the evaluation of Eqs. (3.34)

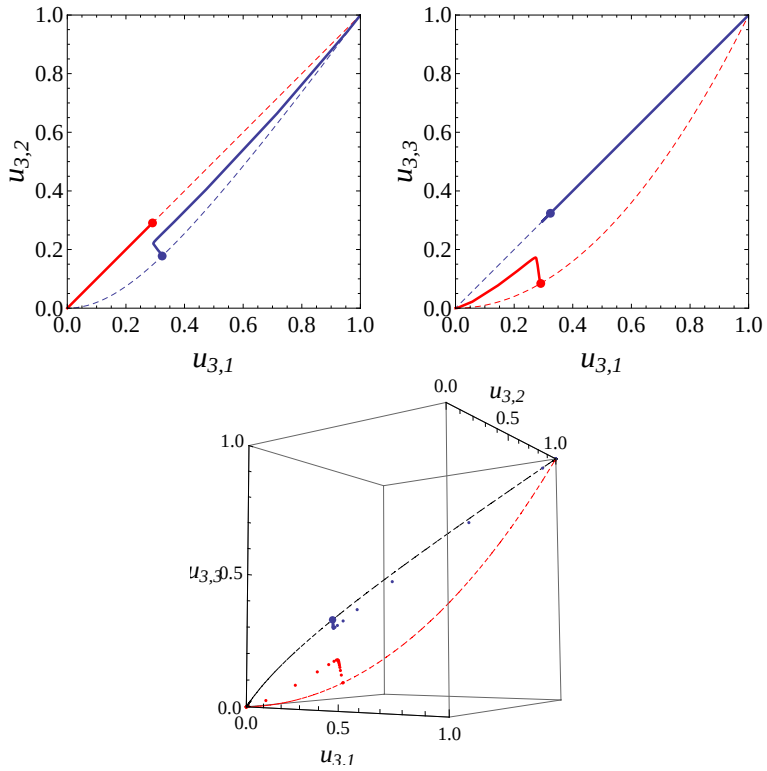

Figure 5.1: The renormalization flow of the 3-replicated $\pm J$ Ising model. The bottom plot is the points expressing the renormalized relative Boltzmann factors for both of the original and dual systems at each renormalization step. The thick curves represent the renormalization flows in the two panels on the top. The dashed curves express the points of the relative Boltzmann factors. (see also Fig. 4.2.)

and (3.35),

$$u_3(\{\phi_{ij}^{\alpha}\}) = \frac{\cosh\left\{K(1+\sum_{\alpha=1}^{3}\cos\pi\phi_{ij}^{\alpha}\right\})}{\cosh 4K} \tag{5.1}$$

$$u_3^*(\{\phi_{ij}^{\alpha}\}) = \sum_{\tau=\pm 1}\frac{\mathrm{e}^{K\tau}}{2^3\cosh^3 K}\prod_{\alpha=1}^{3}\left(\mathrm{e}^{K\tau}+\mathrm{e}^{-K\tau}\cos\pi\phi_{ij}^{\alpha}\right), \tag{5.2}$$

where $\phi_{ij}^{\alpha}=\phi_i^{\alpha}-\phi_j^{\alpha}$. The multicritical point for the 3-replicated $\pm J$ Ising model defined on the square lattice is confirmed to be located at the predicted point by the conjecture (4.2) within its error bars in Ref. [88]. Also on hierarchical lattices, such estimations are worthwhile to be considered. We calculate numerically the location of the multicritical point for the replicated $\pm J$ Ising model following the procedure of the renormalization group on the hierarchical lattices in this section. For example,

we consider the following recursion relation for the 3-replicated $\pm J$ Ising model on one of the self-dual hierarchical lattices depicted in Fig. 4.4, similarly to the case of the non-random Ising model as in Eq. (4.25),

$$Au_3^{(r)}(\{\phi_{ij}^{\alpha}\}) = \sum_{\{\phi_k^{\alpha}\}} u_3^{(r-1)}\left(\phi_{i1}^{\alpha}\right) u_3^{(r-1)}\left(\phi_{i2}^{\alpha}\right) u_3^{(r-1)}\left(\phi_{12}^{\alpha}\right) u_3^{(r-1)}\left(\phi_{1j}^{\alpha}\right) u_3^{(r-1)}\left(\phi_{2j}^{\alpha}\right), \tag{5.3}$$

The numerical evaluation of this recursion relation for both the original and dual relative Boltzmann factors gives us the renormalization flow described as in Fig. 5.1.

The specialty of the hierarchical lattice does not change the functional form of the partition function by the renormalization, and permits us to describe the renormalization flow in the same space $(u_{3,1}, u_{3,2}, u_{3,3})$ expressing the change of the relative Boltzmann factors before the renormalization. On other two-dimensional lattices, other types of interactions are generated after the renormalization. Therefore we cannot describe the change of the relative Boltzmann factors in the same space. The flow from two lines go toward fixed points located away from them, depending on the value of the given coupling K, that is the initial condition. One fixed point at $(u_{3,1}, u_{3,2}, u_{3,3}) = (1, 1, 1)$ expresses the point corresponding to the paramagnetic phase. Therefore the renormalization flow is absorbed into this point, given the high-temperature initial condition as in Fig. 5.1. On the other hand, the corresponding dual point moves toward another fixed point at $(u_{3,1}, u_{3,2}, u_{3,3}) = (0, 0, 0)$ corresponds to the ferromagnetic phase as in Fig. 5.1.

From the observation of such behaviors of the renormalization flows related by the duality, we recognize the existence of an unstable fixed point for the original and the dual n-replicated $\pm J$ Ising model as in Fig. 5.2. We consider the trajectory of the relative Boltzmann factors with the replica number n. For simplicity, we write the representative point of the relative Boltzmann factor as $(u_1, u_2, \cdots, u_n)$. The initial conditions, the original relative Boltzmann factors $(u_1, u_2, \cdots, u_n)$, are denoted by the solid line in Fig. 5.2 and the corresponding the dual ones $(u_1^*, u_2^*, \cdots, u_n^*)$ are expressed by the dashed line on the same space as in Fig. 5.2. We consider the projections on the two-dimensional plane (u_1, u_2) for the relative Boltzmann factors as in Fig. 5.2, for convenience. The renormalized system also has a representative point in the same space as in Fig. 5.2, because of the specialty on the hierarchical lattice. We express such a development of relative Boltzmann factors at each renormalization step on the n-dimensional hyperspace as $(u_1^{(r)}, u_2^{(r)}, \cdots, u_n^{(r)})$, where the superscript means the number of renormalization steps. Therefore we can depict the renormalization flow following the arrows emanating from p_c and d_c to C, p_h and d_l to P, and p_l and d_h to F. Here F is the fixed point corresponding to the low-temperature limit, and P expresses the fixed point of the high-temperature limit. The renormalization flow from the multicritical point p_c reaches the unstable fixed

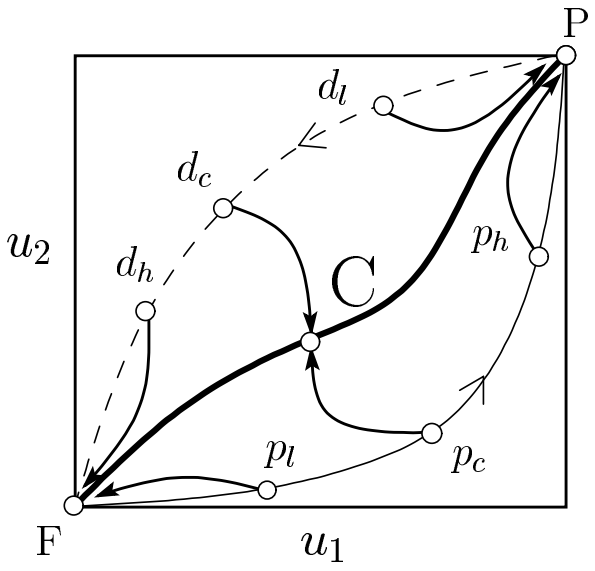

Figure 5.2: A schematic picture to consider the renormalization flow and the duality for the replicated $\pm J$ Ising model.

point C, $(u_1^{(\infty)}, u_2^{(\infty)}, \cdots, u_n^{(\infty)})$. On the other hand, there is the point d_c related with p_c by the duality. We expect that the renormalization flow from this dual point d_c also reaches the same unstable fixed point C because p_c and d_c represent the same multicritical point. Considering the above property of the renormalization flow as well as the duality, we find that the duality relates two trajectories of the renormalization flow from p_c and from d_c, tracing the renormalization flows at each renormalization. In other words, after a sufficient number of renormalization steps, the thin curve representing the original system and the dashed curve for the dual system both approach the common renormalized system depicted as the bold line in Fig. 5.2, which goes through the fixed point C. We estimate the initial condition aiming at this unstable fixed point to determine the location of the multicritical point for the replicated $\pm J$ Ising model and we show the obtained results for several self-dual hierarchical lattices with the replica number 3 as well as 4 in Table 5.1.

Similarly to the results for the quenched limit $n \to 0$ obtained in the previous chapter, the multicritical point does not precisely but closely located at the conjectured point by Eq. (4.2) for the replica number 3 and beyond as in Table 5.1. Therefore the conjecture (4.2) is not always satisfied for arbitrary replica numbers on the hierarchical lattices. This is considered to be one of the reasons why the multicritical point for the $\pm J$ Ising model is slightly away from the conjecture as found in the previous chapter.

b	n	p_c	$p_{\text{numerical}}$	$p_c - p_{\text{numerical}}$
2	$n \to 0$	0.889972	0.8915(6)	−0.0015(6)
	1	0.821797	0.821797	0
	2	0.788675	0.788675	0
	3	0.769563	0.768851	0.000713
	4	0.757348	0.755451	0.001897
3	$n \to 0$	0.889972	0.8903(2)	−0.0003(2)
	1	0.821797	0.821797	0
	2	0.788675	0.788675	0
	3	0.769563	0.769022	0.000542
	4	0.757348	0.755942	0.001406
4	$n \to 0$	0.889972	0.8892(6)	0.0007(6)
	1	0.821797	0.821797	0
	2	0.788675	0.788675	0
	3	0.769563	0.769649	−0.000086
	4	0.757348	0.757763	−0.000415
5	$n \to 0$	0.889972	0.8895(6)	0.0004(6)
	1	0.821797	0.821797	0
	2	0.788675	0.788675	0
	3	0.769563	0.7705020	−0.000939
	4	0.757348	0.7601328	−0.002785
6	$n \to 0$	0.889972	0.8890(6)	0.0010(6)
	1	0.821797	0.821797	0
	2	0.788675	0.788675	0
	3	0.769563	0.771376	−0.001813
	4	0.757348	0.762313	−0.004965

Table 5.1: Differences between p_c by the conjecture equation $x_0(K,K) = x_0^*(K,K)$, and $p_{\text{numerical}}$ by the exact renormalization analysis for the n-replicated $\pm J$ Ising model on several self-dual hierarchical lattices. For $n \to 0$, $p_{\text{numerical}}$ denotes the results obtained in Ref. [104] by Nobre's technique [105], also shown for comparison.

The way to improve the conjecture is inspired by this observation of the renormalization flow. As seen in Fig. 5.1, the original and dual relative Boltzmann factors give the initial conditions for the recursion relation of the renormalization flow. In addition, a careful observation of the renormalization flow in Fig. 5.1 enables us to recognize the fact that, after each step of renormalization, the renormalization flow goes in some direction once (toward the unstable fixed point C as in Fig. 5.2), and then is absorbed into the fixed point depending on the initial condition. In other words, two points of the relative Boltzmann factors after the renormalization approach the unstable fixed point closer than those before the renormalization. This means we can improve the precision of the conjecture, if we assume the reason for the failure of the precise prediction by the conjecture is mainly in the fact that two lines expressing the relative Boltzmann factors do not always coincide for the replicated spin systems. From this assumption, we suggest a way to improve the conjecture to derive a more precise location of the multicritical point in the next section.

5.2 Improvement by Renormalization

In the previous section, we observed the change of the relative Boltzmann factors by the renormalization on the hierarchical lattices. Then we found the fact that two points describing the original and dual relative Boltzmann factors near the multicritical point approach each other after the renormalization as in Fig. 5.2. The unstable fixed point of the renormalization is located between these points. If two points of the relative Boltzmann factors coincide, we can predict the critical point as the solution of Eq. (4.2) as the fixed point of the duality, similarly to the non-random Ising model. We thus propose here an improved version of the conjecture as follows,

$$x_0^{(r\to\infty)}(K,K) = x_0^{*(r\to\infty)}(K,K), \tag{5.4}$$

where $x_0^{(r)}$ and $x_0^{*(r)}$ are the original and dual principal Boltzmann factors after r-step renormalization, respectively. However the infinite-step renormalization is not so easy to be evaluated.

If we recall that we could obtain the close point to the location of the multicritical point on the hierarchical lattices even by the conventional version of the conjecture (4.2), we assume that Eq. (4.2) is an approximation for the location of the multicritical point. We expect that the improved conjecture by the one-step ($r = 1$) renormalization, which can be easily calculated analytically or numerically, becomes a more precise approximation. The observation of the renormalization flow as in Fig. (5.1) convinces us that the representative points of the relative Boltzmann factors are closer to the unstable fixed point after the one-step renormalization. Therefore

we consider the improved conjecture by the one-step renormalization below, and show several results by this calculation.

5.3 Improvement for Replicated Systems

We numerically evaluate the suitable recursion relation for each self-dual hierarchical lattice, similarly to Eq. (5.3). By equating the obtained principal Boltzmann factors for the original and dual replicated $\pm J$ Ising models,

$$x_0^{(1)}(K,K) = x_0^{*(1)}(K,K), \tag{5.5}$$

we obtain the results shown as in Table 5.2. All results are in good agreement with the numerical estimations as in Table 5.2. Comparison of Table 5.2 with Table 5.1 clearly indicates remarkable improvements. Therefore the improvement of the conjecture is successful even by one step of the renormalization.

In the next section, we show the results by the improved conjecture for the quenched random spin systems on the hierarchical lattices by the extrapolation to the limit $n \to 0$.

5.4 Improvement for Quenched Systems

In this section, we report the results by the improved conjecture in Eq. (5.5) and evaluate its performance compared with the conventional conjecture for the quenched systems ($n \to 0$).

The conventional conjecture as in Eq. (4.2) yields an equation that the binary entropy $H(p)$ equals to $1/2$ for self-dual hierarchical lattices as in Eq. (4.11). Similarly to this relation, the improved conjecture gives an equation in terms that the entropy given by the values of the renormalized couplings takes some value as described below. After a one-step renormalization, we obtain again the replicated random-bond Ising model on the hierarchical lattice with the renormalized couplings $\{K_{ij}^{(1)}\}$ and their distribution function $P^{(1)}(K_{ij})$. The original and dual principal Boltzmann factors for the replicated random-bond Ising model after one-step renormalization are given as

$$x_0^{(1)}(K,K) = \int dK_{ij} P^{(1)}(K_{ij}) \mathrm{e}^{nK_{ij}} \tag{5.6}$$

$$x_0^{*(1)}(K,K) = \int dK_{ij} P^{(1)}(K_{ij}) \left(\frac{\mathrm{e}^{K_{ij}} + \mathrm{e}^{-K_{ij}}}{\sqrt{2}} \right)^n, \tag{5.7}$$

b	n	$p_c^{(1)}$	$p_{\text{numerical}}$	$p_c^{(1)} - p_{\text{numerical}}$
2	1	0.821797	0.821797	0
	2	0.788675	0.788675	0
	3	0.769048	0.768851	0.000197
	4	0.755986	0.755451	0.000535
3	1	0.821797	0.821797	0
	2	0.788675	0.788675	0
	3	0.769138	0.769022	0.000116
	4	0.756250	0.755942	0.000308
4	1	0.821797	0.821797	0
	2	0.788675	0.788675	0
	3	0.769629	0.769649	−0.000020
	4	0.757619	0.757763	−0.000144
5	1	0.821797	0.821797	0
	2	0.788675	0.788675	0
	3	0.769968	0.770502	−0.000534
	4	0.758461	0.760133	−0.001672
6	1	0.821797	0.821797	0
	2	0.788675	0.788675	0
	3	0.769947	0.771376	−0.001429
	4	0.758300	0.762313	−0.004013

Table 5.2: The results by the improved conjecture $x_0^{(1)}(K) = x_0^{*(1)}(K)$.

b	p_c	$p_c^{(1)}$	$p_{\rm numerical}$	$p_c^{(1)} - p_{\rm numerical}$
2	0.889972	0.892025	0.8915(6)	−0.0005(6)
3	0.889972	0.890340	0.8903(2)	0.0000(2)
4	0.889972	0.889204	0.8892(6)	0.0000(6)
5	0.889972	0.889522	0.8895(6)	0.0000(6)
6	0.889972	0.889095	0.8890(6)	0.0000(6)

Table 5.3: The results for the quenched limit ($n \to 0$) by the improved conjecture for the self-dual hierarchical lattices.

where the distribution function is given by,

$$P^{(1)}(K_{ij}) = \int \left\{ \prod_{\rm unit} dK_{ij}^{(0)} P(K_{ij}^{(0)}) \right\} \delta(K_{ij} - K_{ij}^{(1)}(\{K_{ij}^{(0)}\})). \tag{5.8}$$

Here we use the couplings $\{K_{ij}^{(1)}\}$ obtained by the calculation of the recursion such Eq. (4.25). The product runs over the bonds on the unit cell of the hierarchical lattice. The initial condition (K, K) is given by the point on the Nishimori line. Using the principal Boltzmann factors defined in Eqs. (5.6) and (5.7), we take the leading term of the replica number $n \to 0$ of the equation $x_0^{(1)}(K, K) = {x_0}^{*(1)}(K, K)$ and obtain the improved conjecture for the quenched random spin system as

$$\int dK_{ij} P^{(1)}(K_{ij}) \log_2 \{1 + \exp(-2K_{ij})\} = \frac{1}{2}. \tag{5.9}$$

The left-hand side of this equation is written as $H^{(1)}(p)$. Equation (5.9) gives the results as the locations of the multicritical points for the self-dual hierarchical lattices shown in Table 5.3. We also find that the improved conjecture gives results depending on the feature of each hierarchical lattice because the prediction for the self-dual hierarchical lattice is different from each other, which was not found in the case by the conventional conjecture.

The improved conjecture also succeeds in leading to the relation between the multicritical points on the mutually dual pairs. It is straightforward to apply the improved conjecture to the mutually dual pairs, similarly to the case of the conventional conjecture [100] as, by consideration of the product of two partition functions,

$$H^{(1)}(p_a) + H^{(1)}(p_b) = 1, \tag{5.10}$$

where p_a and p_b denote the locations of the multicritical points on mutually dual pairs. We estimate the values of the left-hand side of Eq. (5.10) for several pairs of

Lattice	p_a	p_b	value
1	0.9338(7)	0.8265(6)	1.002(7)
2	0.8149(6)	0.9487(7)	0.984(9)
3	0.7526(5)	0.9720(7)	0.993(9)
4	0.8712(6)	0.9079(6)	1.007(6)
5	0.8700(6)	0.9081(7)	1.011(6)
6	0.9337(7)	0.8266(6)	1.003(7)
7	0.9084(6)	0.8678(6)	0.996(6)
8	0.9065(6)	0.8686(6)	1.003(6)

Table 5.4: The results by the improved conjecture for the mutually dual pairs. We estimate values of the left-hand side of Eq. (5.10) by the improved conjecture, shown on the right-most column of this Table.

hierarchical lattices in Figs. 4.6 and 4.7. The obtained results are given in Table 5.4. We use the values of the locations of the multicritical points obtained by Nobre's method, as in Table 4.2, to compare the performance of the improved conjecture with that of the conventional conjecture in Eq. (4.27). We cannot find improvement for all the cases, because we estimate the left-hand side of Eq. (5.10) by use of the values for exact locations of two multicritical points given by stochastic approaches. Equation (5.10) is not evaluated by a sufficient number of the renormalization steps, but the first approximation for the multicritical point on the hierarchical lattice. Therefore the improvement does not always work well. Nevertheless, especially for the number 1 and 6 of the hierarchical lattices with the maximum differences 2% as in Table 4.2, the improvement is greatly successful because both of the deviations become less than 0.3% as in Table 5.4.

We can also see the performance of the improved conjecture from another point of view, the phase boundary. We can predict the phase boundary by the improved conjecture without the Nishimori-line condition $K_p = K$, that is,

$$x_0^{(1)}(K_p, K) = x_0^{*(1)}(K_p, K), \tag{5.11}$$

The phase boundary is described for the $\pm J$ Ising model on the self-dual hierarchical lattice with $b = 3$ scale length in Fig. 5.3. The critical point $T_c = 2.26919$ for the non-random Ising model is exactly reproduced by this equation. The slope from this point is estimated as

$$\frac{1}{T_c}\left.\frac{dT}{dp}\right|_{T=T_c} = 3.30712. \tag{5.12}$$

This value is closer to the numerical result 3.23(3) by Nobre [105] than the value 3.41421 by the conventional conjecture. Therefore we can consider that it is success-

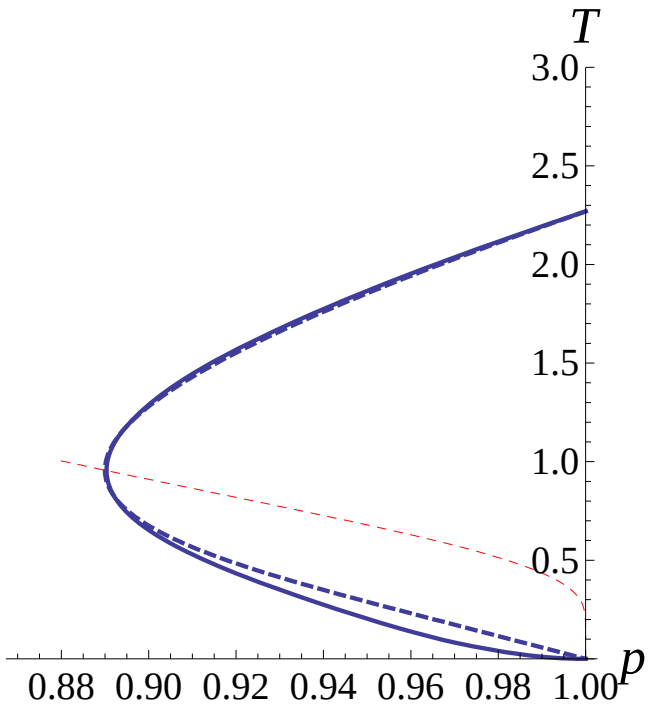

Figure 5.3: Conjectured phase diagram for the $\pm J$ Ising model on the self-dual hierarchical lattice with the scale factor $b = 3$.The solid line describe the conjectured phase boundary by the improved version and the dashed line expresses one by the conventional one. The thin dashed line is the Nishimori line.

ful to derive a more consistent phase boundary with the one predicted by another result. Nevertheless the conjectured phase boundary is inaccurate especially in the low-temperature region under the Nishimori line. The phase boundary is expected to be similar to one on the square lattice as in Fig. 1.6, or slightly reentrant toward the ferromagnetic phase in the region under the Nishimori line [105]. We cannot find the critical point p_0 with a non-zero value in the ground state, for which the existing results are listed in Table 1.2, by the improved conjecture as in Fig. 5.3. Nobre numerically investigated the location of p_0 and estimated as $p_0 = 0.8951(3)$ [105]. Therefore we have to further develop a theory even for the low-temperature region in the future but it should be emphasized that we have obtained an analytical approach to derive an approximate but accurate location of the multicritical point, the special critical point on the Nishimori line, and the slope of the critical points of T_c. We have not seen a theory to derive the locations of the precise critical points by such a simple equation as Eq. (5.11).

In the next chapter, we develop an improved version of the conjecture applicable

to regular lattices such as square, triangular, hexagonal lattices.

Chapter 6

Improved Conjecture for Regular Lattices

In this chapter we propose an improved version of the conjecture for the derivation of more precise locations of the critical points on the regular lattices. In the previous chapter, the structure of the hierarchical lattices enabled the renormalization group analysis to give the exact calculation. On the other hand the renormalization group analysis for the regular lattice is usually reduced to an approximate tool to derive the location of the critical point, because many-body interactions appear after the renormalization to prevent us from iterating the renormalization. If we attempt to construct the recursion relation for the coupling constants, we introduce some approximations such as the abandonment of such many-body interactions. The improved conjecture for the hierarchical lattice has been successful within satisfactory precision even by a one-step renormalization. Therefore we may not need to iterate the renormalization, depending on desired precision. In addition, as seen in the previous chapter, we sum over internal sites only in a unit cell of each hierarchical lattice. This calculation gives an equivalent quantity to the partition function for a small system, which consists of the product over the edge Boltzmann factors only on the unit cell of the hierarchical lattice. Therefore we expect to be able to also construct the improved conjecture for the regular lattice, if we consider the summation of the partition function on a limited range of the regular lattices. We regard this quantity as the principal Boltzmann factor for the improved conjecture on the regular lattices. The obtained results as will be seen below give an answer for the location of the multicritical point for the $\pm J$ Ising model on the square lattice with the precision to the fourth decimal point.

6.1 Formalism

We first review the improved conjecture for the hierarchical lattice and consider the application for the regular lattices. In the previous chapter, we found that the conventional conjecture could not give the exact solution. We have proposed, for the practical application, the improved conjecture by the one-step renormalization as an approximation with higher precision than the conventional one. In this calculation, we consider the summation over the internal sites on the unit cell of the hierarchical lattices for parallel spins at both ends. This is the principal Boltzmann factor after the renormalization. We can regard this renormalized principal Boltzmann factor as the partition function defined on the unit cell of the hierarchical lattice under the constraint that the spins at both ends are paralell. For example, we find this replacement explicitly for the Ising model on the self-dual hierarchical lattice in Fig. 4.4, from Eq. (4.25), in

$$Ae^{K^{(1)}} = \sum_{S_1,S_2} e^{K^{(0)}(S_1+S_2+S_1S_2+S_1+S_2)} \tag{6.1}$$

$$\Longleftrightarrow \quad Z(K) = \overline{\sum_{\{S_i\}}} \prod_{\langle ij\rangle}^{\text{unit}} e^{K^{(0)}S_iS_j} \tag{6.2}$$

where the overline means the summation over internal spins S_1 and S_2 on the unit cell of the hierarchical lattice in Fig. 4.4 with the edge spins up S_i and $S_j = 1$. The product runs over the nearest neighboring pairs on the unit of the hierarchical lattice.

Going back to our purpose, we attempt to construct the improved conjecture for the random spin systems on the regular lattice. If we consider the development of the conjecture in the same direction as the improvement on the hierarchical lattices, we need the principal Boltzmann factor after the summation over internal sites included in a limited range of the regular lattice. We call the limited range of the regular lattice a small system in this thesis. When we take the summation over the internal sites, we impose the fixed boundary condition on all the spins on the boundary of the small system. We establish an improved version of the conjecture on the regular lattice below, following the above consideration.

6.1.1 Square Lattice

The starting point of the establishment of the improved conjecture is the exact duality relation for the n-replicated partition function. We first restrict ourselves to the case for the random-bond Ising model on the square lattice as in Eq. (3.38) for simplicity. It is straightforward to extend the following procedure to other random spin systems and other lattices. As shown in Fig. 6.1, we consider to trace out a

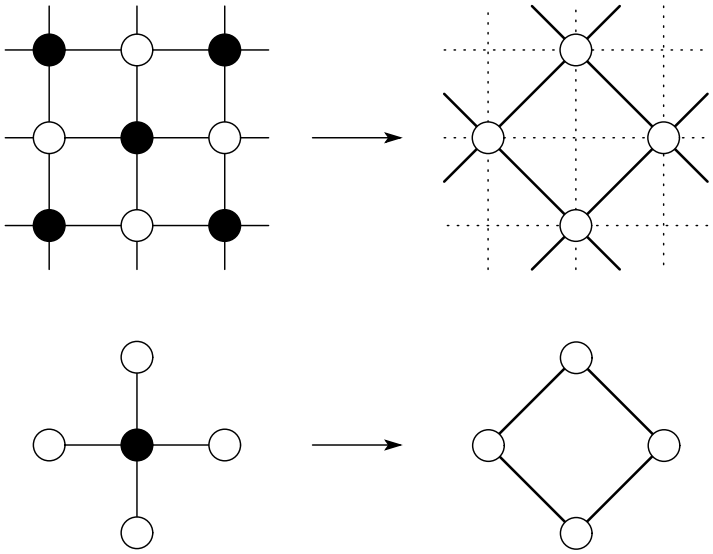

Figure 6.1: The example of the summation for the square lattice and the small system. The top figures describe one of the types of the summation for the square lattice. The bottom figures express the small system for the evaluation of the principal Boltzmann factor.

part of the spins on the square lattice. Then the exact duality relation (3.38) is reduced to

$$Z_n^{(s)}(x_0^{(s)}, x_1^{(s)}, \cdots, x_n^{(s)}) = Z_n^{(s)}(x_0^{*(s)}, x_1^{*(s)}, \cdots, x_n^{*(s)}). \tag{6.3}$$

Here $Z_n^{(s)}$ represents the reduced partition function by the summation of a part of spins on the square lattice. The superscript s distinguishes the type of the approximations, which are different types of the summation as considered below. The quantity $x_k^{(s)}$ is the edge Boltzmann factor including many-body interactions generated after the summation. We take a small system of the square lattice as in Fig. 6.1 and define the principal Boltzmann factors after the summation to establish the improved version of the conjecture, following the previously considered idea,

$$x_0^{(s)} = \left[\left\{ \sum_{\{S_i\}}^{\text{part}} \prod_{\langle ij \rangle} \mathrm{e}^{\beta J_{ij} S_i S_j} \right\}^n \right]_{\text{av}} \tag{6.4}$$

$$x_0^{*(s)} = \left[\left\{ \sum_{\{S_i\}}^{\text{part}} \prod_{\langle ij \rangle} \frac{1}{\sqrt{2}} \left(\mathrm{e}^{\beta J_{ij}} + \mathrm{e}^{-\beta J_{ij}} S_i S_j \right) \right\}^n \right]_{\text{av}}, \tag{6.5}$$

where the overline means the summation over internal spins in the small system of the square lattice as the filled circle in Fig. 6.1 with the other spins fixed in up directions $\{S_i\} = 1$. The word "part" represents that the product runs over the bonds of the small system under consideration. These principal Boltzmann factors can be regarded as partition functions after the configurational average and application of the replica method defined on the small system under the fixed boundary condition as shown in Fig. 6.1.

We then assume that a single equation gives the critical points for any number of n, similarly to the conventional conjecture,

$$x_0^{(s)} = x_0^{*(s)}. \tag{6.6}$$

By the extrapolation of the quenched limit $n \to 0$ of this equation, we obtain the improved conjecture for the square lattice as follows,

$$\left[\log Z^{*(s)}(\beta, \{J_{ij}\})\right]_{\rm av} - \left[\log Z^{(s)}(\beta, \{J_{ij}\})\right]_{\rm av} = 0. \tag{6.7}$$

We need the configurational average for J_{ij} of the logatihmic terms by two partition functions $Z^{(s)}$ and $Z^{*(s)}$ defined on the small system,

$$Z^{(s)}(\beta, \{J_{ij}\}) = \overline{\sum_{\{S_i\}} \prod_{\langle ij \rangle}^{\rm part}} {\rm e}^{\beta J_{ij} S_i S_j} \tag{6.8}$$

$$Z^{*(s)}(\beta, \{J_{ij}\}) = \overline{\sum_{\{S_i\}} \prod_{\langle ij \rangle}^{\rm part}} \frac{1}{\sqrt{2}} \left({\rm e}^{\beta J_{ij}} + {\rm e}^{-\beta J_{ij}} S_i S_j \right), \tag{6.9}$$

where the asterisk represents that the edge Boltzmann factor is given in a different form obtained after the duality for the random-bond Ising model as shown above. We can estimate the location of the multicritical point and other critical points by the above relation (6.7) as detailed below. Similarly to the shown case on the square lattice, we can derive the improved version of the triangular lattice.

6.1.2 Triangular Lattice

We use the replicated version of the duality relation for two partition functions on the triangular lattice in Eq. (3.42) to establish the improved conjecture for the triangular lattice. We restrict ourselves to the case for the random-bond Ising model on the triangular lattice. We give several remarks on the face Boltzmann factor on the triangular lattice. The original face Boltzmann factor has three edge Boltzmann factors denoted as x defined on the bonds of the elementary triangle as in Eq. (3.39). On the other hand, the dual face Boltzmann factor has three dual edge Boltzmann factors x^* as in Eq. (3.41). In addition this face Boltzmann factor is defined on

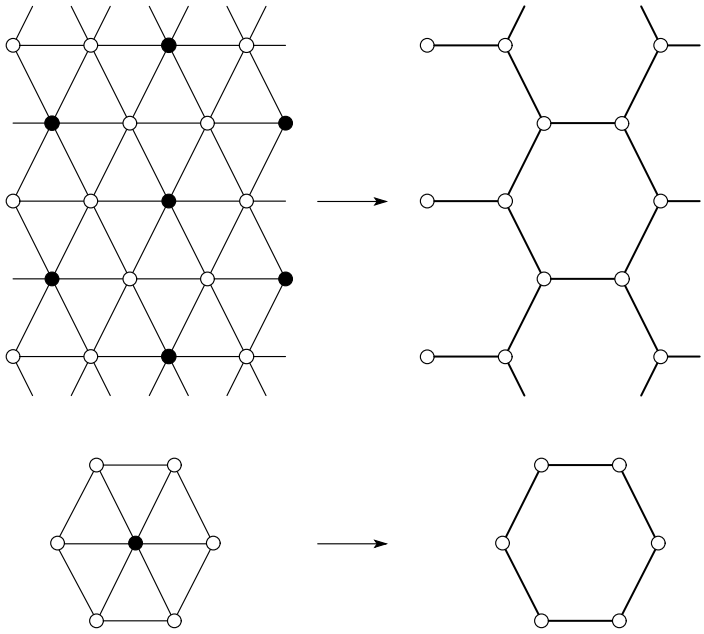

Figure 6.2: The example of the summation for the triangular lattice and the small system. The top figures express one of the types of the summation for the triangular lattice. The bottom figures express the small system for the evaluation of the principal Boltzmann factor.

the bonds on the star shape as in Fig. 2.9. In the dual face Boltzmann factor, the summation over the spin at the center of the star is included, which corresponds the star-triangle transformation.

Similarly to the case of the square lattice, we consider the summation over a part of the spins on the triangular lattice as in Fig. 6.2, and the exact duality relation (3.42) for the triangular lattice is reduced to,

$$Z^{(s)}_{\mathrm{TR},n}(A^{(s)}_0, A^{(s)}_1, \cdots, A^{(s)}_n) = Z^{(s)}_{\mathrm{TR},n}(A^{*(s)}_0, A^{*(s)}_1, \cdots, A^{*(s)}_n), \tag{6.10}$$

where $Z^{(s)}_{\mathrm{TR},n}$ represents the reduced partition function by the summation over a part of spins on the triangular lattice. The quantity $A^{(s)}_k$ is the face Boltzmann factor after the summation. We define the principal Boltzmann factor after the summation

over a part of the triangular lattices as,

$$A_0^{(s)} = \left[\left\{ \overline{\sum_{\{S_i\}}} \prod_{\triangle}^{\text{part}} \exp\left(\beta J_{12} S_1 S_2 + \beta J_{23} S_2 S_3 + \beta J_{31} S_3 S_1\right) \right\}^n \right]_{\text{av}} \tag{6.11}$$

$$A_0^{*(s)} = \left[2^{-\frac{n}{2} N_s^{(s)}} \left\{ \overline{\sum_{\{S_i\}}} \sum_{\{S_0\}} \prod_{\triangle}^{\text{part}} \frac{1}{\sqrt{2}} \left(\mathrm{e}^{\beta J_{10}} + \mathrm{e}^{-\beta J_{10}} S_1 S_0\right) \right.\right.$$
$$\left.\left. \times \frac{1}{\sqrt{2}} \left(\mathrm{e}^{\beta J_{20}} + \mathrm{e}^{-\beta J_{20}} S_2 S_0\right) \frac{1}{\sqrt{2}} \left(\mathrm{e}^{\beta J_{30}} + \mathrm{e}^{-\beta J_{30}} S_3 S_0\right) \right\}^n \right]_{\text{av}}, \tag{6.12}$$

where $N_s^{(s)}$ is equal to the number of the up-pointing triangles included in the small system. The overline means the summation over internal spins included in the small system of the triangular lattice as the filled circles in Fig. 6.2 with the other spins (the white-colored sites) up $\{S_i\} = 1$. The word "part" above the product symbol represents over the up-pointing triangles in the small system as in Fig. 6.2. The summation over S' means the star-triangle transformation. We can establish the improved conjecture for the triangular lattice by an equation of these principal Boltzmann factors after the summation $A_0^{(s)} = A_0^{*(s)}$ and by the extrapolation to the quenched limit of $n \to 0$,

$$\left[\log Z_{\text{TR}}^{*(s)}(\beta, \{J_{ij}\})\right]_{\text{av}} - \left[\log Z_{\text{TR}}^{(s)}(\beta, \{J_{ij}\})\right]_{\text{av}} = 0. \tag{6.13}$$

Again we consider the configurational average for J_{ij} of the logarithmic terms by the partition functions $Z_{\text{TR}}^{*(s)}$ and $Z_{\text{TR}}^{*(s)}$ defined on the small system of the triangular lattice as,

$$Z_{\text{TR}}^{(s)}(\beta, \{J_{ij}\}) = \left[\overline{\sum_{\{S_i\}}} \prod_{\triangle}^{\text{part}} \exp\left(\beta J_{12} S_1 S_2 + \beta J_{23} S_2 S_3 + \beta J_{31} S_3 S_1\right) \right]_{\text{av}} \tag{6.14}$$

$$Z_{\text{TR}}^{*(s)}(\beta, \{J_{ij}\}) = \left[2^{-\frac{1}{2} N_s^{(s)}} \overline{\sum_{\{S_i\}}} \sum_{\{S_0\}} \prod_{\triangle}^{\text{part}} \frac{1}{\sqrt{2}} \left(\mathrm{e}^{\beta J_{10}} + \mathrm{e}^{-\beta J_{10}} S_1 S_0\right) \right.$$
$$\left. \times \frac{1}{\sqrt{2}} \left(\mathrm{e}^{\beta J_{20}} + \mathrm{e}^{-\beta J_{20}} S_2 S_0\right) \frac{1}{\sqrt{2}} \left(\mathrm{e}^{\beta J_{30}} + \mathrm{e}^{-\beta J_{30}} S_3 S_0\right) \right]_{\text{av}}. \tag{6.15}$$

Before detailed calculations for the determination of the locations of the critical points, we consider the physical meaning of the improved conjecture from a different point of view.

6.2 Frustration Entropy and Multicritical Point

Here we consider the physical meaning of the improved conjecture, especially by consideration of the case of the square lattice for simplicity. The second term $Z^{(s)}$ on the left-hand side of Eq. (6.7) can be reduced to the entropy of distribution of frustration under the Nishimori-line condition $\beta = \beta_p$ for the small system under the fixed boundary condition as in Fig. 6.1, because the second term $Z^{(s)}$ on the left-hand side of Eq. (6.7) is the same as the free energy for the random-bond Ising model defined on the small system as in Eq. (3.29). Therefore we can obtain another expression of the second term $Z^{(s)}$ on the left-hand side of Eq. (6.7) as, for the case of the $\pm J$ Ising model for instance, similarly to Eq. (3.30),

$$\begin{aligned}&\left[\log Z^{(s)}(\beta, \{J_{ij}\})\right]_{\rm av} \\ &\quad = -\beta \left[F^{(s)}\right]_{\rm av} = \frac{1}{2^{N_s^{(s)}} (2\cosh \beta_p J)^{N_B^{(s)}}} \sum_{\{J_{ij}\}} Z^{(s)}(\beta_p, \{J_{ij}\}) \log Z^{(s)}(\beta, \{J_{ij}\}).\end{aligned} \tag{6.16}$$

On the other hand, the first term $Z^{*(s)}$ on the left-hand side of Eq. (6.7), which is generated from the dual principal Boltzmann factor after the summation, is not in a gauge invariant form, because the gauge transformation defined as in Eqs. (3.12) and (3.13) gives another expression of $Z^{*(s)}$,

$$Z_G^{*(s)}(\beta, \{J_{ij}\}) \;=\; \overline{\sum_{\{S_i\}} \prod_{\langle ij \rangle}^{\rm part}} \frac{1}{\sqrt{2}} \left({\rm e}^{\beta J_{ij} \sigma_i \sigma_j} + {\rm e}^{-\beta J_{ij} \sigma_i \sigma_j} S_i \sigma_i S_j \sigma_j \right). \tag{6.17}$$

This is different from the case for the second term $Z^{(s)}$ on the left-hand side of Eq. (6.7). The duality, however, transforms the first term $Z^{*(s)}$ on the left-hand side of Eq. (6.7) into another partition function in the gauge invariant form. For instance, in the case of the small system as in Fig. 6.3, the duality is the same as the simple case as shown in Fig. 2.5. Therefore we can use the relation (2.29) as follows, by setting $q = 2$,

$$Z^{(s)}[x^*] = 2^{N_s^{(s)} - \frac{N_B^{(s)}}{2} - 1} Z_{\rm D}^{(s)}[x], \tag{6.18}$$

where $N_B^{(s)}$ is the number of bonds, and $N_s^{(s)}$ is that of sites in the small system of the original square lattice. We give a remark that we use here x^* on the left-hand side of this relation. The partition function expressed by Eq. (6.9) is defined on the small lattice as in Fig. 6.3 and has the dual edge Boltzmann factor x^*. We apply the duality to this partition function. Therefore the partition function (6.9)

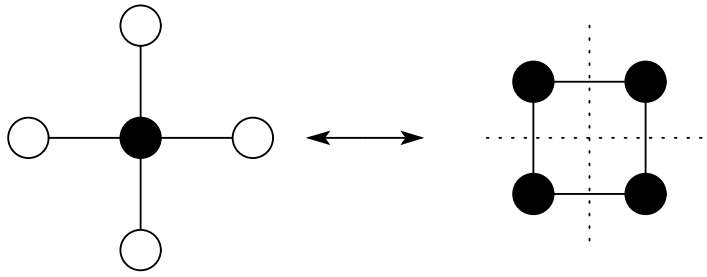

Figure 6.3: The dual lattice for the small system in Fig. 6.1. The black colored sites are free spins as the targets of the summation and the white ones are fixed in the up-pointing directions.

is the start point of the duality and we set it on the left-hand side of Eq. (6.18). The application of the duality for the small system as in Eq. (6.18) enables us to explicitly write the resulting partition function $Z_{\rm D}[x]$ in the following form, which is gauge invariant,

$$Z_{\rm D}^{(s)}(\beta, \{J_{ij}\}) \;=\; \overline{\sum_{\{S_i\}} \prod_{\langle ij \rangle}^{\rm part(D)} {\rm e}^{\beta J_{ij} S_i S_j}}, \tag{6.19}$$

where the 'part(D)' expresses the product over the bonds on the dual lattice for the small system as in Fig. 6.3. This partition function is in a gauge invariant form and the configurational-averaged quantity of its logarithm is the same as the free energy of the random-bond Ising model defined on the dual lattice for the small lattice. We use the relation (6.18) and rewrite the first term $Z^{*(s)}$ on the left-hand side of Eq. (6.7) as,

$$\left[\log Z^{*(s)}(\beta, \{J_{ij}\})\right]_{\rm av} = \left[\log Z_{\rm D}^{(s)}(\beta, \{J_{ij}\})\right]_{\rm av} + \left(N_s^{(s)} - \frac{N_B^{(s)}}{2} - 1 \right) \log 2. \tag{6.20}$$

The first term on the right-hand side of this relation can be reduced to the entropy of the distribution of frustration, because this is the free energy of the random-bond Ising model defined on the dual lattice for the small system, as, similarly to Eq. (3.30),

$$\begin{aligned} &\left[\log Z_{\rm D}^{(s)}(\beta, \{J_{ij}\})\right]_{\rm av} \\ &\quad = -\beta \left[F_{\rm D}^{(s)}\right]_{\rm av} = \frac{1}{2^{N_{\rm D}^{(s)}} (2\cosh \beta_p J)^{N_B^{(s)}}} \sum_{\{J_{ij}\}} Z_{\rm D}^{(s)}(\beta_p, \{J_{ij}\}) \log Z_{\rm D}^{(s)}(\beta, \{J_{ij}\}). \end{aligned} \tag{6.21}$$

Here $N_D^{(s)}$ expresses the number of sites of the dual lattice of the small system, which is equal to that of the plaquettes of the original small system. In the case of the small system of the square lattice as in Fig. 6.3, $N_s^{(s)} = 1$, $N_B^{(s)} = 4$, $N_D^{(s)} = 4$. The above considerations enable us to rewrite Eq. (6.7) as,

$$\frac{1}{2^{N_D^{(s)}}} S_{\rm D}^{(s)}(\beta_p, \beta) - \frac{1}{2^{N_s^{(s)}}} S^{(s)}(\beta_p, \beta) = \left(\frac{N_B^{(s)}}{2} - N_s^{(s)} + 1 \right) \log 2, \tag{6.22}$$

where

$$S_{\rm D}^{(s)}(\beta_p, \beta) = \sum_{\{J_{ij}\}} \frac{Z_{\rm D}^{(s)}(\beta_p, \{J_{ij}\})}{(2\cosh \beta_p J)^{N_B^{(s)}}} \log \frac{Z_{\rm D}^{(s)}(\beta, \{J_{ij}\})}{(2\cosh \beta J)^{N_B^{(s)}}} \tag{6.23}$$

$$S^{(s)}(\beta_p, \beta) = \sum_{\{J_{ij}\}} \frac{Z^{(s)}(\beta_p, \{J_{ij}\})}{(2\cosh \beta_p J)^{N_B^{(s)}}} \log \frac{Z^{(s)}(\beta, \{J_{ij}\})}{(2\cosh \beta J)^{N_B^{(s)}}}. \tag{6.24}$$

It is straightforward to obtain the same relation for the Gaussian Ising model by use of the following quantities,

$$S_{\rm D}^{(s)}(J_0, \beta) = \int \prod_{\langle ij \rangle}^{\rm part\,(D)} dJ_{ij} I(J_{ij}) Z_{\rm D}^{(s)}(J_0, \{J_{ij}\}) \log Z_{\rm D}^{(s)}(\beta, \{J_{ij}\}) \tag{6.25}$$

$$S^{(s)}(J_0, \beta) = \int \prod_{\langle ij \rangle}^{\rm part} dJ_{ij} I(J_{ij}) Z^{(s)}(J_0, \{J_{ij}\}) \log Z^{(s)}(\beta, \{J_{ij}\}), \tag{6.26}$$

where $I(J_{ij})$ is defined in Eq. (3.21).

If we set $\beta = \beta_p$ for the $\pm J$ Ising model and $\beta = J_0$ for the Gaussian Ising model, we find that equation (6.22) states that the multicritical point is located where the difference between two entropies of the distribution of frustration takes a special value. Its physical meaning is not obvious yet. This problem should be considered in the future.

If the improvement affects the predictions not only of the multicritical point but also the critical points as shown in the case for the slope of the critical points in the previous chapter, we can apply the improved conjecture to the random spin systems without gauge symmetry. The absence of the Nishimori line on the phase diagram does not permit us to rewrite Eq. (6.7) in term of the entropy of the distribution of frustration as in Eq. (6.22). However the above discussions by the duality for the small system are applicable to such random spin systems. We can thus give the

critical points by the following equation for the random spin systems without the Nishimori line,

$$-\beta\left(\left[F_{\mathrm{D}}^{(s)}\right]_{\mathrm{av}}-\left[F^{(s)}\right]_{\mathrm{av}}\right)=\left(\frac{N_B^{(s)}}{2}-N_s^{(s)}+1\right)\log 2. \tag{6.27}$$

Therefore our task to analytically derive the critical points in random spin systems is to estimate the difference between the two free energies on the small system and its dual one. It is straightforward to establish the expression as in Eqs. (6.22) and (6.27) also for the case of the triangular lattice.

In the next section, we show the results for the precise locations of the multicritical points obtained by computing Eq. (6.7) for the square lattice and Eq. (6.13) for the triangular lattice.

6.3 Derivations of Multicritical Points

We derive the location of the multicritical point by the improved conjecture for the regular lattices. Setting $\beta_p = \beta$, the Nishimori-line condition, for Eq. (6.7) or equivalently (6.22), we can predict the location of the multicritical point for the $\pm J$ Ising model as well as the Gaussian Ising model on the square lattice. If we consider a larger range of the summation of spins, (i. e., the small system includes more bonds and sites.) it is expected that the precision of the improved conjecture becomes higher. One of the reasons is that the improved conjecture can include more effects of spatially non-uniform interactions, which are essential features in random spin systems. In other words, the conventional conjecture has been the zeroth approximation without consideration of a form of the lattice and non-uniform interactions in space. The improved conjecture is also an approximation but gives more precise answers than the conventional conjecture, because it is formulated with the consideration of an individual characteristic of the lattice similarly to the case of the hierarchical lattices. We express the type of the approximations by the value of s, which has represented the considered form of the small system. In this thesis, we show the results of three types of approximations for the precise location of the multicritical point on the square lattice by three different sizes of the small systems as in Fig. 6.4 and two types of approximations on the triangular lattice especially for the $\pm J$ Ising model as in Fig. 6.5.

6.3.1 First Approximation for the Square Lattice

We consider the first approximation for the location of the multicritical point on the square lattice by the $s = 1$ small system as shown in Fig. 6.4. To identify

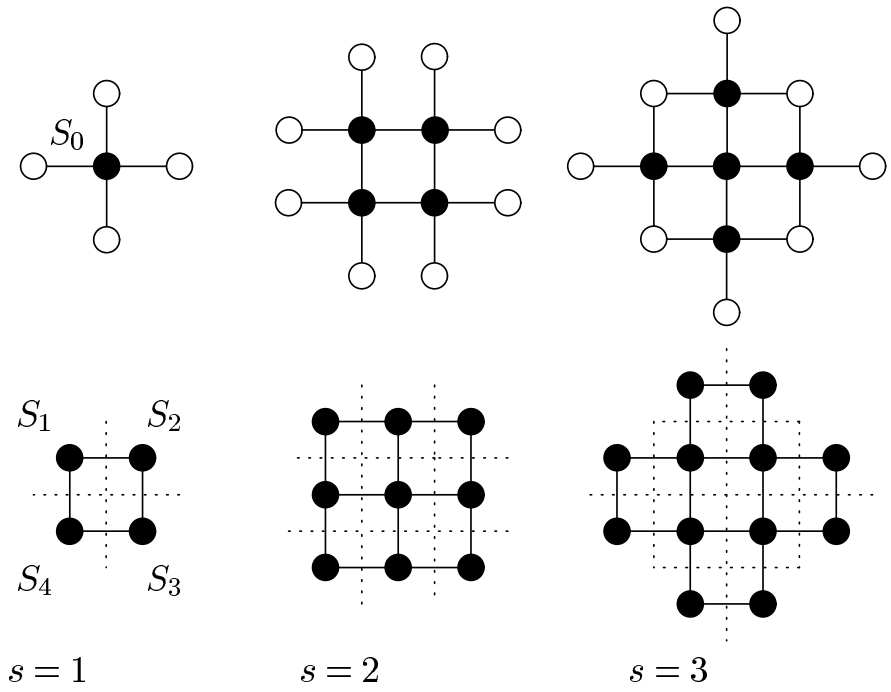

Figure 6.4: Three patterns of the small systems for the improved conjecture on the square lattice. The top figures express the small systems for the evaluations of $Z^{(s)}$ and $Z^{*(s)}$. The bottom figures represent the dual lattices for the small systems, on which the partition functions are denoted by $Z_{\rm D}$. The filled circles are the targets of the summation and white ones are fixed in up directions $\{S_i\} = 1$.

the multicritical point, we evaluate the quantities in Eq. (6.7). We calculate the partition function on the $s = 1$ small system for the square lattice in Eq. (6.8) by the summation over the single site at the center surrounded by four bonds with four spins up, because of the fixed boundary condition. The result is given as

$$\begin{aligned} Z^{(1)}(\beta, \{J_{ij}\}) &= \sum_{S_0=\pm 1} \mathrm{e}^{\beta(J_{01}+J_{02}+J_{03}+J_{04})S_0} \\ &= 2\cosh\{\beta(J_{01}+J_{02}+J_{03}+J_{04})\} \end{aligned} \tag{6.28}$$

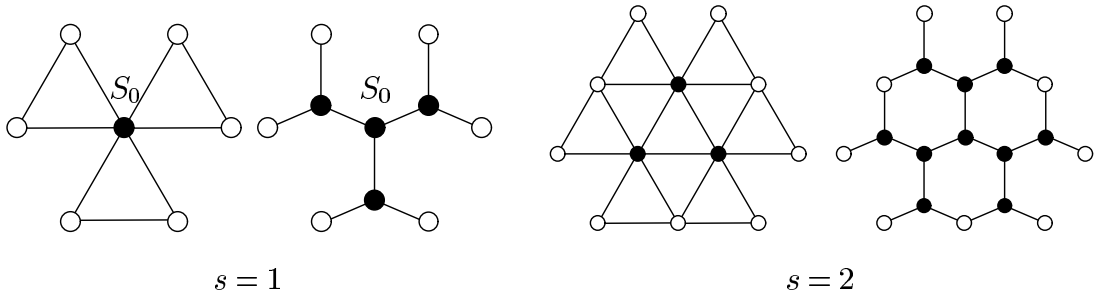

Figure 6.5: Two patterns of the small systems for the improved conjecture on the triangular lattice. The left-hand side for each type of the approximations is for the partition function $Z_{\rm TR}^{(s)}$, and the right-hand side is for the dual partition function $Z_{\rm TR}^{*(s)}$, for which the star-triangle transformation is needed. We use the same symbols in Fig. 2.6.

Another partition function defined on the $s = 1$ small system in Eq. (6.9) is calculated as,

$$\begin{aligned} Z^{*(1)}(\beta, \{J_{ij}\}) &= \left(\frac{1}{\sqrt{2}}\right)^4 \sum_{S_0=\pm 1} \prod_{i=1}^{4} \left(\mathrm{e}^{\beta J_{0i}} + S_0 \mathrm{e}^{-\beta J_{0i}}\right) \\ &= \left(\frac{1}{\sqrt{2}}\right)^4 \left\{ \prod_{i=1}^{4} (2\cosh \beta J_{0i}) + \prod_{i=1}^{4} (2\sinh \beta J_{0i}) \right\}. \end{aligned} \tag{6.29}$$

This quantity is also obtained from the evaluation of the partition function $Z_{\rm D}$ defined on the dual small system by use of the relation (6.18). Then we can explicitly write down the improved conjecture for the location of the multicritical point for the $\pm J$ Ising model on the square lattice as, from Eq. (6.7),

$$\begin{aligned} &\sum_{\tau_{ij}} \frac{1}{2^4} \left(1 + \tanh^4 K_p \prod_{i=1}^{4} \tau_{0i}\right) \log \left(1 + \tanh^4 K \prod_{i=1}^{4} \tau_{0i}\right) \\ &\quad - \sum_{\tau_{ij}} \frac{1}{2} \, \frac{2\cosh\left\{K_p \sum_{i=0}^{4} \tau_{0i}\right\}}{\left(2\cosh K_p\right)^4} \log \frac{2\cosh\left\{K \sum_{i=0}^{4} \tau_{0i}\right\}}{\left(2\cosh K\right)^4} = 2\log 2, \end{aligned} \tag{6.30}$$

where we used the coupling constant $K = \beta J$ and its sign τ_{ij}. Setting $K = K_p$, we solve this equation and obtain $p_c^{(1)} = 0.890725$. This result is listed in Table 6.1 with other approximations for the location of the multicritical points on the square lattice to see the performance of the improvement and to compare the improved conjecture with the existing results.

For the Gaussian Ising model, we have to evaluate the quadruple integration over four bonds $\{J_{ij}\}$ as,

$$\int_{-\infty}^{\infty}\prod_{i=1}^{4}P(J_{0i})dJ_{0i}\log\left\{\prod_{i=1}^{4}(2\cosh\beta J_{0i})+\prod_{i=1}^{4}(2\sinh\beta J_{0i})\right\}$$
$$-\int_{-\infty}^{\infty}\prod_{i=1}^{4}P(J_{0i})dJ_{0i}\log\{2\cosh\{\beta(J_{01}+J_{02}+J_{03}+J_{04})\}=2\log 2, \tag{6.31}$$

where $P(J_{ij})$ is the distribution function defined in Eq. (3.5). The numerical manipulation of this equation gives the location of the multicritical point for the Gaussian Ising model on the square lattice as $J_0^{(1)}=1.021564$.

Other approximations for the square lattice by the small systems labeled by $s=2$ and 3 are straightforward to be evaluated. The numerical manipulation of these approximations give the predictions of the location of the multicritical points on the square lattice as $p_c^{(2)}=0.890824$ and $p_c^{(3)}=0.890822$ as listed in Table 6.1.

6.3.2 First Approximation for the Triangular Lattice

We show the calculation of the first approximation of the improved conjecture for the location of the multicritical point of the $\pm J$ Ising model on the triangular lattice. We consider the small system labeled by $s=1$ with three up-pointing triangles as in Fig. 6.5. In this case, it is convenient to define the following quantities,

$$Y(S,\{J_{ij}\}) = e^{\beta(J_{01}+J_{02}S+J_{03}S)} \tag{6.32}$$

$$\begin{aligned} Y^*(S,\{J_{ij}\}) &= \frac{1}{4}\sum_{S'=\pm1}\prod_{i=1}^{2}\left(e^{\beta J_{0i}}+S'e^{-\beta J_{0i}}\right)\left(e^{\beta J_{03}}+S'Se^{-\beta J_{03}}\right) \\ &= \frac{1}{4}\left\{\prod_{i=1}^{2}(2\cosh\beta J_{0i})\left(e^{\beta J_{03}}+Se^{-\beta J_{03}}\right)\right. \\ &\quad \left.+\prod_{i=1}^{2}(2\sinh\beta J_{0i})\left(e^{\beta J_{03}}-Se^{-\beta J_{03}}\right)\right\}, \end{aligned} \tag{6.33}$$

where the locations of the spins S', S, and the sets of $\{J_{0i}\}$ are described in Fig. 6.6. The summation over S' corresponds to the star-triangle transformation. We calculate two partition functions for the small system of the triangular lattice as in

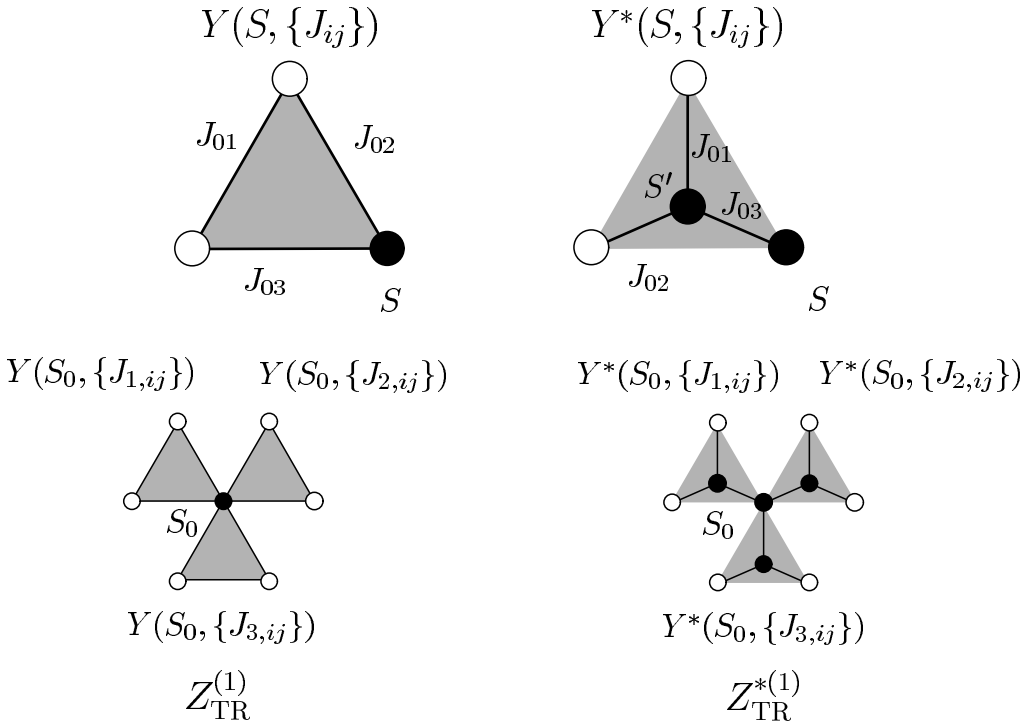

Figure 6.6: The relationships between Y and $Z_{\rm TR}^{(1)}$, and between Y^* and $Z_{\rm TR}^{*(1)}$. The spin S' at the center of the star shape is of the summation for the star-triangle transformation.

Fig. 6.5 as, by use of these quantities,

$$\begin{aligned} Z_{\rm TR}^{(1)}(\beta,\{J_{ij}\}) &= \sum_{S_0=\pm1}\prod_{k=1}^{3} Y(S_0,\{J_{k,ij}\}) \\ &= 2\,\mathrm{e}^{\beta\sum_{k=1}^{3}J_{k,01}}\cosh\{\beta\sum_{k=1}^{3}(J_{k,02}+J_{k,03})\} \end{aligned} \tag{6.34}$$

$$\begin{aligned} Z_{\rm TR}^{*(1)}(\beta,\{J_{ij}\}) &= \sum_{S_0=\pm1}\prod_{k=1}^{3} Y^*(S_0,\{J_{k,ij}\}) \\ &= 2^3\left\{\prod_{k=1}^{3}\left(\prod_{i=1}^{2}\cosh\beta J_{k,0i}+\prod_{i=1}^{2}\sinh\beta J_{k,0i}\right)\right. \\ &\quad \left.+\prod_{k=1}^{3}\left(\prod_{i=1}^{2}\cosh\beta J_{k,0i}\sinh\beta J_{k,03}+\prod_{i=1}^{2}\sinh\beta J_{k,0i}\cosh\beta J_{k,03}\right)\right\}. \end{aligned} \tag{6.35}$$

Substituting these quantities into Eq. (6.13), we can obtain the first approximation of the improved conjecture for the location of the multicritical point of the $\pm J$ Ising model on the triangular lattice. The result is given as $p_c^{(1)} = 0.835957$, which is also listed in Table 6.1 with the one by another approximation by the numerical manipulation of the $s = 2$ small system in Fig. 6.5.

6.3.3 First Approximation for the Potts Spin Glass

As another application of the improved conjecture, let us consider the Potts spin glass defined in Eq. (4.13). We estimate the location of the multicritical point for the Potts spin glass by the first approximation for the square lattice by use of the $s = 1$ small lattice. The Potts spin glass has the edge Boltzmann factor as,

$$x(\phi_{ij}) = \mathrm{e}^{\beta J \delta(\phi_{ij}+l_{ij})}, \tag{6.36}$$

and the dual one,

$$x^*(\phi_{ij}) = \frac{v}{\sqrt{q}} \left\{ \mathrm{e}^{\mathrm{i}\frac{2\pi}{q} l_{ij}\phi_{ij}} + \frac{q}{v}\delta(\phi_{ij}) \right\}, \tag{6.37}$$

where $v \equiv \mathrm{e}^K - 1$, ϕ_{ij} represents the difference between the nearest neighboring spins between 0 and $q-1$ and l_{ij} is the random variable following the distribution function (4.14). Therefore the partition functions as in Eq. (6.7) for the small system are given as,

$$Z^{(1)}(\beta; \{l_{ij}\}) = \left[\overline{\sum_{\{\phi_i\}} \prod_{\langle ij \rangle}^{\text{part}} \mathrm{e}^{\beta J \delta(\phi_{ij}+l_{ij})}} \right]_{\text{av}} \tag{6.38}$$

$$Z^{*(1)}(\beta; \{l_{ij}\}) = \left[\overline{\sum_{\{\phi_i\}} \prod_{\langle ij \rangle}^{\text{part}} \frac{v}{\sqrt{q}} \left\{ \mathrm{e}^{\mathrm{i}\frac{2\pi}{q} l_{ij}\phi_{ij}} + \frac{q}{v}\delta(\phi_{ij}) \right\}} \right]_{\text{av}}. \tag{6.39}$$

We can carry out the summation over ϕ_0 at the center of the $s = 1$ small system as in Fig. (6.4) as,

$$\begin{aligned} Z^{(1)}(\beta, \{l_{ij}\}) &= \sum_{\phi_0=0}^{q-1} \mathrm{e}^{\beta J \{\delta(\phi_0+l_{01})+\delta(\phi_0+l_{02})+\delta(\phi_0+l_{03})+\delta(\phi_0+l_{04})\}} \\ &= q + 4v + v^2 \sum_{i \neq j} \delta(l_{0i}, l_{0j}) + v^3 \sum_{i \neq j \neq k} \delta(l_{0i}, l_{0j}, l_{0k}) + v^4 \delta(l_{01}, l_{02}, l_{03}, l_{04}), \end{aligned} \tag{6.40}$$

where $i \neq j$ means the summation over different pairs among four bonds, and $i \neq j \neq k$ expresses the summation over all combinations of different three bonds among four bonds.

$$\begin{aligned} Z^{*(1)}(\beta, \{l_{ij}\}) &= \left(\frac{v}{\sqrt{q}}\right)^4 \sum_{\phi_0=0}^{q-1} \prod_{i=1}^{4} \left\{ \mathrm{e}^{\mathrm{i}\frac{2\pi}{q} l_{oi}\phi_0} + \frac{q}{v}\delta(\phi_0) \right\} \\ &= \frac{v^4}{q^2} \left\{ \left(1+\frac{q}{v}\right)^4 - 1 + q\delta\left(\sum_{i=1}^{4} l_{0i}\right) \right\}. \end{aligned} \tag{6.41}$$

We rewrite Eq. (6.7) as follows, from these quantities,

$$\left[\log \left\{ \frac{(q+v)^4 - v^4 + qv^4\delta\left(\sum_{i=1}^{4} l_{0i}\right)}{q + 4v + v^2 \sum_{i\neq j} \delta(l_{0i}, l_{0j}) + v^3 \sum_{i\neq j\neq k} \delta(l_{0i}, l_{0j}, l_{0k}) + v^4\delta(l_{01}, l_{02}, l_{03}, l_{04})} \right\} \right]_{\mathrm{av}} = 2\log q, \tag{6.42}$$

where the configurational average for the random variables $\{l_{0i}\}$ on the four bonds follows the distribution function as in Eq. (4.14). We can estimate the location of the multicritical point for the Potts spin glass on the square lattice as $p_c^{(1)} = 0.0791462$ for $q = 3$, $p_c^{(1)} = 0.0626157$ for $q = 4$, and $p_c^{(1)} = 0.0520578$ for $q = 5$. These results are shown in Table 6.1 in comparison with those by the conventional conjecture.

6.4 Discussion

We discuss the performance of the improved conjecture and explain the features found in Table 6.1 where all the obtained results by the improved conjecture in this thesis are shown.

At first, we remark the predictions for the location of the multicritical point of the $\pm J$ Ising model. All of the improved results for the $\pm J$ Ising model on the square lattice indicate higher values about $p_c \approx 0.8908$ than $p_c^{(0)} = 0.8900$ by the conventional conjecture. As the size of the small system increases, the prediction of p_c converges to some value about $p_c = 0.8908$. If we compare the results by the $s = 2$ and $s = 3$ small systems, the difference between two approximations is found at the sixth decimal point. We desire the precision to the fourth digit in the fraction to conclude the confliction between $p_c \approx 0.8900$ and $p_c \approx 0.8908$. For this purpose, the improved conjecture gives a satisfactory answer that the multicritical point is located at $p_c \approx 0.89082$. Its validity is not proved. We therefore cannot completely deny the possibility that the multicritical point locates at $p_c \approx 0.8900$ as estimated

Type	Conjecture	Numerical result
SQ $\pm J$	$p_c^{(0)} = 0.889972$ [87, 88]	0.8905(5) [56]
	$p_c^{(1)} = 0.890725$	0.8906(2) [57]
	$p_c^{(2)} = 0.890824$	0.8907(2) [58]
	$p_c^{(3)} = 0.890822$	0.8900(5) [59]
		0.8894(9) [60]
		0.89081(7) [62]
SQ Gaussian	$J_0^{(0)} = 1.021770$ [87, 88]	1.02098(4) [61]
	$J_0^{(1)} = 1.021564$	
TR $\pm J$	$p_c^{(0)} = 0.835806$ [101]	0.8355(5) [59]
	$p_c^{(1)} = 0.835956$	
	$p_c^{(2)} = 0.835985$	
HEX $\pm J$	$p_c^{(0)} = 0.932704$ [101]	0.9325(5) [59]
	$p_c^{(1)} = 0.932611$	
	$p_c^{(2)} = 0.932593$	
SQ Potts($q = 3$)	$p_c^{(0)} = 0.079731$ [87, 88]	0.079-0.080 [102]
	$p_c^{(1)} = 0.079146$	
SQ Potts($q = 4$)	$p_c^{(0)} = 0.063097$ [88]	
	$p_c^{(1)} = 0.062616$	
SQ Potts($q = 5$)	$p_c^{(0)} = 0.052467$ [88]	
	$p_c^{(1)} = 0.052058$	

Table 6.1: SQ denotes the square lattice, TR expresses the triangular lattice, and HEX means the hexagonal lattice.

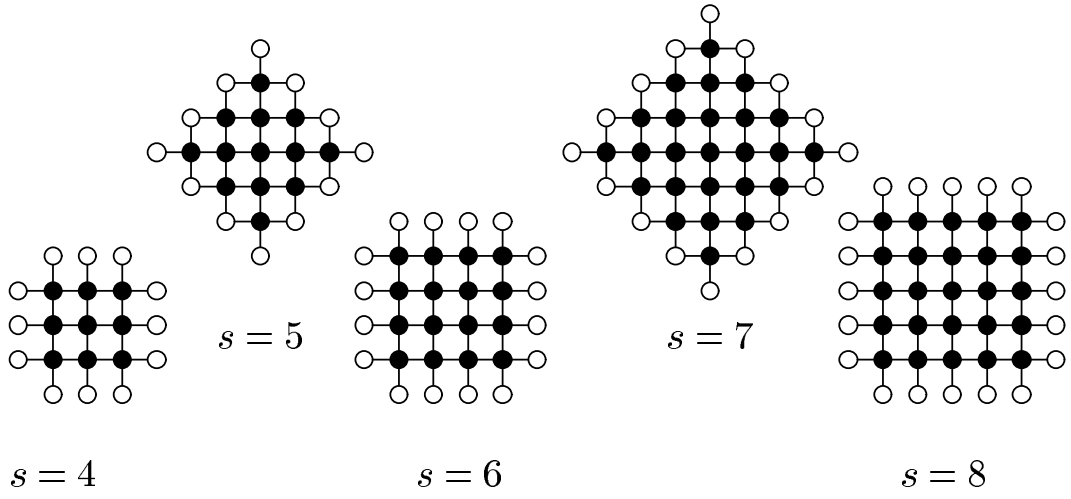

Figure 6.7: Further approximations for estimations of slope of T_c. The numbers of bonds in each pattern are 24 ($s = 4$), 36 ($s = 5$), 40 ($s = 6$), 64 ($s = 7$), and 60 ($s = 8$).

in other studies [59, 60]. However the following discussions support our conclusion $p_c \approx 0.89082$ from a different point of view.

The phase boundary can be predicted by the improved conjecture without the restriction of the Nishimori-line condition, similarly to the conventional conjecture. Unfortunately the improved conjecture fails again to derive a precise phase boundary especially under the Nishimori line similarly to the case of the hierarchical lattice as in Fig. 5.3. Nevertheless we find the improvement of estimations of the slope of the critical point T_c of the non-random Ising model. We concentrate on the estimations of the slope and show the results below by use of not only $s = 1$, $s = 2$, and $s = 3$ small systems but also various ones as in Fig. 6.7. The computing time of the order $\sim O(2^{N_B^{(s)}})$ is needed in general for the calculation of the improved conjecture, in particular for that of the configurational average on $\{J_{ij}\}$, whose number is given as $N_B^{(s)}$. However, the configurational average becomes much simpler, when we consider a calculation only around T_c to estimate the slope of T_c, at which only a single bond at most becomes the antiferromagnetic interaction. Therefore we can deal with further approximations to estimate the value of the slope of T_c by various small lattices as in Fig. 6.7. The obtained values are listed in Table 6.2. We perform two types of the approximations by the different forms of the small lattices with many cross shapes and with many squares as in Fig. 6.7. Two types of the approximations give different values but, in any cases, the increase of the size of the small system

Number	Value of slope	Number	Value of slope
$s = 0$	3.41421	$s = 0$	3.41421
$s = 1$	3.33658	$s = 2$	3.30267
$s = 3$	3.31272	$s = 4$	3.28461
$s = 5$	3.29352	$s = 6$	3.27345
$s = 7$	3.28161	$s = 8$	3.26586
exact	3.20911 [106]	exact	3.20911 [106]

Table 6.2: The slope of the critical point of T_c for the $\pm J$ Ising model on the square lattice. We distinguish the approximations by the form of the small lattice as in Fig. 6.7. The left-hand side table gives the results by the small systems with many cross shapes. The right-hand side table shows the ones with many squares. For the comparison, we write the result by the conventional conjecture denoted by $s = 0$.

shows the behavior of convergence to the exact solution 3.20911 of the slope of T_c by Domany [106]. Therefore it is considered that the improved conjecture gives a systematic way to derive the precise locations of the critical points in random spin systems. We need to consider the approximation by the use of the large size of the small system, depending on the desirable precision. Going back to the location of the multicritical point, we observe the difference between two approximations by $s = 2$ and $s = 3$ and find conversion to the fifth digit. As a conclusion, the improved conjecture is successful in giving the precise answer of the location of the multicritical point with the precision to the fifth digit, $p_c \approx 0.89082$.

The improved conjecture is applicable to the diluted Ising model by the evaluation of Eq. (6.7) and use of the distribution function in Eq. (4.33). We investigate the values of the slope of T_c similarly to the case of the $\pm J$ Ising model, to evaluate the performance of the improvement. We show the results for the slope of the critical points T_c for the diluted Ising model in Table 6.3. These values also converge to the exact solution 1.32926 [110], similarly to the case for the $\pm J$ Ising model. From this point of view, the improved conjecture is a systematic approach to lead to the precise locations of the critical points in random spin systems as well as such a special point as the multicritical point.

The improved conjecture gives the predictions for the location of the multicritical point of the $\pm J$ Ising model on the triangular lattice by consideration of two different small lattices as in Fig. 6.5 as shown in Table 6.1. The results for the hexagonal lattice are estimated by use of the relation (4.10) as listed in Table 6.1. From these predictions, we conclude the location of the multicritical point, with the precision to the fourth digit, for the triangular lattice as $p_{\rm TR} = 0.8360$ and for the hexagonal lattice as $p_{\rm HEX} = 0.9326$. A remarkable support for these results is also found in the slope of T_c for the triangular lattice. We estimate the values of the slope of T_c for

Number	Value of slope	Number	Value of slope
$s = 0$	1.34254	$s = 0$	1.34254
$s = 1$	1.33780	$s = 2$	1.33561
$s = 3$	1.33626	$s = 4$	1.33442
$s = 5$	1.33500	$s = 6$	1.33367
$s = 7$	1.33420	$s = 8$	1.33316
exact	1.32926 [110]	exact	1.32926 [110]

Table 6.3: The slope of the critical point of T_c for the diluted Ising model on the square lattice. The left-hand side table gives the results by the small systems with many cross shapes. The right-hand side table shows the ones with many squares. For the comparison, we write the result by the conventional conjecture denoted by $s = 0$.

Number	Value of slope	Number	Value of slope
$s = 0$	2.78984	$s = 0$	1.19248
$s = 1$	2.77566	$s = 1$	1.19137
$s = 2$	2.77146	$s = 2$	1.19104
exact	2.73072	exact	1.18777

Table 6.4: The slope of the critical point of T_c for the $\pm J$ Ising model on the triangular lattice in the left-hand side and for the diluted Ising model on the triangular lattice in the right-hand side. The results by the conventional conjecture are expressed by $s = 0$.

each small system. The exact value of the slope of T_c can be estimated as 2.73072 by the same calculation as the case of the square lattice [106]. The results are shown in Table 6.4. These estimations also show that the improved conjecture can give the precise locations of the critical points with the behavior of the convergence to the exact solutions. We apply the improved conjecture to the diluted Ising model on the triangular lattice and calculate the value of the slope of the critical points. The results show again the similar behavior converging to the exact solution, which is obtained by the same procedure as the case on the square lattice [110], as shown in Table 6.4.

We also apply the improved conjecture to the Gaussian Ising model on the square lattice only by the use of the $s = 1$ small system. The resulting value is $J_0^{(1)} = 1.02156$, which is slightly modified, about 0.2%, from the figure by the conventional conjecture $J_0^{(0)} = 1.021770$. Therefore we need further approximations for the determination of the location of the multicritical point for the Gaussian Ising model with the precision to the fourth digit. If we compare the quantitative difference of improvement for the $\pm J$ Ising model with the one for the Gaussian Ising

model, we find the improvement for the Gaussian model is a smaller change than the one 0.8% for the $\pm J$ Ising model. This is why the distance between two points of solutions by the conventional conjecture for the replicated system for the Gaussian Ising model is closer than that for the $\pm J$ Ising model as in Figs. 4.2 and 4.3. In other words, the conventional conjecture has been considered to give the close location to the answer for the multicritical point of the Gaussian Ising model. If we take account into this observation and the improved conjecture on the hierarchical lattices, the duality can give the exact location of the critical point when two of the original and dual relative Boltzmann factors coincide perfectly or have an intersection as the fixed point as found for the 2-replicated $\pm J$ Ising model as in Fig. 3.3. We can thus give a conclusion that the conventional conjecture cannot give an exact solution, but is an approximation for the location of the critical points in random spin systems. Its performance is considered to be determined by the deviation between the two representative points of the original and dual relative Boltzmann factors for the solution of the conventional conjecture.

The results are also given for the Potts spin glasses as in Table 6.1. These show the deviations at the fourth digit from the predictions by the conventional conjecture as found between $p_c^{(0)} = 0.079731$ and $p_c^{(1)} = 0.079146$ for $q = 3$, between $p_c^{(0)} = 0.063097$ and $p_c^{(1)} = 0.062616$ for $q = 4$, and between $p_c^{(0)} = 0.052467$ and $p_c^{(1)} = 0.052058$ for $q = 5$. If we give provisional conclusions for the locations of the multicritical points for the Potts spin glasses on the square lattice, we remark $p_c = 0.079 - 0.080$ for $q = 3$, $p_c = 0.062 - 0.063$ for $q = 4$, and $p_c = 0.052$ for $q = 5$. Further approximations are needed for the decisive precision to the fourth decimal point.

In addition, we remark that the improved conjecture works well for the diluted Villain model as well as shown cases above [114].

If we need the precise location of the critical points in the random spin systems, we consider the summation over spins in the small system taken from the considered lattice, the improved conjecture. This may be a unique way to analytically derive the location of the critical points in random spin systems with very high precision. In addition, a possible way of the application of the improved conjecture as a numerical implementation is considered. The algorithm is very simple. We estimate the difference between the free energies with different edge Boltzmann factors as in Eq. (6.7) or equivalently between the ones defined on two different lattices as in Eq. (6.27). Moreover it is possible to directly analyze the verticality of the phase boundary under the Nishimori line as in Fig. 1.6. Of course, in the low-temperature region under the Nishimori line, the improved conjecture is still not a satisfactory tool. If we consider a sufficiently large size of the small system, we may obtain the critical point p_0 in the ground state. As another direction, we use the properties on the Nishimori line and consider the relationship between the improved conjecture and its specialty. One of the relationships is found as the expression in terms of the

entropy of the distribution of entropy. We should study this physical meaning in the future.

In this thesis, we restrict ourselves to considering the random spin systems in two-dimensional systems. However we can apply the duality to other dimensional systems. For example, the duality can be transform the random-bond Ising model on the three-dimensional cubic lattice into the random-plaquette gauge model on the three-dimensional cubic lattice. The random-plaquette gauge model is an attractive one in terms of the quantum toric code [73, 74]. An accuracy threshold to correct error of the quantum toric code corresponds to the location of the multicritical point on the random-plaquette gauge model with the random couplings following $\pm J$ distribution function on the three-dimensional cubic lattice. The conventional conjecture relates this threshold with the location of the multicritical point of the $\pm J$ Ising model on the three-dimensional cubic lattice [115]. The improved conjecture also cannot directly derive such an accuracy threshold, but can make more precise relationship between the locations of the multicritical points on the random-bond Ising model and the random-plaquette gauge model than the conventional conjecture does. Similarly to the other spin-glass theory, the improved conjecture furthers the information theory. This means a contribution to both of the classical and quantum information theories.

Chapter 7

Summary

Since the pioneering result by the mean-field theory of the Sherrington and Kirkpatrick model, we have been interested in the random spin systems and have expected the existence of the spin glass phase even for finite dimensional systems. For finite-dimensional systems, it has been difficult to elucidate properties in the random spin systems because very little systematic analytical work exists. We mainly rely on the approximations, the phenomenological techniques and predominantly the numerical simulations. In particular, a great number of numerical studies have been successful in clarifying the critical phenomena at the critical points, estimating the critical exponents, and categorizing the universality classes in random spin systems. Unfortunately different results sometimes have been reported and their validity have been discussed. To clarify the reliability of various numerical approaches, we have to derive the exact or highly precise solutions.

In this thesis, we have shown an analytic study to systematically derive the location of the critical points for finite-dimensional random spin systems. This study is of practical importance to greatly facilitate the estimation of the critical exponents and to give benchmarks for the reliability of the numerical approaches. For these purposes, we considered the duality with the replica method in random spin systems mainly through investigations of the $\pm J$ Ising model.

The duality has been a useful technique to establish the relationship between two different models in non-random spin systems as in Chapter 2. Coincidence of two lines expressing the representative points of the relative Boltzmann factor related with each other by the duality permits us to derive the exact location of the critical point. On the other hand, we cannot obtain such a satisfactory relationship in random spin systems before and after the duality.

An argument using the gauge symmetry is a piece of the rigorous and exact techniques. In the special subspace on the phase diagram, the Nishimori line, we can calculate the exact value of the internal energy, evaluate the upper bound for the specific heat and prove several correlation inequalities. Though the duality does

not always work well for the random spin systems, we assume that a single equation gives the prediction of the critical point similarly to the non-random spin systems as mentioned in Chapter 4, the conventional conjecture. This ansatz has given some results in good agreement to the third digit with existing results by numerical simulations and estimations. These successful predictions have been considered to be justified by a special property on the Nishimori line, but several cases on the hierarchical lattices show that the conjecture is not always valid.

We have then attempted, in Chapter 5, to construct the improved conjecture with high precision beyond the conventional conjecture using the idea of the renormalization group analysis, that is to sum over a part of degrees of freedom to elucidate precisely properties near the critical point. This improved conjecture gives predictions of the closer locations of the multicritical points to exact answers obtained by the renormalization group analysis on the hierarchical lattices than the conventional conjecture. The improved conjecture seems to be able to derive the critical points in several regions, as well as the multicritical point on the Nishimori line, though we unfortunately cannot obtain perfect answers for the locations of the critical points, especially in the low-temperature region. However this study has given a basis for the improvement of the conjecture on regular lattices.

The improved conjecture has been proposed for the regular lattices in Chapter 6. In this case, the renormalization group analysis does not work well because many-body interactions are generated after the renormalization. Therefore we do not iterate the renormalization but attempt to perform the summation over the degrees of freedom in a limited range of the regular lattice under the consideration. Instead of the iteration of the renormalization, we consider the summation over the larger size of the small systems. In this formulation, the improved conjecture has an appealing feature that the phase transition across the multicritical point occurs when the entropy of the distribution of frustration takes a special value. This physical meaning will become a significant problem on the phase transition in the random spin systems. Though the improvement of the critical points in the low-temperature region under the Nishimori line has been unsatisfactory, we have obtained the location of the multicritical point for the $\pm J$ Ising model on the square, the triangular, and the hexagonal lattices with the precision to the fourth digit. In addition, the slopes of the critical points for several random-bond Ising models have been estimated and have shown the behaviors converging to the exact solutions. From these results, the improved conjecture is successful in deriving the precise location of the critical points in several regions in random spin systems.

The improved conjecture is a meaningful step, since discovery of the Nishimori line, to construct an analytic theory, which may be a unique way to lead us to exact solutions in finite-dimensional random spin systems. It should be emphasized that we have proposed a systematic approach to derive the location of the critical points, because we can propose the suitable approximation by the analysis of the

small lattice, and can give the answer with the desired precision. One of the possible applications of the improved conjecture is thus considered to be a numerical implementation to estimate the precise location of the critical point. Then we will obtain a sufficiently precise value to be regarded as the exact solution. It will be the benchmark of the reliability of various numerical approaches before challenges toward the unsolved problems related with the nature of the spin glasses.

In addition, the connection with the gauge invariance shows an appealing aspect of the improved conjecture. The value of the entropy of the distribution of frustration characterizes the phase transition on the Nishimori line. Therefore the improved conjecture gives slight but another step to understand the deep meaning of the gauge invariance in the spin glass. There is a further interesting problem that the phase transition on the Nishimori line is related with problems on both of the classical and quantum information processing. Analytic properties of the improved conjecture will elucidate profound relationship among three different fields, the spin-glass, the classical and the quantum information theories. Such hidden properties behind the nature of the spin glass are possibly clarified only through the exact solutions and analytic analyses. The line of our study is essential to truly understand the physics on the spin glass and beyond.

Bibliography

[1] K. Binder and A. P. Young, Rev. Mod. Phys. **58**, 801 (1986).

[2] M. Mézard, G. Parisi, and M. Virasoro, *Spin Glass Theory and Beyond* (World Scientific, 1986) .

[3] H. Nishimori, *Statistical Physics of Spin Glasses and Information Processing: An Introduction* (Oxford Univ. Press, Oxford, 2001).

[4] M. A. Ruderman and C. Kittel, **96**, 99 (1954).

[5] T. Kasuya, Prog. Theor. Phys. **16**, 45 (1956).

[6] K. Yosida, Phys. Rev. **106**, 893 (1957).

[7] V. Cannella and J. A. Mydosh, Phys. Rev. B **6**, 4220 (1972).

[8] H. Maletta and W. Felsch, Phys. Rev. B **20**, 1245 (1979)

[9] O. Meschede, F. Steglich, W. Felsch, and H. Maletta, and W. Zinn, Phys. Rev. Lett. **44**, 102 (1980).

[10] G. E. Brodale, R. A. Fischer, W. E. Fogle, N. E. Philips, and J. van Chen, J. Magn. Mag. Mat. **31-34**, 1331 (1983).

[11] G. Toulousse, Commun. Phys. **2**, 115 (1977).

[12] J Vannimenus and G. Toulousse, J. Phys. C: Solid State Phys. **10**, L537 (1977).

[13] S. F. Edwards and P. W. Anderson, J. Phys. F **5**, 965 (1975).

[14] D. Sherrington and S. Kirkpatrick, Phys. Rev. Lett. **35**, 1792 (1975).

[15] S. Kirkpatrick and D. Sherrington, Phys. Rev. B **17**, 4384 (1981).

[16] C. De. Dominicis, M. Gabay, H. Orland, and T. Garel, J. Phys. (Paris) **41**, 923 (1980).

[17] A. J. Bray and M. A. Moore, J. Phys. C: Solid State Phys. **13**, L469 (1980).

[18] A. J. Bray and M. A. Moore, J. Phys. C: Solid State Phys. **13**, L907 (1980).

[19] M. Kac, Trondheim Theoretical Physics Seminar, Nordita, Publ. No, 286 (1968).

[20] S. F. Edwards, in *Proceedings of the Third International Conference on Amorphous Materials*, edited by R. W. Douglas and B. Ellis, (Wiley, New York), p. 279 (1970).

[21] T. F. Lin, J. Math. Phys. **11**, 1584 (1970).

[22] S. F. Edwards, in *Polymer Networks*, edited by A. J. Chompff and S. Newman, (Plenum, New York), p. 83 (1971).

[23] A. Bladin, J. Physique C **6**, 1568 (1978).

[24] A. J, Bray and M. A. Moore, Phys Rev. Lett. **41**, 1069 (1978).

[25] G. Parisi, Phys. Rev. Lett. **43**, 1754 (1979).

[26] R. G. Palmer, Adv. Phys. **31**, 669 (1982).

[27] M. Mézard, G. Parisi, N. Sourlas, G. Toulouse, and M. Virasoro, Phys. Rev. Lett. **52**, 1156 (1984).

[28] M. Mézard, G. Parisi, N. Sourlas, G. Toulouse, and M. Virasoro, J. Phys. (Paris) **45**, 843 (1984).

[29] D. J. Thouless, P. W. Anderson, and R. G. Palmer, Philos. Mag. **35**, 593 (1977).

[30] T. C. Lubensky, Phys. Rev. B **11**, 3573 (1975).

[31] A. P. Young and R. B. Stinchcombe, J. Phys. C **8**, L535 (1975).

[32] A. B. Harris, T. C. Lubensky, and R. J. Chen, Phys. Rev. Lett. **36**, 415 (1976).

[33] R. J. Chen and T. C. Lubensky, Phys. Rev. B **16**, 2106 (1977).

[34] H. Nishimori, Prog. Theor. Phys. **66**, 1169 (1981).

[35] R. N. Bhatt and A. P. Young, Phys. Rev. Lett. **54**, 924 (1985).

[36] R. N. Bhatt and A. P. Young, Phys. Rev. B **37**, 5606 (1988).

[37] A. T. Ogielski and I. Morgenstein, Phys. Rev. Lett. **54**, 928 (1985).

[38] A. T. Ogielski and I. Morgenstein, Phys. Rev. B **32**, 7384 (1985).

[39] I. Morgenstein and K. Binder, Phys. Rev. B **22**, 288 (1980).

[40] A. J. Bray and M. A. Moore, J. Phys. C **17**, L463 (1984).

[41] R. R. P. Singh and S. Chakravarty, Phys. Rev. Lett. **57**, 245 (1986).

[42] Y. Ozeki, J. Phys. Soc. Jpn. **59**, 3531 (1990).

[43] H. G. Katzgraber, M. Körner and A. P. Young, Phys. Rev. B **73** 224432 (2006).

[44] I. A. Campbell, K. Hukushima and H. Takayama, Phys. Rev. B **76** 13442 (2007).

[45] D. S. Fisher and D. A. Huse, J. Phys. A. **20** L997 (1987).

[46] D. A. Huse and D. S. Fisher, J. Phys. A. **20** L1005 (1987).

[47] D. S. Fisher and D. A. Huse, Phys. Rev. B **38** 386 (1988).

[48] H. Nishimori, J. Phys. Soc. **55**, 3305 (1986).

[49] A. Georges and P. Le Doussal, *unpublished Preprint* (1988).

[50] P. Le Doussal and A. B. Harris, Phys. Rev. Lett. **61** 625 (1988).

[51] P. Le Doussal and A. B. Harris, Phys. Rev. B **40** 9249 (1989).

[52] Y. Ozeki and H. Nishimori, J. Pys. Soc. Jpn. **56** 1568 (1987). (Addendum: **56** 2992 (1987).)

[53] Y. Ozeki and H. Nishimori, J. Phys. Soc. Jpn. **56** 3265 (1987).

[54] R. R. P. Singh and J. Adler, Phys. Rev. B **54**, 364 (1996).

[55] Y. Ozeki and N. Ito, J. Phys. A: Math. Gen. **31**, 5451 (1998).

[56] F. D. A. Aarão Reis, S. L. A. de Queiroz, and R. R. dos Santos, Phys. Rev. B **60**, 6740 (1999).

[57] A. Honecker, M. Picco, and P. Pujol, Phys. Rev. Lett. **87**, 047201 (2001).

[58] F. Merz and J. T. Chalker, Phys. Rev. B **65**, 054425 (2002).

[59] S. L. A. de Queiroz, Phys. Rev. B **73**, 064410 (2006).

[60] N. Ito and Y. Ozeki, Physica A **321**, 262 (2003).

[61] M. Picco, A. Honecker, and P. Pujol, J. Stat. Mech. P09006 (2006).

[62] M. Hasenbusch, F. P. Toldin, A. Pelissetto, and E. Vicari, Phys. Rev. E **77**, 051115 (2008).

[63] R. R. P. Singh, Phys. Rev. Lett. **67**, 899 (1991).

[64] M. Hasenbusch, F. P. Toldin, A. Pelissetto, and E. Vicari, Phys. Rev. B **76**, 184202 (2007).

[65] I. A. Gruzberg, N. Read, and A. W. W. Ludwig, Phys. Rev. B **63**, 104422 (2001).

[66] S. Cho and M. P. A. Fisher, Phys. Rev. B **55**, 1025 (1997).

[67] J. T. Chalker, N. Read, V. Kagalovsky, B. Horovitz, Y. Avishai, and A. W. W. Ludwig, Phys. Rev. B **65**, 012506 (2001).

[68] A. Mildenberger, F. Evers, R. Narayanan, A. D. Mirlin, and K. Damle, Phys. Rev. B **73**, 121301(R) (2006).

[69] N. Sourlas, Europhys. Lett. **25**, 159 (1994).

[70] H. Nishimori, Physica A **205**, 1 (1994).

[71] Y. Iba, J. Phys. A: Math. Gen. **32**, 3875 (1999).

[72] H. Nishimori, Physica A **315**, 243 (2002).

[73] E. Dennis, A. Kitaev, A. Landahl, and J. Preskill, J. Math. Phys. **43**, 4452 (2002).

[74] C. Wang, J. Harrington, and J. Preskill, Ann. Phys. (NY) **303**, 31 (2003).

[75] G. Grinstein, C. Jayaprakash, and Michael Wortis, Phys. Rev. B **19**, 260 (1979).

[76] H. Freund and P. Grassberger, J. Phys. A: Math. Gen. **22**, 4045 (1989).

[77] J. Bendish, U. Derigs and A. Metz, Discrete Applied Mathematics **22**, 139 (1994).

[78] N. Kawashima and H. Rieger, Europhys. Lett. **39**, 85 (1997).

[79] J. A. Blackman, J. R. Gonçalves, and J. Poulter, Phys. Rev. E **58**, 1502 (1998).

[80] C. Amoruso and A. K. Hartmann, Phys. Rev. B **70**, 134425 (2004).

[81] J. Edmonds, Can. J. Math. **17**, 449 (1965).

[82] F. Barahona, R. Maynard, R. Rammal, and J. P. Uhry, J. Phys. A. **15**, 673 (1982).

[83] F. Barahona, J. Phys. A **15**, 3241 (1982).

[84] H. Kitatani, J. Phys. Soc. Jpn. **61**, 4049 (1992).

[85] H. A. Kramers and G. H. Wannier, Phys. Rev. **60**, 252 (1941).

[86] F. Y. Wu and Y. K. Wang, J. Math. Phys. **17**, 439 (1976).

[87] H. Nishimori and K. Nemoto, J. Phys. Soc. Jpn. **71**, 1198 (2002).

[88] J.-M. Maillard, K. Nemoto and H. Nishimori, J. Phys. A **36**, 9799 (2003).

[89] A. N. Berker and S. Ostlund, J. Phys. C **12**, 4961 (1979).

[90] R. B. Griffiths and M. Kaufman, Phys. Rev. B **26**, 5022R (1982).

[91] M. Kaufman and R. B. Griffiths, Phys. Rev. B **30**, 244 (1984).

[92] M. Hinczewski and A. N. Berker, Phys. Rev. B **72**, 144402 (2005).

[93] L. Onsager, Phys. Rev. **65**, 117 (1944).

[94] R. J. Baxter, *Exactly solved models in statistical mechanics* (Academic Press, London, 1982).

[95] F. Y. Wu, Rev. Mod. Phys. **54**, 235 (1982).

[96] M. Ohzeki and H. Nishimori, J. Phys. Soc. Jpn. **126**, 977 (2007).

[97] F. Y. Wu and R. K. P. Zia, J. Phys. A: Math. Gen. **14** 721 (1981).

[98] A. Georges, D. Hansel, P. Le Doussal and J. -M. Maillard, J. Physique **48**, 1 (1987).

[99] H. Nishimori, J. Stat. Phys. **126**, 977 (2007).

[100] K. Takeda, T. Sasamoto and H. Nishimori, J. Phys. A **38**, 3751 (2005).

[101] H. Nishimori and M. Ohzeki, J. Phys. Soc. Jpn. **75**, 034004 (2006).

[102] J. L. Jacobsen and M. Picco, Phys. Rev. E **65**, 026113 (2002).

[103] H. Nishimori and M. J. Stephen, Phys. Rev. B **27**, 5644 (1983).

[104] M. Ohzeki, H. Nishimori and A. Nihat Berker, Phys. Rev. E **77**, 061110 (2008).

[105] F. D. Nobre, Phys. Rev. E **64**, 046108 (2001).

[106] E. Domany, J. Phys. C **12**, L119 (1979).

[107] H. Nishimori, J. Phys. C **12**, L905 (1979).

[108] H. Nishimori, J. Phys. C **12**, L641 (1979).

[109] D. Stauffer, *Introduction to Percolation Theory* (Taylor & Francis, London, 1985).

[110] E. Domany, J. Phys. C **11**, L337 (1978).

[111] B. W. Southern and M. F. Thrope, J. Phys. C: Solid State Phys. **12**, 5351 (1979).

[112] B. W. Southern, J. Phys. C: Solid State Phys. **13**, L285 (1980).

[113] A. Aharony and M. J. Stephen, J. Phys. C. Solid State Phys. **13** L407 (1980).

[114] Y. Okabe, private communication.

[115] K. Takeda and H. Nishimori, Nucl. Phys. B **686** 377 (2004).